AN ABSTRACT OF THE THESIS OF

Donald Homer DeBok (Name) for the degree Master of Ocean Engineering (Degree)

in Civil Engineering (Major Department) presented on December 8, 1977

Title: A LARGE SCALE MODEL STUDY OF PLACED STONE BREAKWATERS

Abstract approved: Redacted for Privacy

Dr. Charles K. Sollitt

The results of three hydraulic model tests to evaluate the stability of a placed stone breakwater are presented and discussed. The prototype breakwater was designed to protect offshore power and port facilities in 60 feet of water and was tested at scale ratios of 1:10, 1:20, and 1:100. The armor layer tested is formed from quarried stones of irregular parallelepiped shapes, individually placed long axis perpendicular to the plane of the surface. The resultant breakwater is relatively smooth, densely packed and very stable. Stability, runup, rundown, and reflection are evaluated for a variety of water depth, wave height, and periods. Analysis of the damage induced in the models shows that the placed stone armor is approximately as stable as dolos. Runup, rundown, and reflection response is similar to rough impermeable slopes. Comparison of large and small scale results demonstrate that relative increases in drag forces at lower Reynolds numbers decrease stability and runup in small scale models.

A Large Scale Model Study of Placed Stone Breakwaters

by

Donald Homer DeBok

A THESIS

submitted to

Oregon State University

in partial fulfillment of
the requirements for the
degree of

Master of Ocean Engineering

Completed December 8, 1977

Commencement June 1978

APPROVED:

Redacted for Privacy

Professor of Civil Engineering
in charge of major

Redacted for Privacy

Head of Department of Civil Engineering

Redacted for Privacy

Dean of Graduate School

Date thesis is presented December 8, 1977

Typed by Type-Ink for Donald Homer DeBok

ACKNOWLEDGEMENTS

This study was sponsored by the Umpqua Navigation Division of Bohemia Corporation, Eugene, Oregon. Mr. O.H. Hinsdale of Portland, Oregon was a motivating force in making this study a reality. Dean F. J. Burgess, Prof. J. H. Nath and Prof. L.S. Slotta of Oregon State University negotiated the terms of the research grant.

A major portion of the work was conducted by Lt. DeBok, U.S. Coast Guard, in partial fulfillment of the requirements of the Master of Ocean Engineering degree at Oregon State University. The experimental studies were ably assisted by Mr. T. L. Dibble and Mr. E.J. Jones. Dr. C.K. Sollitt, Dept. of Civil Engineering at Oregon State University, was the Principal Investigator.

TABLE OF CONTENTS

LIST OF FIGURES

LIST OF FIGURES (continued)

LIST OF FIGURES (continued)

LIST OF FIGURES (continued)

LIST OF TABLES

LIST OF SYMBOLS

A_c	Characteristic area
A^*	Dimensionless area
a	Area
B	Thompsen's dimensionless wave damage coefficient
b	Width of the breakwater
C_D	Drag coefficient
C_r	Reflection coefficient
d	Depth of the water
F_D	Drag force
F_r	Froude number
F_s	Resistance force
g	Acceleration of gravity
H	Wave height
H_b	Breaking wave height
H_i	Incident wave height
H_{max}	Maximum wave height in a partial standing wave envelope
H_{min}	Minimum wave height in a partial standing wave envelope
H_o	Deep water wave height
H_r	Reflected wave height
H_{ZD}	Zero damage wave height
i	Subscript identifying direction
J	Number of stones displaced from the breakwater

j	Subscript identifying the coordinate orthogonal to the direction of motion
K_D	Hudson's stability coefficient
K_r	Reflection coefficient
K_s	Shoaling coefficient
k_s	Static resistance coefficient
L	Characteristic length
N_{ZD}	Thomsen's zero damage stability coefficient
P	Characteristic pressure
p	Pressure
p^*	Dimensionless counterpart of pressure
R_d	Rundown
R_e	Reynolds number
R_u	Runup
s	Specific gravity
T	Wave period
t	Time
t^*	Dimensionless counterpart of time
U	Characteristic Velocity
u	Velocity
u^*	Dimensionless counterpart of velocity
V	Unit volume
V^*	Dimensionless counterpart of unit volume
W	Weight

W'	Submerged Weight
x	Spatial dimension in the direction of motion
x^*	Dimensionless counterpart to distance in the direction of motion
α	Breakwater slope
γ	Weight density
δ	Phase shift of the wave
η	Surface profile of the wave
η_i	Surface profile of the incident wave
η_r	Surface profile of the reflected wave
λ	Wave length
λ_o	Deep water wave length
μ	Iribarren's friction coefficient, dynamic viscosity
ν	Kinematic viscosity
ρ	Mass density
Φ	Measure of a materials ability to disipate wave energy

A LARGE SCALE MODEL STUDY OF PLACED STONE BREAKWATERS

CHAPTER I

INTRODUCTION

1.1 Scope

This report describes a hydraulic model study of a placed stone breakwater design for the Umpqua Division of Bohemia Corporation. The study investigates the suitability of the design for creating artificial islands around offshore nuclear power plants and investigates the effects of model scale on placed stone breakwater research. This specific application requires a structure which will withstand waves near the breaking condition in water depths varying from 40 to 60 feet.

The placed stone technique utilized in this design requires the use of stones quarried in the shape of rectangular blocks. These stones are set individually such that the long axis is perpendicular to the slope of the breakwater. This closely packed arrangement increases stability even though the decrease in porosity causes greater runup.

The design was exposed to a test program of monochromatic waves (constant amplitude and period for any single test run). Wave heights were increased in successive cases until structure failure was

achieved. Both wave period and water depth were varied to achieve a variety of exposure conditions. Testing was conducted at three model scales (1:10, 1:20, 1:100) to provide a means of estimating scale effects. These models appear in Fig. 1-1, 1-2, and 1-3 respectively.

Four major objectives were sought:

1. Determination of the no damage wave height for a range of water depths and wave periods.
2. Determination of the stability parameter, K_D, of Hudson's formula, for this design.
3. Comparison of runup data for this structure with that for other armor shapes.
4. Investigation of the effect of model scale on stability and runup.

The structure was found to be exceptionally stable with a K_D of 30 at the 1:10 scale. Runup was greater than that on rubble mound and relative runup increased with decreasing scale and increasing wave period. No damage wave heights increased with increasing model size.

1.2 Background

The placed stone technique examined in this research has been developed over the past 20 years by the Portland District of the U.S. Army Corps of Engineers and the Umpqua Division of Bohemia Corporation. The following account of this development draws heavily on articles written by Kidby, Powell and Roberts (28) and on the

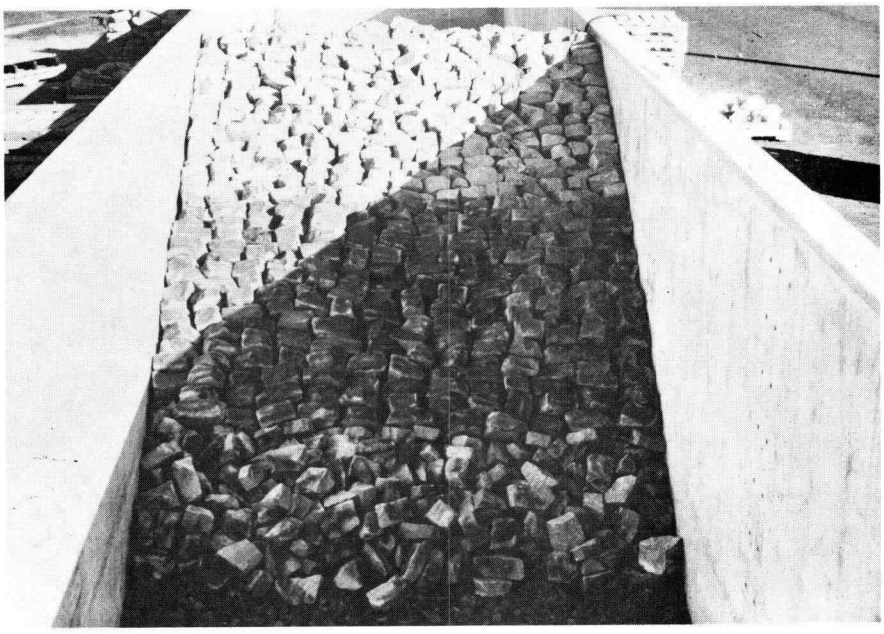

Fig. 1-1. 1:10 Scale Model

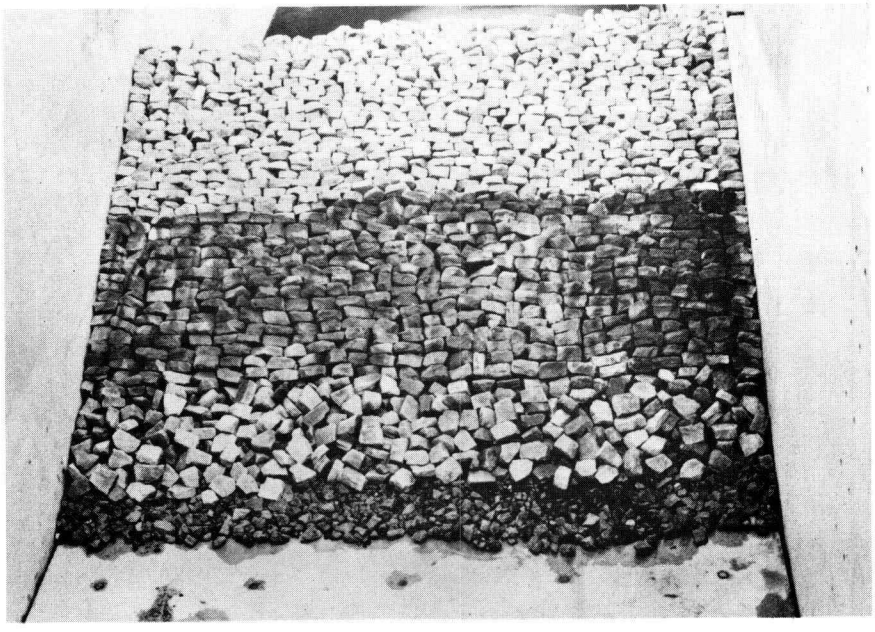

Fig. 1-2. 1:20 Scale Model

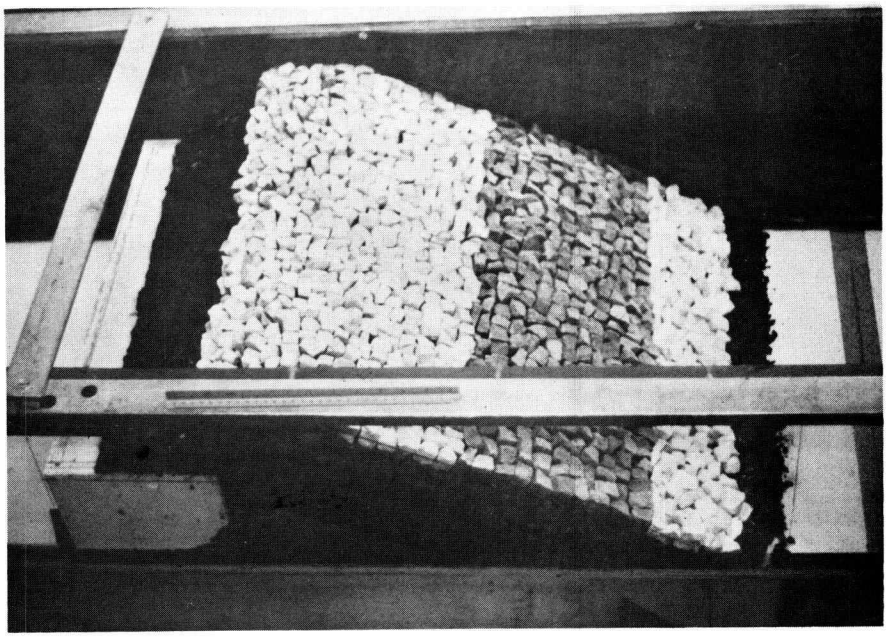

Fig. 1-3. 1:100 Scale Model

PROTOTYPE BREAKWATER SECTION

DIMENSIONS IN FEET

MATERIAL	SIZE (TON)
A+	25-35
A	15-25
A-	10-15
B	6-12
B-	3-6
C	0-3

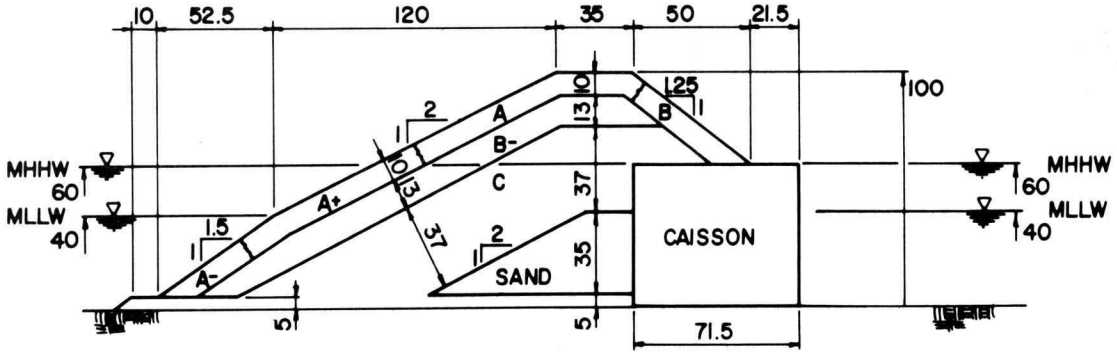

Fig. 1-4. Prototype Breakwater Dimensions

Corps of Engineers surveillance report of the Umpqua River South Jetty (46).

During the 1950's several jetties on the Oregon-Washington coast were constructed, repaired or lengthened. Except for the south jetty at Coquille River, work was performed using pell mell placement by bulldozer. Stones in the armor layer of the Coquille jetty were placed individually by crane. During subsequent storms, this jetty received significantly less damage than other structures. Observation of Coquille jetty indicated that a relatively high percentage of stones had been placed long axis perpendicular to the slope. Based on this knowledge, the jetties on the Rogue River (1959-1960) were constructed in a similar fashion. Each stone above low water was placed with its long axis perpendicular to jetty length and tilted slightly toward the core. These structures have survived very well despite severe wave conditions experienced in the 1960's.

The success of the Coquille and Rogue River jetties prompted the Portland District to sponsor a hydraulic model study of a similar design. The model study was conducted in conjunction with the design of the south jetty of the Siuslaw River at the U.S. Army Corps of Engineers Waterways Experiment Station, Vicksburg, Mississippi, in 1961. The study (26) concluded that:

1. The design was suitable for the application.
2. The placement improves stability but in view of limited tests,

designs using the technique should consider the apparent improved stability only as an added safety factor.

3. Appreciable overtopping occurred in higher waves.

The model was scaled at 1:50 and the stone size used would be equivalent to a 1:60 model of the design breakwater. The Siuslaw design used random placement up to the low water mark. The extension of placed stone below low water, as in the current design, may be a significant design improvement.

Jetties designed and constructed in the Portland District since 1960 have used placed stone armor. These works include Yaquina Bay south jetty, Tillamook Bay south jetty, and Umpqua River south jetty. A total of 11 projects have been completed using the technique. Umpqua south jetty has been systematically observed by the Portland District (46), and damage to the armor has been minor. Some portions of the jetty have subsided, probably due to erosion at the toe.

The overall success of these works prompted Umpqua Navigation, a Division of Bohemia, Inc., to fund this research. The stability tests were conducted at a large scale ratio to minimize scale effects inherent in small models and to supplement the Waterway Experiment Station Study.

1.3 Breakwater Description

The breakwater modeled in this research (Fig. 1-4) was designed to protect an offshore nuclear power plant in 50 feet of

water. Crest height is 100 feet off the ocean floor. The inner core is sand and the outer core is quarry rock. An intermediate layer of 3 to 12 ton stones (B minus stones), 13 feet thick covers the outer core. The armor layer is 10 feet thick and is composed of four classes of stone referred to as A minus, A select, A and B. The A minus stone (10 to 15 tons) is randomly placed from the toe to 10 feet below the low water mark at a slope of 1:1.5. From this point to the point of highest expected water level (60 feet above the toe), A select rock, 25 to 35 tons, is placed. At the low water point (40 feet) the slope changes from 1:1.5 to 1:2. The remaining area of the seaward face and the entire crest is of A stone, 15 to 25 tons. The backface, which extends down to the high water mark, is of B stone, 6 to 12 tons. A concrete caisson forms the backside of the breakwater below high water. All stones of type A select, A, and B are placed individually with the long axis perpendicular to the jetty face. These stones are specially quarried and selected for their rectangular parallelepiped shape.

The stones used in the 1:10 and 1:20 scale models were quarried and classified by Umpqua Navigation. The stones used in the 1:100 scale model were split from larger stones and classified by the investigators. All models were constructed by the investigators after instruction by Umpqua personnel. Table 1-1 compares, at full scale, the mean weights of the stones used in the models. Data on

Table 1-1. Mean Weight and Standard Deviation of Model Stones Compared at Prototype Scale

Classification of stones	Prototype weight (short tons)	Mean Weight			Standard Deviation		
		1:10	1:20	1:100	1:10	1:20	1:100
B minus	3 to 12	6.3	7.3	6.2	1.9	2.7	2.2
B	6 to 12	8.9	9.4	9.1	2.1	2.0	1.7
A minus	10 to 15	12.7	12.1	13.3	2.8	2.4	1.4
A select	25 to 35	29.0	28.4	28.9	3.9	3.5	2.6
A	15 to 25	19.2	20.3	19.7	2.8	2.5	2.8

distribution of stone sizes are provided in Appendix B and a pictorial essay showing the phases of model construction is contained in Appendix A.

CHAPTER II

REVIEW OF IMPORTANT CONCEPTS

2.1 Introduction

The interaction of a group of waves with a rubble mound breakwater has not been adequately described by any independent theory. In lieu of analytical models, hydraulic models have been developed to assist in quantifying complex processes of engineering interest. The application of hydraulic modeling techniques to a real problem requires an appreciation of the physical processes involved and for the capabilities and limitations of hydraulic models.

Breakwater modeling and interpretation of the results for design application requires some understanding of four major topics:

1. The fundamentals of wave motion.
2. Hydraulic modeling procedures and the effect of approximate modeling techniques.
3. The factors which affect the stability of a breakwater.
4. Runup behavior on permeable slopes.

The discussion provided herein is intended to provide some background necessary to understand this report and to provide a review of related investigations.

2.2 Wave Description

There are several important properties of waves fundamental to any wave-structure interaction study. These properties are most conveniently described in terms of linear wave theory. The discussion presented is intended primarily to familiarize the reader with the technique used to determine the incident and reflected wave properties from the raw data. A more complete description of the solution and applications of wave theory is provided by Ippen (23).

The most significant parameters of a wave are the period of oscillation, T, and the vertical distance from crest to trough, H. The period is essentially fixed at the generation point and combined with the water depth, establishes the wave length (λ). The height is also constant when the wave travels over a flat bottom or in water that is deep compared to the wave length. In water shallower than one-half wave length, the amplitude varies with the depth of water.

The height is limited in two ways; by wave steepness

$$\frac{H_b}{\lambda} = \frac{1}{7}$$

in deep water, and by relative height

$$\frac{H_b}{d} = 0.78$$

in shallow water, where λ is the wave length and d is the water depth. These are commonly accepted breaking limits (23). In terms of this

study, at the greatest expected water depth (60 feet) the maximum unbroken wave height capable of reaching the breakwater is 46.8 feet. Energy reflected by the breakwater will tend to increase the combined wave steepness thereby reducing the maximum attainable wave height at the breakwater.

A useful explanation of wave behavior is provided by the theory of small amplitude waves, generally called Airy or linear wave theory. It is the first order approximation to the solution of the boundary value problem for surface waves in an ideal fluid. The solution is, as the name implies, linear, and many of its simplified capabilities arise from this linearity. The solution closely describes waves of small amplitude and is approximate for steep waves. Though inaccurate in some respects, for example, pressures near the surface, it is particularly useful in others, such as refraction at nonbreaking heights.

The profile of a progressive wave (η) described by linear theory is a simple sinusoid

$$\eta = \frac{H_i}{2} \sin \left(\frac{2\pi x}{\lambda} - \frac{2\pi t}{T} \right)$$

This wave is propagating in the positive x direction during time, t. Since the solutions at the first order are linear, the combination of several waves may be accomplished by simple addition; it is not necessary to resolve the boundary value problem. Therefore

$$\eta_{total} = \sum_{j=1}^{n} \eta_j$$

describes the water surface of n waves interacting.

Of primary concern in this research is the reduction of the incident wave height from the water surface profile in front of the breakwater. It can be assumed that a wave reflected by a breakwater is of the same frequency as the incident wave, only altered in phase, amplitude and direction. These waves may be written as

$$\eta_i = \frac{H_i}{2} \sin \left(\frac{2 \pi x}{\lambda} - \frac{2 \pi t}{T}\right)$$

and

$$\eta_r = \frac{H_r}{2} \sin \left(\frac{2 \pi x}{\lambda} + \frac{2 \pi t}{T} + \delta\right)$$

where δ is the phase shift and the subscripts i and r refer to the incident and reflected waves, respectively. Any subsequent reflection from the wave generator plate can be shown to superimpose with the incident wave to form one wave of the same frequency. In time a steady state will exist such that all waves traveling toward the breakwater may be treated as a single incident wave train, and all waves traveling away from the breakwater may be treated as a single reflected wave train.

The superposition of incident and reflected waves yields a partial standing wave as shown in Fig. 2-1. The envelope is stationary when a steady state has been achieved. This standing wave

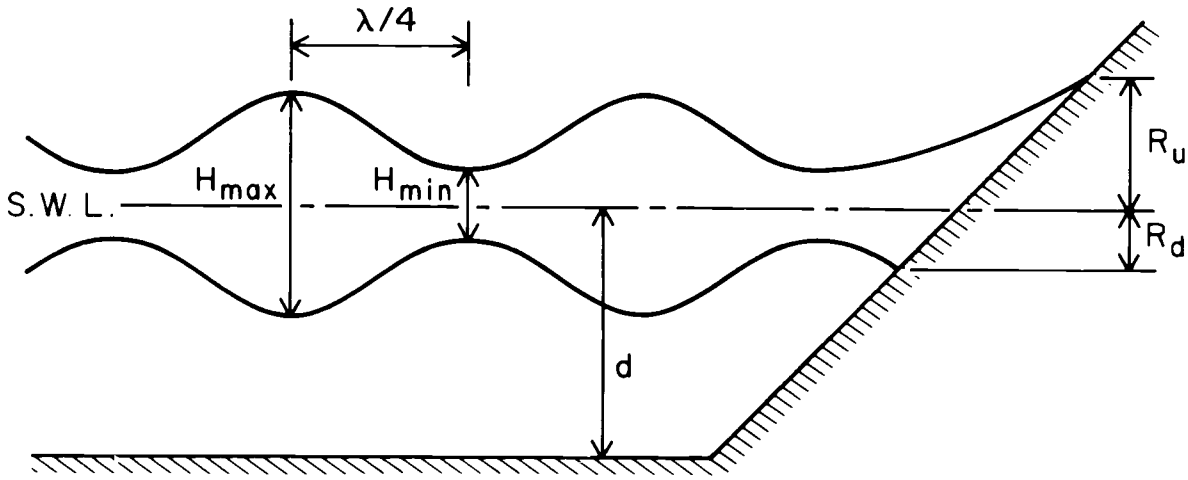

Fig. 2-1. Partial Standing Wave Envelope in Space

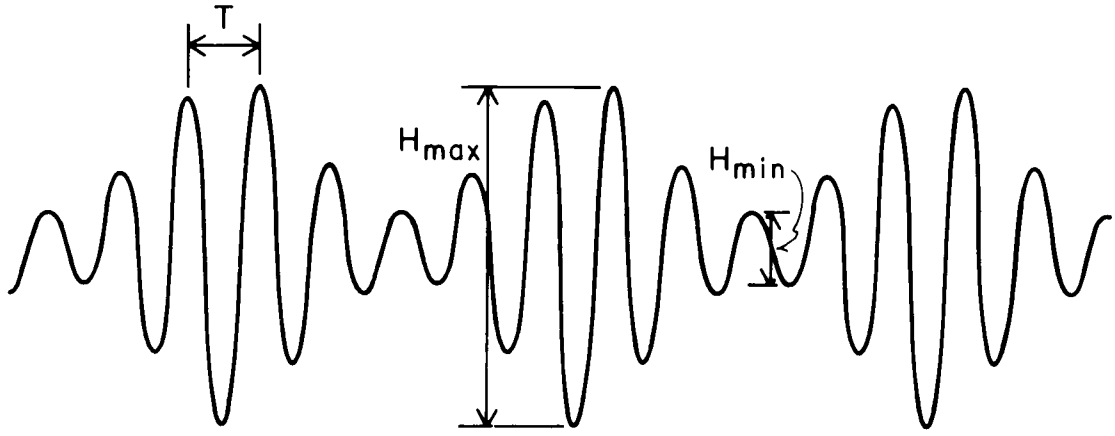

Fig. 2-2. Partial Standing Wave Profile in Time

envelope may be profiled by slowly moving a wave gauge perpendicular to the crest line. Using this method, relative maxima or minima are found every quarter wave length of the incident wave, Fig. 2-2. The maximum points exist where the incident and reflected waves are in phase (crests superimpose with crests and troughs superimpose with troughs) and the minimum points exist where the incident and reflected waves interfere (troughs subtract from crests). The maxima are the summation of wave heights.

$$H_{max} = H_i + H_r$$

The minima are the difference of the wave heights.

$$H_{min} = H_i - H_r$$

The incident wave height (H_i) may be found by summing the above.

$$H_i = \frac{H_{max} + H_{min}}{2}$$

The reflected wave height (H_r) may be found by subtracting the above.

$$H_r = \frac{H_{max} - H_{min}}{2}$$

The reflection coefficient (K_r) is defined as the ratio of the reflected and incident wave height.

$$K_r = \frac{H_r}{H_i} = \frac{H_{max} - H_{min}}{H_{max} + H_{min}}$$

The use of higher order wave theories to solve the problem of partial reflection is greatly complicated by nonlinear terms. If the

water surfaces of the waves were combined linearly for higher order theories, the solution would be identical to that presented above. Higher order solutions do not permit simple superposition of wave velocity and pressure fields and a boundary value problem must be reformulated.

Goda (13, 14) solved the boundary value problem for partial reflection to a third order approximation. An iterative technique utilizing graphical solutions is used to determine the incident wave height and reflection coefficient, accurate to the third order, from the measured maxima and minima. Calculated variation of wave heights due to nonlinear effects was small (less than 5%) in the majority of the test conditions. In the case of the longer waves (13.5, 16.0 seconds) that were profiled in the same depth of water as the toe of the breakwater, the calculated variation became significant. These conditions in which the calculated variation exceeded 5% (the anticipated error of measuring techniques) were corrected using Goda's method. The error in reflection coefficient was considerably greater than 5% and the reflection coefficient results have been corrected.

In the majority of the test runs, it was necessary to measure the standing wave envelope in water deeper than that at the toe of the breakwater. Since wave height varies with water depth, the direct measurements do not describe either the incident wave height (H_i) or

the deep water height (H_o). Deepwater heights were calculated using relationships derived from linear wave theory.

This relationship is formulated by requiring that the wave energy flux through the water column remain constant at all depths. This requirement precludes the long term accumulation or depletion of wave energy at intermediate depths. The energy flux, according to linear wave theory (23), is equal to the product of the energy density and the energy propagation rate. The energy density is proportional to square of the wave height. Hence, the wave height ratio at any two depths is inversely proportional to the square root of the energy propagation rates at the depths of interest. The Shore Protection Manual (45) tabulates this ratio, referenced to the deep water condition, and presents the results as a shoaling coefficient, K_s.

$$K_s = \frac{H}{H_o}$$

where H is the height at the depth, d. The shoaling coefficient is solely a function of the relative depth, d/λ_o, which is the ratio of the water depth to the deep water length ($\lambda_o = 5.127T^2$ in English units). The ratio of the shoaling coefficients at any two depths yields the ratio of the wave heights at those respective depths.

$$\frac{H_1}{H_2} = \frac{H_1/H_o}{H_2/H_o} = \frac{K_{s_1}}{K_{s_2}}$$

The wave height is measured at one location using the wave envelope technique. Then, the wave height at another location can be calculated by using the relative depths at both locations to determine K_{s_1} and K_{s_2} and

$$H_2 = \left(\frac{K_{s_2}}{K_{s_1}}\right) H_1$$

2.3 Hydraulic Modeling

The use of hydraulic models in testing breakwater stability has been developed to provide increased information to the designer. The small scale model has enabled investigators to study the effect of such variables as armor shape, armor weight, breakwater slope and special placement techniques. The application of modeling to a structure under wave action requires the consideration of three types of forces: 1) gravitational forces, (2) viscous forces (real fluid effects), and 3) inertial forces. The relationship between the forces and the limitations introduced by approximate modeling techniques are important to the understanding of this study.

The necessary scaling parameters for modeling hydraulic processes are obtained by casting the governing fluid mechanics equations in a dimensionless format. The Navier-Stokes equations are accepted as the appropriate description for incompressible, isothermal fluid motions. The equations state that acceleration of a

fluid mass results from an imbalance of gravitational, pressure and viscous forces. In tensor notation (sum on double subscripts), the equations are written

$$\underbrace{\frac{\partial u_i}{\partial t}}_{\text{unsteady accel.}} + \underbrace{u_j \frac{\partial u_i}{\partial x_j}}_{\text{convective accel.}} = \underbrace{g_i}_{\text{gravity}} - \underbrace{\frac{1}{\rho}\frac{\partial p}{\partial x_i}}_{\text{pressure gradient}} + \underbrace{\nu \frac{\partial}{\partial x_j}\left(\frac{\partial u_i}{\partial x_j}\right)}_{\text{viscous shear}}$$

where
- u = velocity
- p = pressure
- x = spatial dimension
- t = time
- g = acceleration due to gravity
- ρ = mass density
- ν = viscosity
- i = subscript identifying the direction of motion
- j = subscript identifying other orthogonal coordinate directions

Dimensionless velocities, pressures, lengths, and times are formed by choosing characteristic scaling quantities to represent the magnitude and units for each quantity of interest. Then each dimensional dependent and independent variable is expressed as a product of a dimensionless variable with the appropriate characteristic quantity. The characteristic quantities are

- L = characteristic length (e.g. wave height or length)
- T = characteristic time (e.g. wave period)
- U = characteristic velocity (e.g. crest water particle velocity)
- P = characteristic pressure (e.g. hydrostatic pressure component)

If superscript asterisks are used to identify dimensionless variables, then the relationships between dimensional variables and their

dimensionless counterparts are

$$u = U\, u^*$$
$$p = P\, p^*$$
$$\mathbf{x} = L\, \mathbf{x}^*$$
$$t = T\, t^*$$

Substitution into the Navier-Stokes equation yields

$$\frac{U}{T}\frac{\partial u_i^*}{\partial t^*} + \frac{U^2}{L} u_j^* \frac{\partial u_i^*}{\partial x_j^*} = g_i - \frac{P}{L}\frac{\partial p^*}{\partial x_i^*} + \nu \frac{U}{L^2}\frac{\partial}{\partial x_j^*}\left(\frac{\partial u_i^*}{\partial x_j^*}\right)$$

Dividing through by U^2/L,

$$\left[\frac{L}{TU}\right]\frac{\partial u_i^*}{\partial t^*} + u_j^* \frac{\partial u_i^*}{\partial x_j^*} = \left[\frac{g_i L}{U^2}\right] - \left[\frac{P}{\rho U^2}\right]\frac{\partial p^*}{\partial x_i^*} + \left[\frac{\nu}{UL}\right]\frac{\partial}{\partial x_j^*}\left(\frac{\partial u_i^*}{\partial x_j^*}\right)$$

Now each quantity with an asterisk superscript is dimensionless and dimensional homogeneity requires that each bracketed quantity be dimensionless as well. A check with any convenient system of units will verify the latter. Since the above equation is dimensionless, it must hold in any system of units. Furthermore, it must hold at any model scale if the same process is being described in completely similar systems. The latter statement is true because the dimensional variables and their respective characteristic quantities remain proportional at all scales, in all systems of units, so that their ratios (the dimensionless, superscripted variables) are the same at all scales. Consider, for example, the $\mathbf{x}_i$ spatial dimension. Suppose it is made dimensionless by using the wave length as a characteristic quantity. If the model scale is changed by a factor of

n, both x_i and L change by a factor of n so that the ratio, $x_i^* = nx/nL$, remains the same at both scales. A similar argument may be presented for u, p and t. Hence, all dimensionless variables and functions of dimensionless variables are identical in completely similar systems. It follows that the dimensionless accelerations and stresses expressed in the above equation must be the same in model and prototype. And, because the entire equation is equally valid at both scales, the bracketed dimensionless scaling factors must be identical in model and prototype. If the subscripts m and p are used to identify model and prototype, then complete similarity requires that

$$\left[\frac{L}{TU}\right]_m = \left[\frac{L}{TU}\right]_p$$

$$\left[\frac{g_i L}{U^2}\right]_m = \left[\frac{g_i L}{U^2}\right]_p$$

$$\left[\frac{P}{U^2}\right]_m = \left[\frac{P}{U^2}\right]_p$$

$$\left[\frac{\nu}{U L}\right]_m = \left[\frac{\nu}{U L}\right]_p$$

The first term represents the ratio of unsteady to convective accelerations and is a recognition of kinematic similarity. It may be rewritten as

$$\frac{U_m}{U_p} = \frac{L_m/T_m}{L_p/T_p}$$

This states the intuitively obvious requirement that velocities scale according to the ratio of the length divided by time.

The second term represents the ratio of gravitational forces to inertial forces (gravitational force per unit mass divided by inertia per unit mass) and is commonly referred to as Froude scaling. The Froude number is usually defined as the square root of the inverse of this quantity,

$$F_r = \frac{U}{(g\ L)^{1/2}} = \text{Froude Number}$$

The third term represents the ratio of pressure forces to inertial forces and is commonly referred to as Euler scaling. In free surface flows, however, it is permissible to scale the characteristic pressure, P, using the hydrostatic pressure component. For a given depth, d, below the still water level, the hydrostatic pressure is simply

$$p = \rho g d$$

Since d scales with the length scale L,

$$P = [\ \rho g L]$$

Then

$$\left[\frac{P}{\rho\ U^2}\right] = \left[\frac{\rho g L}{\rho\ U^2}\right] = \left[\frac{gL}{U^2}\right]$$

Hence, Euler scaling reduces to Froude scaling for free surface phenomena.

The fourth term represents the ratio of viscous forces to inertial forces and is commonly referred to as Reynold's scaling. The Reynolds number is usually defined as the inverse of this quantity,

$$R_e = \frac{U L}{\nu}$$

Now the dimensionless Navier-Stokes equation may be written,

$$\left[\frac{L/T}{U}\right] \frac{\partial u_i^*}{\partial t^*} + u_j^* \frac{\partial u_i^*}{\partial x_j^*} = \frac{1}{F_r^2}\left(1 - \frac{\partial p^*}{\partial x_i^*}\right) + \frac{1}{R_e} \frac{\partial}{\partial x_j^*}\left(\frac{\partial u_i^*}{\partial x_j^*}\right)$$

Kinematically and dynamically similar models must respond identically to the above equation for properly modeled processes. Thus, the three dimensionless ratios must be equal in model and prototype,

$$\left[\frac{L/T}{U}\right]_m = \left[\frac{L/T}{U}\right]_p , \quad F_{r_m} = F_{r_p} \text{ and } R_{e_m} = R_{e_p} .$$

The kinematic term is necessary to scale the velocity term. Length, time and velocity scales are usually chosen to make this term close to unity. The Froude number controls two forces in the equation and it is readily apparent why it is so important to maintain this term in free surface phenomena. The magnitude of the Fourde number is also close to unity. The Reynolds number controls the viscous or frictional term in the equation of motion. It can be seen that for small R_e, this term will be important. But large R_e makes this term negligible with respect to other terms in the equation. Since R_e is

equal to the product of the length and velocity scale, it is clear that large models tend to increase R_e and therefore make viscous effects less important in modifying the overall process.

Froude scaling requires that

$$F_r = \frac{U_m}{(gL_m)^{1/2}} = \frac{U_p}{(gL_p)^{1/2}}$$

Since gravity is the same in both model and prototype

$$\frac{U_m}{U_p} = \left(\frac{L_m}{L_p}\right)^{1/2}$$

i.e., velocities scale according to the square root of the length ratio. Kinematic similarity requires that

$$\frac{U_m}{L_m/T_m} = \frac{U_p}{L_p/T_p}$$

or

$$\frac{T_m}{T_p} = \frac{U_p}{U_m}\,\frac{L_m}{L_p} = \frac{L_p}{L_m}\left(\frac{L_m}{L_p}\right)^{1/2}$$

Hence

$$\frac{T_m}{T_p} = \left(\frac{L_m}{L_p}\right)^{1/2} = \frac{U_m}{U_p}$$

Thus, if the model is dimensioned to be one one-hundredth of the linear dimensions of the prototype, the model time and velocities occur in ratios of one-tenth of that observed in the prototype. Scaling

factors for other model properties can be developed using a similar approach.

If, in addition to Froude and kinematic scaling, Reynolds scaling is also observed, then

$$\frac{U_m L_m}{\nu_m} = \frac{U_p L_p}{\nu_p}$$

or

$$\frac{\nu_m}{\nu_p} = \frac{U_m L_m}{U_p L_p} = \left(\frac{L_m}{L_p}\right)^{3/2}$$

Thus, for exactly similar systems, the viscosity of the fluid must be varied to maintain Reynolds scaling. For large model scales, this is nearly impossible. For instance, if $L_m/L_p = 1/100$ then

$$\frac{\nu_m}{\nu_p} = \frac{1}{1000}$$

If the prototype fluid is water, no known fluids exist to yield a viscosity as small as 1/1000 that of water. The easy way out of this predicament is to ignore Reynolds scaling and hope for the best. This, however, is justified only if the Reynolds number is large. The only way to maintain a large Reynolds number and still use the same fluid in model and prototype is to make the model as large as possible. Ideally, the model should be equal to the prototype in scale, then all similarities would be maintained. This, of course, is not

practical so it is necessary to compromise and make the model large, but smaller than full scale, and to use water as the modeling fluid.

Ignoring Reynolds similarity produces an unscaled variation in some properties of the model and this is commonly referred to as a scale effect. Several investigators have observed such variations; on breakwater stability, Dai and Kamel (6) and Thomsen, Wohlt and Harrison (44); on overtopping of structures, Cross and Sollitt (4); and on transmission of waves through permeable structures, Johnson, Kondo and Wallihan (27), Sollitt and Cross (41), and Wilson and Cross (51). By conducting tests at three scales, the effect of ignoring Reynolds similarity is isolated from the parameters of interest. If the models behave similarly then Reynolds effects are negligible and the models are sufficiently large.

Breakwater stability scale effects can be demonstrated by observing the form of the governing force equations. Stability is a function of the body forces' ability to resist the dynamic forces imposed by the wave velocity field. The body forces are characterized by the product of the material weight and a dimensionless resistance which includes the effect of unit shape, strength and special placement. This resistance force may be written:

$$F_s = k_s \gamma V$$

where k_s is the static resistance coefficient, γ is the weight density and V is the unit volume. Dynamic forces are best characterized by

the drag force experienced by an individual stone,

$$F_D = C_D \rho A \frac{U^2}{2}$$

where C_D is the dimensionless drag coefficient, ρ is the mass density, A is the projected area, and U is the approach velocity. A ratio of F_D/F_s less than unity indicates a stable condition.

By substituting dimensionless equivalents and noting that ρ, γ, g and k_s are constants, the ratio of forces for both the model and the prototype becomes

$$\frac{F_D}{F_s} = \frac{C_D L^2 A^* \rho L g U^{*2}/2}{\gamma k_s L^3 V^*}$$

Since $\gamma = \rho g$

$$\frac{F_D}{F_s} = C_D \frac{A^* U^{*2}}{V^* 2k_s}$$

If A^*, V^*, U^* and k_s are identical in both model and prototype, the force ratio is maintained only if C_D is constant. This is not true in all cases. The drag coefficient is dependent on Reynolds number, displaying a generally exponential decay with increasing Reynolds number. Thus drag forces are overestimated in small models, thereby indicating less stable conditions than exist in the prototype.

Experimentally, Dai and Kamel (6) have measured 15 to 50% reduction in no damage wave heights for model scales reduced by a factor of 15. Tests by the Army Corps of Engineers, Coastal

Engineering Research Center (CERC) (44) indicated no damage wave height decreases of 33% or more for decreasing model size by ten-fold.

2.4 Breakwater Stability and Design

During the first third of this century, the state of the art in breakwater design was much as it had been since antiquity. Designers evaluated the success of breakwaters exposed to similar conditions and adjusted sizes accordingly. Since the first design formula appeared in 1933, research has removed much of the guesswork from this design process. One of the primary advances, though not considered in this paper, is the increased accuracy with which waves at a site can be predicted. Advances in theoretical understanding and the application of small scale model tests have greatly increased the probability that a breakwater will be as stable as designed.

Incident wave forces causing structural instability in a rubble mound pose a physical situation that defies a precise mathematical description. An approximate analysis of a single rock on a slope under wave attack does, however, provide an indication of the form of the equation relating the weight of the stone and the destabilizing wave height. Figure 2-3 depicts such a single stone which is prevented from rolling. To be removed, the stone must be lifted from its position by forces imparted by the water. Considering only the

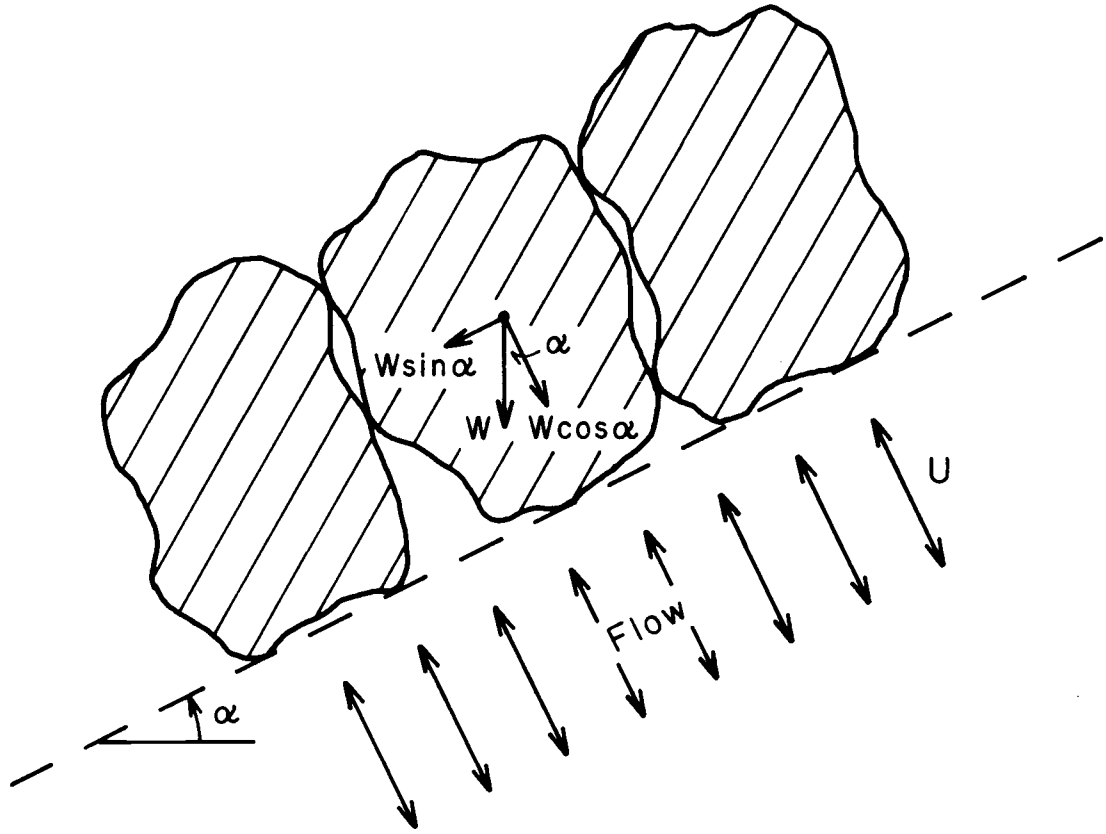

Fig. 2-3. Stability Definition Sketch

drag forces exerted by water flowing out of the breakwater, the destabilizing force is equal to the drag force previously discussed.

$$F_u = F_D = C_D \rho A \frac{U^2}{2}$$

The submerged weight (W') of the stone is given by the equation

$$W' = W \left(\frac{s - 1}{s}\right)$$

where W is the weight of the stone and s is the specific gravity of the stone. The stone will be unstable when:

$$W \left(\frac{s - 1}{s}\right) \cos \alpha \leq C_D \quad A \frac{U^2}{2}$$

The velocity of a water particle under a breaking wave is nearly equal to the phase speed. Since the outrushing velocity is scaled proportional to the incident wave particle velocity

$$U^2 = \frac{H^2}{T^2}$$

In deep water

$$\lambda \propto T^2$$

where $\propto$ is to be interpreted as "proportional to, "

so:

$$U^2 \propto \frac{H^2}{\lambda}$$

A wave breaks in deep water when

$$H \approx \lambda / 7$$

Therefore:

$$U^2 \propto H$$

A shallow water breaking wave behaves according to

$$U^2 \propto C^2 = g\,d$$

and $$H = 0.8\,d$$

Hence a similar result is obtained

$$U^2 \propto H$$

From this argument, it can be inferred that the proportionality holds for intermediate depths as well.

The projected area of the stone is related to the weight of the stone by the following proportionality,

$$A \propto L^2 \propto (Vol)^{2/3} = \left(\frac{W}{s\gamma}\right)^{2/3}$$

Combining these results produces the following relationship,

$$W \left(\frac{s-1}{s}\right) \cos\alpha \geq C_D \left(\frac{W}{s\gamma}\right)^{2/3} \frac{H}{2}$$

Assuming that γ and C_D are constant, then the following proportionalities hold.

$$H \propto \frac{W^{1/3}\,(s-1)\cos\alpha}{s^{1/3}}$$

$$W \propto \frac{H^3\,s}{(s-1)^3\cos^3\alpha}$$

This form is similar to that presented by most investigators of breakwater stability. The equations most prominently advanced are of the form

$$W \propto \frac{H^3 s}{(s - 1)^3 f(\alpha)}$$

where f (α) is trigonometric function of the slope angle, α.

Castro (2), as recounted by others, proposed the first design formula in 1933. It was reasoned that the destructive action was proportional to wave energy. The energy was expressed in terms of wave height in the formula

$$W = \frac{0.704 H^3 s}{(\cot \alpha + 1)(s - 1)^3 (\cot \alpha - \frac{s}{2})^{1/2}}$$

This equation was generally rejected by engineers due to the interrelation of specific gravity and slope.

Iribarren (27), as related by de Carvalho and Vera Cruz (7), introduced the first version of his formula in 1938.

$$W = \frac{K H^3 s}{(\cos \alpha - \sin \alpha)^3 (s - 1)^3}$$

where K = 0.015 for quarry stones

K = 0.019 for artificial blocks

The formula was derived from analytical considerations and values of K were based on observed damage of two breakwaters. The original

formula and a version adapted by Hudson (17) were used by designers for several years.

Several other formulas were proposed before model testing results were available. They are listed herein as an indication of general agreement for the form of the equations.

1. Mathews (7), 1948

$$W = \frac{0.00149\, H^2\, T\, s}{(\cos\alpha - 0.75 \sin\alpha)^2\, (s-1)^3}$$

2. Epstein and Terrel (8), 1949

$$W = K\, \frac{H^3\, s}{(s-1)^3\, (\mu - \tan\alpha)^3}$$

where μ is a coefficient of friction

3. Rudolf (16), 1950

$$W = \frac{0.0162\, H^2\, T\, s}{\tan^3 (45 - \frac{\alpha}{2})\, (s-1)^3}$$

During the period 1942-1950 the applicability of small scale breakwater model tests was studied at the U.S. Army Engineers Waterways Experiment Station. It was determined that hydraulic models provide excellent design information on most phases of breakwater construction. It was further concluded that Iribarren's formula as modified by Hudson,

$$W = \frac{K\, H^3\, s\, \mu^3}{(\mu \cos\alpha - \sin\alpha)^3\, (s-1)^3}$$

was suitable for development of experimental coefficients. Hudson (17) found that the evaluation of μ (necessary to evaluate K) was difficult. This friction coefficient showed great variation with the placement of stones. The Iribarren formula was abandoned and a new formula was adopted. The now popular formula of Hudson is given by the equation

$$W = \frac{\gamma_r H^3}{K_D (s - 1)^3 \cot \alpha}$$

where K_D is an experimentally determined coefficient that may vary with the armor type, design wave characteristics and allowable damage and γ_r equals $s \gamma_{water}$. K_D for most of the common armor shapes has been determined for breaking and nonbreaking waves. K_D is currently the most common value used to evaluate and compare breakwater armor layers. The stability of the models studied in this research will be compared to other armor units using Hudson's K_D.

Hudson's formula is by no means the ultimate formula for the designer. It allows variation of only three parameters in the design. The formula combines all the effects of interlocking, porosity, special placement, wave period, wave steepness and fronting beach slope into one coefficient. Furthermore, the analytical considerations used to develop the formula ignore the effect of inertial forces. As the state of the art in breakwater building advances, the need for more

sophisticated design equations increases. Some authors have advanced new methods to evaluate breakwater stability, while others have sought to develop K_D's for the proliferation of armor shapes currently available. At the same time several investigators have worked to determine the effect of variables other than wave height and breakwater slope.

Svee (42, 43) separated breakwater failures into those caused by uprushing water and those caused by downrushing water. For runup damage a form similar to Hudson's was proposed and a form similar to Iribarren's was developed for rundown failures. In both cases the leading coefficient was calculated using measured hydraulic properties. The formula was used to evaluate the stability of the Svee block, a "V" shaped block placed in a pattern similar to this study.

Rogan (37) criticized the no damage criteria most commonly used with Hudson's formula. The destruction of the armor layer (onset of damage to under layers) was applied as a criteria in his research. It was argued that such damage was easier to measure and provided a more accurate evaluation of actual stability. Font (9, 10) supported the use of this criteria and pointed out the importance of storm duration as a variable when comparing advanced stages of damage.

Paul and Baird (36) also advanced the idea that the no damage wave height may not be the most cost effective design for a breakwater. A "modes of failure diagram" was described that would indicate the type of failure expected for a given wave height. It was proposed that a handbook of such diagrams be developed for the common armor types used. Diagrams for dolosse and quarry stones were presented.

Thomsen, Wohlt and Harrison (44) employed a dimensionless damage parameter in comparing stability of large and small scale models. The damage was calculated by the number of units displaced or by the area disrupted. These results are of particular interest to this study as they include large and small scale tests of random quarry stones and placed quarry stones.

To evaluate the effectiveness of the "placed stone" technique, it will be compared to shapes which most closely resemble it: cubes, rectangular blocks, Svee blocks, and quarry stones. The dolos, generally accepted as the most effective armor unit, will also be compared. The different scales tested in this research will be compared using Hudson's K_D, modes of failure diagrams and dimensionless damage parameters.

The U.S. Army Engineer's Shore Protection Manual (45) lists Hudson's stability coefficients for several common armor shapes. Of

interest to this study are the values for dolosse, random placed angular quarry stones and special placed angular quarry stones.

Merrifield and Zwamborn (31) reported the development and testing of the dolos. Dolosse were compared to rectangular blocks, tetrahendrons and tetrapods. Comparison was also made with results of Delft Laboratory tests on cubes. The Hudson K_D for dolosse was nearly an order of magnitude greater than that for rectangular or cubic blocks.

d'Angremond, Span, van der Weide, and Woestenek (5), and Paape and Walther (35) give results of tests that involved quarry stones and cubes. The results were similar with cubes being somewhat more effective on a per unit weight basis.

The Waterways Experiment Station (26), in evaluating designs for the south jetty of the Siuslaw River in Oregon, studied a placed stone technique similar to that used in this research. The model tested used placed stone only in the active zone (area between high and low water). It was concluded that the placed stone method did improve stability but that the difficulty in field placement of the stones would preclude application on prototypes. Kidby (28) reanalyzed these experiments and noted a significant increase in stability for an increased number of armor stone layers.

Several investigators have found variation between tests that is unexplained by Hudson's formula. It is generally accepted that K_D

and cot α adequately describe the variations in structure geometry so long as interlocking is not the primary source of armor strength. There is, however, considerable evidence that the combination of K_D and wave height is an insufficient description of the wave action. To assist the designer in this respect, Hudson's coefficients are generally given for both breaking and nonbreaking waves. Whether a wave breaks or not is a function of wave height, wave length (period), water depth, slope of the bottom and reflection from the structure. If K_D is different for breaking and nonbreaking waves, then it must vary as some function of period, water depth and beach slope.

Hudson (18) demonstrated that breakwater stability was relatively independent of periods. Despite the fact that these conclusions were drawn from waves in relatively deep water, this independence was initially accepted for the general case. The literature does not indicate total independence of stability and period but considers any dependency as minor.

Some evidence of the effects of period can be found in the work of Ahrens (1). Variation of stability was noted and compared with breaker type. The collapsing breaker as described by Galvin (11) caused greater damage than plunging or surging breakers. In Galvin's classification, collapsing waves are intermediate to surging and plunging breakers and are described as functions of depth, beach slope, wave height and period.

Carstens, Tørum, and Traetteberg (3) concluded that damage was more closely related to runup than to wave height. Several works that will be discussed later indicate that runup is dependent on wave steepness.

In testing breakwaters for Nawiliwili Harbor (19), a strong influence of relative depth (d/λ) and wave steepness was noted. Nagai (33) observed that the depth of water significantly altered the amount of overtopping experienced by a structure.

Oullett (34), after normalizing tests of several investigators, states that bottom slope and water depth are responsible for changes in wave characteristics. This change in form was not considered nearly as important as changes in the height of the wave. The author also offered the opinion that damage should be correlated to wave runup and that the modes of failure diagram should be adopted rather than Hudson's K_D.

It seems apparent that in breakwaters where the height of the wave is a significant portion of the water depth, stability may vary with factors other than wave height. The effect of these factors is not fully understood, but it appears that they cause an alteration in the shape of the wave. This alteration changes the rate of application and spatial distribution of wave induced forces on the breakwater armor units. Any attempt to provide a single universal damage coefficient would seem to be against the better judgment of

contemporary researchers. At best, a structure can be determined to be stable for conditions which are identical to those created in the laboratory.

2.5 Runup on Permeable Structures

The height of runup is an important engineering design parameter as it establishes the structure height necessary to prevent overtopping. The limiting of overtopping is important to the design of causeways, dikes, seawalls, revetments and breakwaters. Offshore facilities protected by man-made islands may not be able to tolerate overtopping, thus, runup becomes a critical design factor.

The interaction of a nonuniform velocity field with a composite structure is such a complicated process that most predictive investigations of runup are limited in scope. Two approaches are: theoretical analysis of the idealized cases and hydraulic model studies in which one or more of the governing parameters is varied systematically. The results of both methods show reasonable correlation and provide the engineer with some specific results for use in design. This, by no means, indicates that a satisfactory solution to wave runup is at hand. Hydraulic models of each specific design still provide the most straightforward results.

There is no exact mathematical means of predicting runup. Some approximate theories have been advanced but are generally

intended for smooth slopes and low slope angles. Analytical solutions to runup on a breakwater suffer in two specific areas: (1) inability of wave theory to describe the breaking process, and (2) inability to account for varying structure shape.

Le Mehaute, Koh and Hwang (30) provide an excellent summation of the predictions provided by various theoretical approaches. For a given H/λ and d/λ decreasing slopes increase runup for angles greater than those causing breaking. Runup in breaking waves decreases with decreasing slope. Nonbreaking waves of greater steepness cause greater runup whereas increasing steepness in breaking waves moves breaking offshore, thereby decreasing runup. The relative wave height H/d becomes an increasingly important parameter in waves of greater length.

The introduction of a structure in which permeability varies with distance from the face (e.g. a rubble mound breakwater) poses complications that may never be solved analytically. Investigators have, therefore, sought to supplement available theories with experimentally derived relationships. These experiments provide practical design data and form a basis of knowledge to which the results of this study may be compared.

The U.S. Army Corps of Engineers' Shore Protection Manual (45) provides a good summary of runup data useful to the engineer. As presented, the data primarily consider the effect of wave steepness

and structure slope. Several authors have studied the effects of varying armor material, water depth at toe, slope in front of structure and type of breaker, as well as wave height and length.

Granthem's (15) early wave flume tests investigated the effects of slope, 15^{o}, 30^{o}, 45^{o}; relative depth, $0.066 < d/\lambda < 0.434$ and wave steepness, $0.012 < H/\lambda < 0.112$. Relative runup was found to increase with increasing wave steepness for a slope of 15^{o}. Increasing steepness reduced runup for slope angles of 30^{o} and 45^{o}. For a given wave, maximum runup was developed on a slope of 30^{o}. The slopes tested were impermeable except for one series. Riprap on the slope reduced runup but no quantitative results were given. General agreement with theoretical investigations was obtained.

Saville (40) conducted extensive testing of runup on smooth slopes in which both structure slope and depth of water were evaluated for several heights and periods. Results were similar to those of Granthem. Greatest runup was observed on a slope of 1 on 2 except for waves of low steepness. Less steep waves were found to cause greater runup. Tests were made with fronting beaches of two different slopes, 1 on 10 and 1 on 40. Runup was less when the flatter slope was employed, indicating that the different bottom configurations utilized in this study may significantly effect runup results. One riprap structure slope, backed with an impermeable layer, was

tested; runup was reduced by nearly 25%. A more permeable structure could be expected to cause more reduction.

Experiments by Savage (38) provide the most extensive information on surface roughness and permeability. Impermeable slopes artificially roughened by material of 0.2 mm to 10 mm in diameter and permeable slopes of like material were tested. The permeable sections were constructed by placing several layers of material over a solid base. Tests conducted comparing the permeable section to a pile of stones of like size showed little difference in runup. Conclusions reached were limited to waves of low relative height ($H/d < 0.33$). Due to the small size of many of the particles, unscaled viscous force may have been of importance, limiting the usefulness of the experiment to prototype applications. For conditions of constant deepwater steepness, runup on roughened slopes was related to $H_o T/D$ increasing for decreasing diameters, (D). Similarly, runup on a premeable slope was related to by $H_o T^2/k$ where increasing k indicated increasing permeability.

Hunt (22) evaluated the results of several investigators and deduced the following empirical formula for runup on a permeable slope

$$\frac{R}{H} = 2.3 \frac{\tan \alpha}{\left(\frac{H}{T^2}\right)^{1/2}} \Phi$$

where Φ is a measure of the materials' ability to dissipate wave

energy. It was noted that porous material reduces runup more effectively on flatter slopes. Wave energy absorption increased linearly up to a porosity of 50% at which point 90% of the energy was absorbed.

Wassing's (49) summary of experiments conducted at Delft Laboratories, Netherlands, describes runup tests conducted on many variables of interest including slope, structure shape and direction of wave attack. Of particular interest was a study on the effect of dike facing materials on runup. Waves were produced by a wind machine and runup results were compared on the basis of the runup exceeded by 2% of the waves. When compared to a smooth slope neatly placed stones caused a reduction of runup by 10%.

Carstens, Torum and Traetteburg (3), while investigating the effects of irregular waves on breakwaters, observed some variations in runup (measured by the average of the one-third highest wave runup) between a theoretical Neumann spectrum and a measured spectrum. The Neumann spectrum contained more steep waves which seemed to reflect and cause whitecaps ahead of the model, thus reducing runup. Similarly, Van Ooorchot and d'Angremond (47) found the width of the wave spectrum to be important. Wider spectra contain more long waves which, in turn, caused higher runup.

Nagai (33), in investigating overtopping of seawalls, made observations that apply to runup. Depth of water at the toe of the

structure was shown to be important. The greatest runup was observed for waves breaking over the toe rather than on the slope or offshore. As in Saville's work, a fronting beach of 1 on 10 resulted in greater runup than a 1 on 40 beach. In order to estimate the effect of permeability, a series of tests was run using similar shapes (N-shaped armor blocks) with different void ratios. Energy dissipation was generally proportional to the void ratio. This relationship did not hold between differing void shapes (hollow tetrahedron armor blocks). Prototype observations of the final design confirmed the model investigation.

Vera Cruz (48) observed some variation of quantity of overtopping with change of relative depth. No specific conclusions could be made but relative runup decreased with increasing d/L_o. Hudson (18) found the effect of relative depth to be minor, but conceded that it probably existed. The scatter of data taken for the porous slopes tested prevented quantitative conclusions.

The structure slope, fronting beach slope, depth of water at the structure and the deepwater wave steepness control the point and type of breaking wave. Some authors have observed runup variation by classifying the type of breaking wave.

Waves on beaches have been classically separated as surging, spilling and plunging, with surging breakers causing the greatest runup. Galvin (11) classified a collapsing breaker as one which forms

upward as if to plunge then collapses in a surge. Galvin observed that these collapsing breakers caused the greatest runup on beaches. Ahrens (1) observed similar results on riprap.

Weggel (50) observed variations in breaker geometry with beach slope. It was argued that on a steeper slope waves cannot maintain an equilibrium profile. This causes a superelevation in the wave, increasing runup. Inverson (25) observed a superelevation of incident waves that varied with beach slopes. Investigation of slopes of 1:10, 1:20, 1:30, 1:40 and 1:50 showed a 40% increase in wave height on the 1:10 slope as compared to 1:50.

Laboratory investigations reach a general concensus on several relationships. If all other parameters are held constant then:

1. Higher waves cause higher runup, provided waves do not take on a plunging characteristic.
2. Longer waves cause greater runup.
3. Runup is a maximum on slopes of about 30^{o}.
4. Increased porosity decreases runup.

CHAPTER III

TESTING PROGRAM AND FACILITIES

3.1 Introduction

Breakwaters designed to protect offshore power installations must be reliable yet economical. In order to obtain design information which satisfies both of these requirements, extensive hydraulic testing was conducted on models of three different scale ratios (1:10, 1:20, 1:100). The design stability criteria required a breakwater capable of withstanding 13.5 second waves 43 feet high in 60 feet of water. To provide information on this and other severe conditions, a program of several wave periods and water depths was selected.

The 1:10 and 1:20 scale tests were conducted at the Oregon State University Wave Research Facility. The test channel, shown in Fig. 3-1, is 342 feet long, 12 feet wide and 15 feet deep in the test section. Waves are generated by a hinged flap driven by a 150 HP, 3500 psi servo-hydraulic system. Five-foot waves can be produced with 11 feet of water in the test section. The 1:100 scale tests were conducted in the smaller channel shown in Fig. 3-2. The smaller tank is 40 feet long, 2.0 feet wide, and 2.2 feet deep. Waves are produced by a flap type generator driven by a 1/3 HP electric motor.

Fig. 3-1. OSU Wave Research Facility

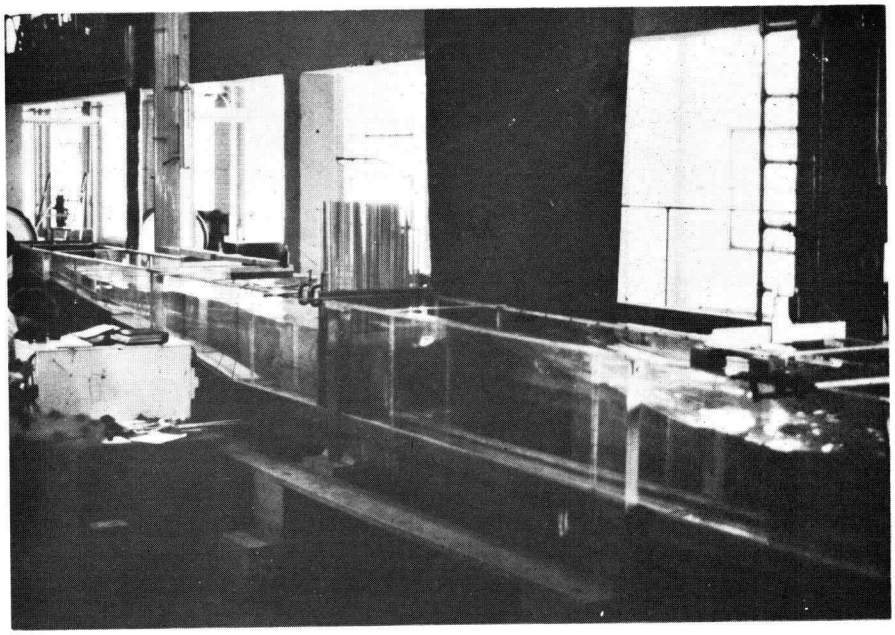

Fig. 3-2. Graf Hall Wave Channel

All tests were conducted using fresh water, thereby necessitating corrections for the density of salt water.

In order to bracket the design period, tests were planned at periods of 10.0 seconds, 13.5 seconds and 16.0 seconds. Ten seconds was chosen as a common design period used for the Atlantic Ocean. Unfortunately, when ten-second waves were scaled for the 1:20 test, a cross channel oscillation developed and the tests on all models were subsequently run at 9.0 seconds. To evaluate longer periods, 16 second waves were selected as the maximum period likely to reach breaking height.

The criteria used in the design of this breakwater was intended for application to a breakwater with uniform armor material. In such a design the highest wave and the deepest water usually present the most adverse conditions. In this breakwater, different armor sizes and placement techniques were used in different locations on the front face. To evaluate all possible stability conditions, namely failure caused by the erosion of A minus stone, tests were conducted at low water (40 feet) and mean water (50 feet) in addition to high water (60 feet).

To determine the no damage wave height, amplitudes were increased on successive runs until failure was observed or until additional increases caused waves to break before reaching the model. A standard exposure of 500 waves was adopted to provide a valid

comparison of damage results. In cases where damage was extensive, testing was terminated at the onset of damage to the under layers.

3.2 Test Procedure

Common procedures were followed on each run. After selecting the generator period and stroke, the wave generator was started. The waves were observed until runup appeared constant, usually 10 to 40 waves. All measurements were taken during this steady state condition.

Variations in the water surface elevation (from which wave heights were calculated) were measured by a Sonic Systems Model 85 Sonic Profiler. This instrument measures distance to the water surface by measuring the travel time for a sonic pulse to propagate to the surface and reflect back to the transducer. To profile the standing wave envelope, the device was moved along the tank and variations in distance were recorded on a Hewlett Packard Model 322 strip chart recorder. The profile was continued until at least two (generally three) nodes and antinodes were observed as shown in Fig. 2-2. In four of the 1:10 test runs, the wave antinodes exceeded the range of the sonic profiler. In these cases the maximums were observed by observation of the wetted profile of the envelope along the wall of the wave channel.

Runup and rundown were measured by reference to a grid placed on the tank wall. Measurements were taken to the nearest inch at the 1:10 and 1:20 scales and to the nearest 1/8 inch at the 1:100 scale. A photographic record of 35 mm still photos and 8 mm movies was made for each test run in the 1:10 and 1:20 scales and for selected tests in the 1:100 scale.

After measurements were taken, the wave machine was stopped (150-200 waves) and a visual inspection was made. Any damage observed at this point was noted and the test was continued to its conclusion. Any test that extended beyond 500 waves was stopped at multiples of 500 waves for inspection. After the completion of the test, the damage was assessed. This was done in two ways:

1. If little damage occurred (i.e. two or three A minus rocks dislodged to bottom of slope), the damage was assessed by counting the displaced rocks without removing the water from the tank.
2. If a large number of A minus rocks were displaced or if A select or A rocks were displaced, the tank was dewatered and the damage was photographed and all loose or displaced rocks were counted. In order to estimate the area of damage on the 1:10 and 1:20 scale test, a one-foot by one-foot wire grid was placed on the face of the breakwater. This grid provided a reference system for sketching the damage area on a data sheet

similar to the one shown in Fig. 3-3. A similar grid with a smaller grid size was used on the 1:100 scale.

After the maximum wave height was generated at any frequency and water depth, the tank was dewatered and the armor layer inspected. Repairs were then made and the next run started.

3.3 1:20 Scale Model

The 1:20 scale model was tested first. It was intended primarily as a stability test with the results to provide an improved testing program for the other models as well as comparisons for scale effects. Model photographs and analysis of the stone sizes are included in Appendices A and B. A total of 43 test runs was made consisting primarily of the most severe conditions attainable.

Initially the breakwater was fronted by long, flat beach shown by the dashed contour in Fig. 3-4 and the photograph in Fig. 3-5. This configuration (hereafter referred to as the flat bottom configuration) was found to be unsatisfactory except for small waves. Wave energy reflected from the model superimposed with the incident wave creating a breaking condition and limited incident wave height to 27 feet. In order to increase the wave height at the breakwater, a slope of 1 on 12 was installed adjacent to the structure (Figs. 3-4 and 3-6). This sloped bottom configuration exposed the breakwater to the full force of the steep but unbroken wave. The sloped bottom created

BREAKWATER DAMAGE RECORD SHEET

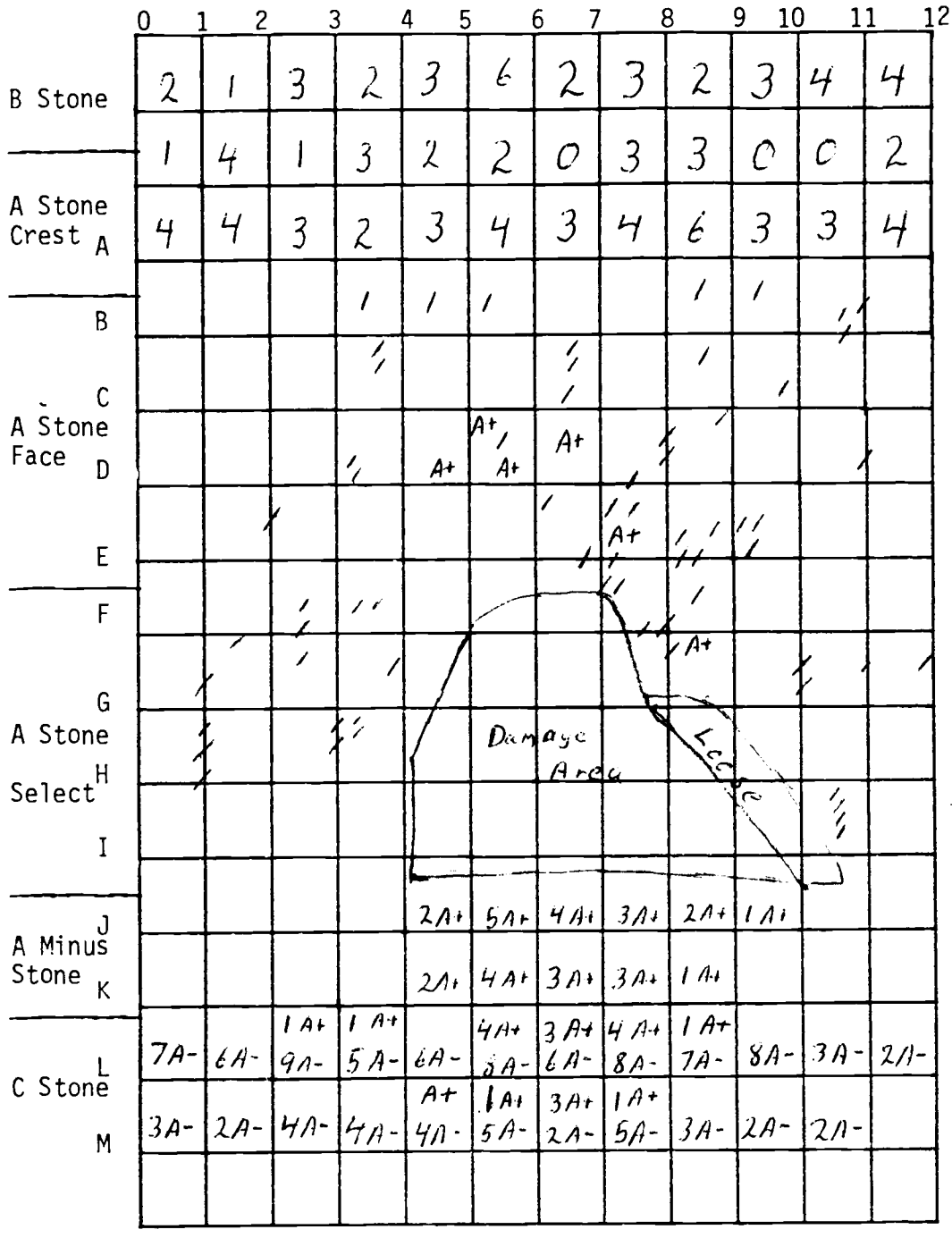

Fig. 3-3. Breakwater Damage Record Sheet

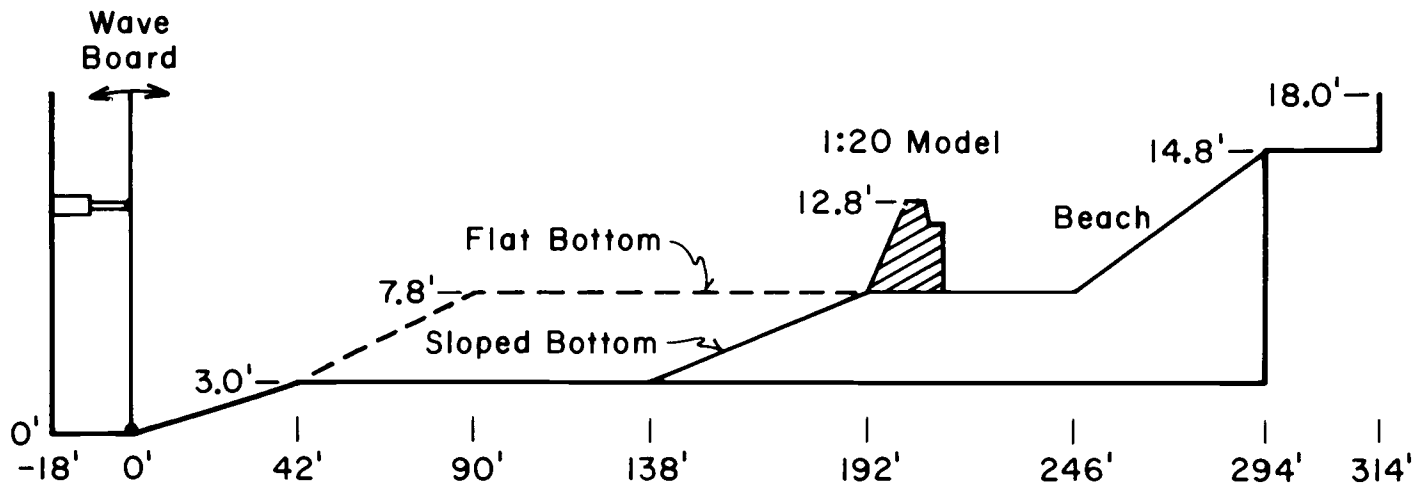

Fig. 3-4. 1:20 Scale Model Bottom Configurations

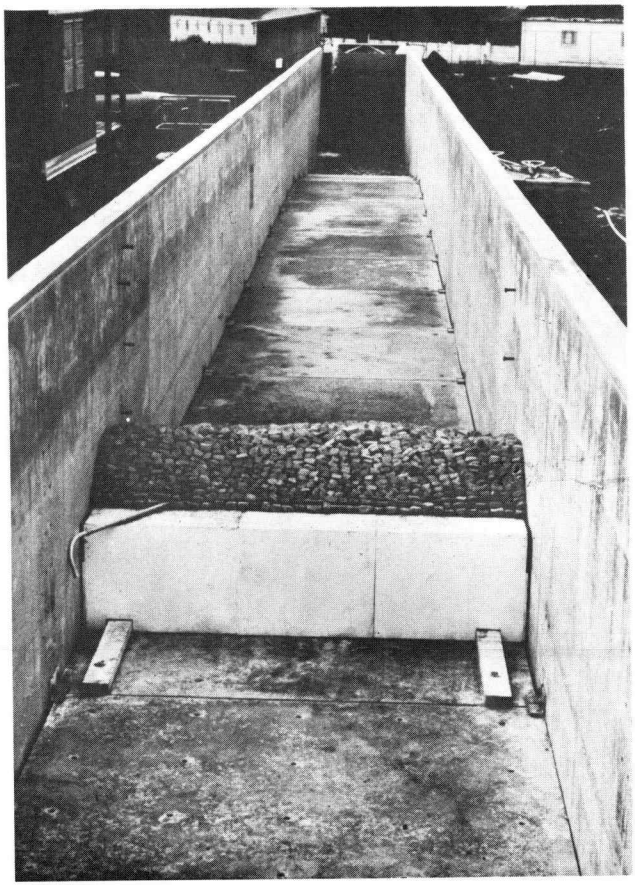

Fig. 3-5. 1:20 Scale Model, Flat Bottom Configuration

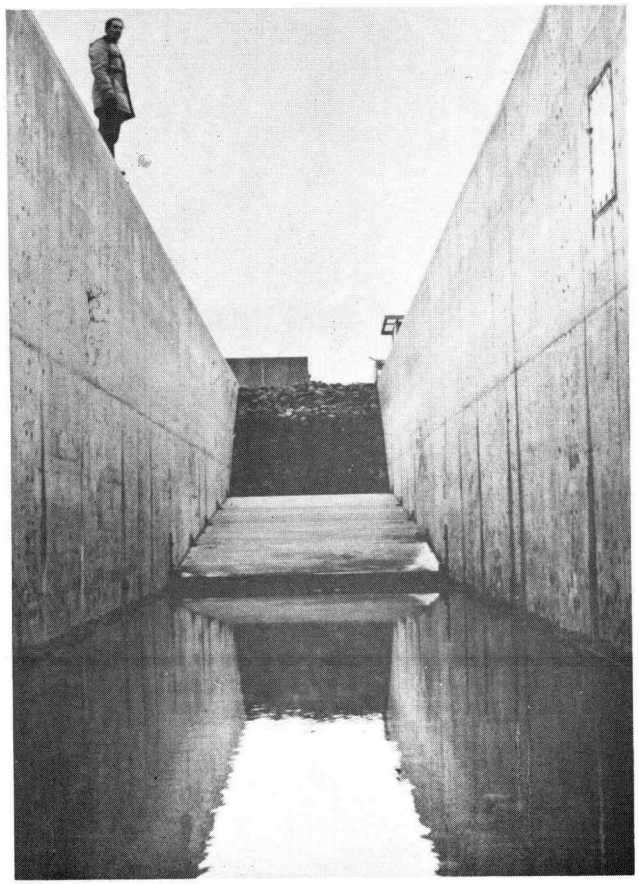

Fig. 3-6. 1:10 Scale Model, Sloped Bottom Configuration

conditions more severe than those associated with gradual slopes common to the sea floor. Testing using both flat and sloped bottoms continued through all of the experiments. Wave height measurements for the sloped bottom were taken from the deeper, flat section fronting the slope. Incident wave heights were calculated by the linear wave theory shoaling technique discussed in Chapter II.

Early in the testing overtopping waves caused failure to the backface of the breakwater. In order to more fully evaluate stability of the frontface, the design was altered by extending the layer of B minus stone onto the backface and replacing the B stone layer with A stone. An intermediate armor layer of B minus stone extending over the backside was also used in the 1:10 and 1:100 models. However, A stone was not placed on the backface of either the 1:10 or 1:100 models.

Two tests were conducted at periods other than 9.0, 13.5 and 16.0 seconds. An 11.2-second wave 40.7 feet high was applied as the wave of maximum height that caused breaking at the interface of the A minus and A select stones. A wave of 18 seconds 48 feet high was applied to test the effect of unusually long waves.

3.4 1:10 Scale Model

The results of the 1:20 scale tests indicated a need for more extensive testing. The 1:10 model (Figs. 3-6 and 3-7) was therefore

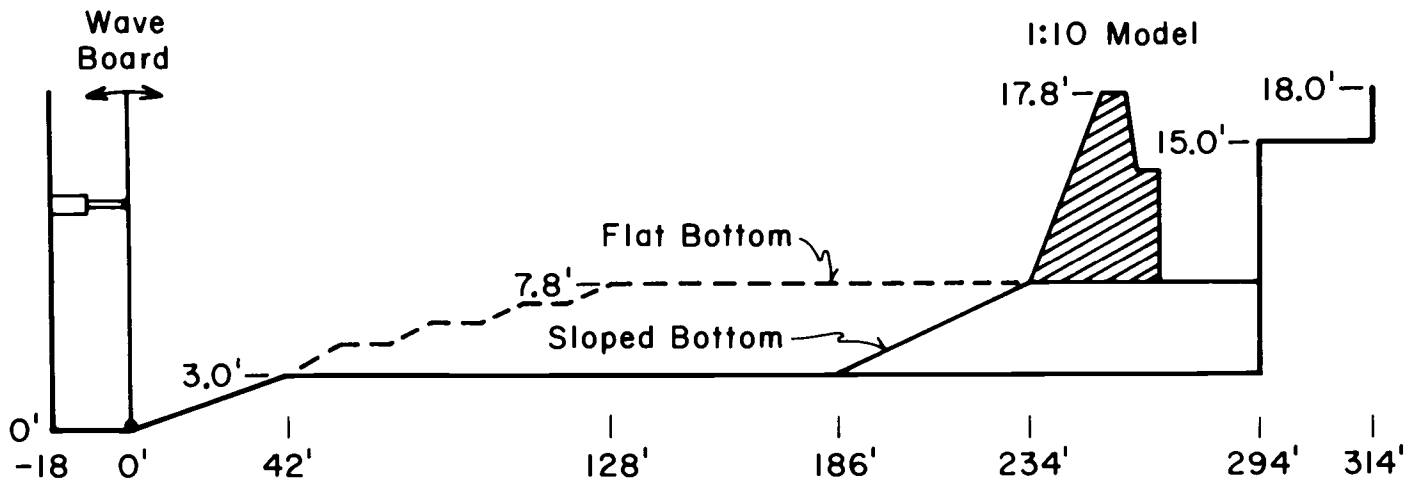

Fig. 3-7. 1:10 Scale Model Bottom Configurations

to 118 test conditions. The additional tests were of two types: 1) relatively small waves to provide more complete runup data and reflection values for non-overtopping conditions; and 2) long duration high wave tests to evaluate the ability to withstand storm conditions.

The flat bottom configuration shown in Fig. 3-7 was utilized in the 1:10 scale test. A more gradual slope was attempted to reduce the interaction of the incident and reflected waves. Again, however, breaking in the shoal section limited the attainable wave height dictating a change to a sloping bottom. The small transmitted wave observed in the 1:20 scale tests allowed relocation of the model near the end of the tank and elimination of the sloping beach.

The most common method for reporting relative runup is to plot it versus some form of wave steepness (H_i/λ, H_o/λ_o, H_o/T^2). The sensitivity of runup, rundown and reflection to wave height and wave length may provide important information to future designs. To provide the additional data needed to evaluate the effect of wave period, several tests were added. Waves equal to one-third of the water depth were tested at several different wave periods (9.0, 10.0, 11.0, 12.0, 13.0, 14.0, 15.0, 16.0 seconds) and at all water depths. Waves equivalent to a 25 foot design wave were also tested at the above period and all water depths.

The 1:10 scale model was found to be very stable and in fact no apparent damage was caused to the A select or A section by any of

the waves tested for durations of 500 waves. To more completely evaluate the ability of the breakwater to withstand long term exposure, five long duration tests were conducted. In one test the model was exposed to a prototype 24 hour storm of 48 foot high 14 second waves. The four other long duration tests were made with a continuous rising water level to simulate a rising tide. The test duration was three hours (9.4 hours in prototype), 30 minutes exposure at low water, two hours of rising water level and 30 minutes at high water. Wave heights were maintained near the maximum. Three tests were conducted at periods of 13 to 14 seconds and one was conducted at periods of 15 to 16.5 seconds.

Since none of the long duration tests caused serious damage to the model, it was necessary to partially dismantle the armor layer to demonstrate random assembly. A section approximately one yard square was removed at the interface between the A select and A stones. The section was reassembled and exposed to the more severe waves with no serious damage.

3.5 1:100 Scale Model

The 1:100 scale testing was designed as a 1:10 replica of the 1:10 model (Fig. 3-7). All lengths except tank width were scaled including distance from the wave board to the model and depth of water in all portions of the tank. A total of 237 wave conditions was tested.

Approximately one-half were tested in the flat bottom condition previously described. This large number of tests was conducted in order to provide an indication of the effect of the sloped bottom. Wave heights from 2.5 feet to the maximum attainable at 9.0, 13.5, and 16.0 second periods were applied to the breakwater. In none of the flat bottom testing was appreciable damage done to the breakwater. On several occasions in the sloped bottom configuration, the front face was severely damaged requiring extensive reconstruction. On three cases the back face sustained severe damage and was rebuilt. Reconstruction did not increase or decrease the integrity of the structure. In some cases, repaired areas remained intact while others failed; in other cases the repaired area failed on consecutive tests. No trend toward regional failure was observed and no wall failures were observed. In short, the damage observed was random in nature.

CHAPTER IV

EVALUATION OF RESULTS

4.1 Introduction

The results of this investigation may be separated into three areas: wave response, structure response and modeling effects. The wave characteristics studied are runup, rundown and reflection; the structural response is evaluated in terms of damage. Each response is analyzed for the individual model and is then compared for the effects of scale and bottom slope.

The wave characteristics are depicted graphically using dimensionless variables. Wave steepness is the most universally applied independent variable in studying runup, rundown and reflection. The deep water form, H_o/T^2, which is proportional to H_o/λ_o, is used in this analysis. Similarly most authors normalize runup and rundown by dividing by wave height. In keeping with the selection of deep water characteristics for the independent variable, the deep water wave height is used in this study. Thus relative runup, R_u/H_o, and relative rundown, R_d/H_o, are used as dependent variables. Reflection coefficients, C_r, however, are evaluated relative to local wave heights. In each case a line depicting a polynomial data fit based on a least squares analysis is plotted. These lines provide a

comparison with the results of previous investigations and allow numerical comparison to determine model effects. A numerical value for scale and bottom effects is developed by taking the percentage difference of the dependent variable (R_u/H_o, R_d/H_o or C_r) for models being compared. By averaging these differences for several values of H_o/T^2 (independent variable) a mean effect is established.

As described previously, breakwater damage is analyzed using the methods of Paul and Baird (36) and Thomsen et al. (44). The results of this analysis is interpreted in terms of Hudson's stability coefficient, K_D, and compared to other shapes. Scale effects are measured by comparing values of K_D and of Thomsen's zero stability coefficient. Since no waves large enough to cause appreciable damage were achieved during the flat bottom tests, the effect of bottom slope on stability is not quantitatively evaluated.

4.2 Runup

Runup is an important measure of a structure's ability to dissipate wave energy. As previously mentioned, some authors have advanced the idea that damage should be correlated with runup. More importantly, runup provides an indication of the crest or berm height necessary to prevent overtopping.

The variables most commonly discussed as affecting runup are wave height, breakwater porosity, face slope, wave length and

water depth. When presenting runup data in the form of dimensionless plots, it is generally accepted that the wave parameters be used as the independent variables with other variables identified as isolines. The most widely encountered presentation of runup data is a plot using deepwater wave steepness (H_o/λ_o or H_o/T^2) as the independent variable and relative runup (R_u/H_o) as the dependent variable.

While other investigations, previously discussed, have studied the effects of slope and porosity, this study is solely concerned with the effects of period, depth, and height. However, since porosity and slope are significant structural parameters and the design being studied is unique, it is necessary to view the results in comparison with breakwaters of similar slope and facing material. Fig. 4-1 illustrates runup plots for studies similar to this study (45). Line A shows runup on a smooth plate for a slope of 1:2 waves with $d/H_o > 3.0$. Line B shows runup on an impermeable graded riprap slope of 1:2 for waves of $d/H_o > 3.0$ and line C shows runup on a permeable riprap slope of 1:2 for waves with $d/H_o > 3.0$. Since the placed stone slope is less permeable and smoother than a random placed but more permeable than an impervious slope, these lines may be considered to form the bounds of expected runup. Lines B and C will, therefore, be used as a basis of comparison for this study and will be plotted on each graph of R_u/H_o versus H_o/T^2.

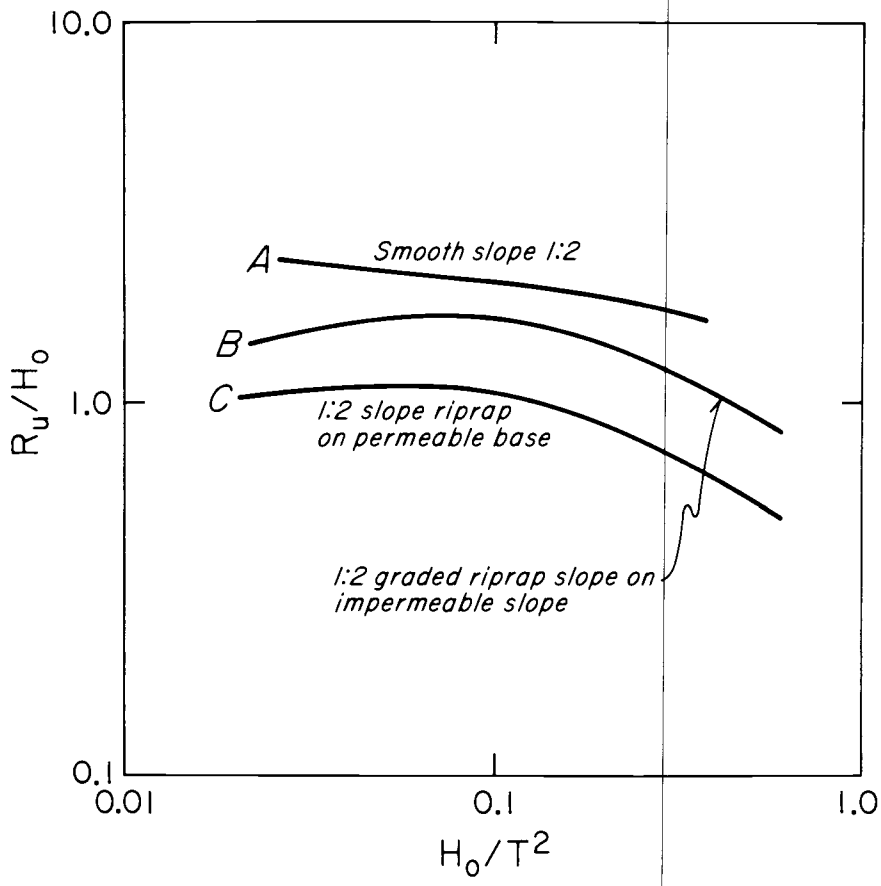

Fig. 4-1. Relative Runup on Similar Surfaces

The anticipated response of runup to variations in period, depth and steepness is shown in Fig. 4-2 and is the result of the following interpretations:

For a given H_o, R_u increases as:

1. Period increases because shoaling is greater in longer waves.
2. Depth decreases, because shallower water increases wave asymmetry, increasing the crest height above the water-line and thereby increasing runup. It is unlikely that depth effects will be discernible since, at the larger depth, runup values for larger waves are curtailed by overtopping.
3. Wave steepness decreases, because steep waves dissipate more energy due to friction and breaking on the breakwater slope. A relative maximum is reached since at some intermediate steepness wave asymmetry increases without appreciably increasing losses on the face of the breakwater.

As described previously, runup was measured utilizing a grid on the wall of the wave channel. This measurement was hampered by splashing and by nonuniform advance of the water. The values of runup used in developing the following discussions and plots represent the average highest vertical rise of the intact portion of the wave over the majority of the slope.

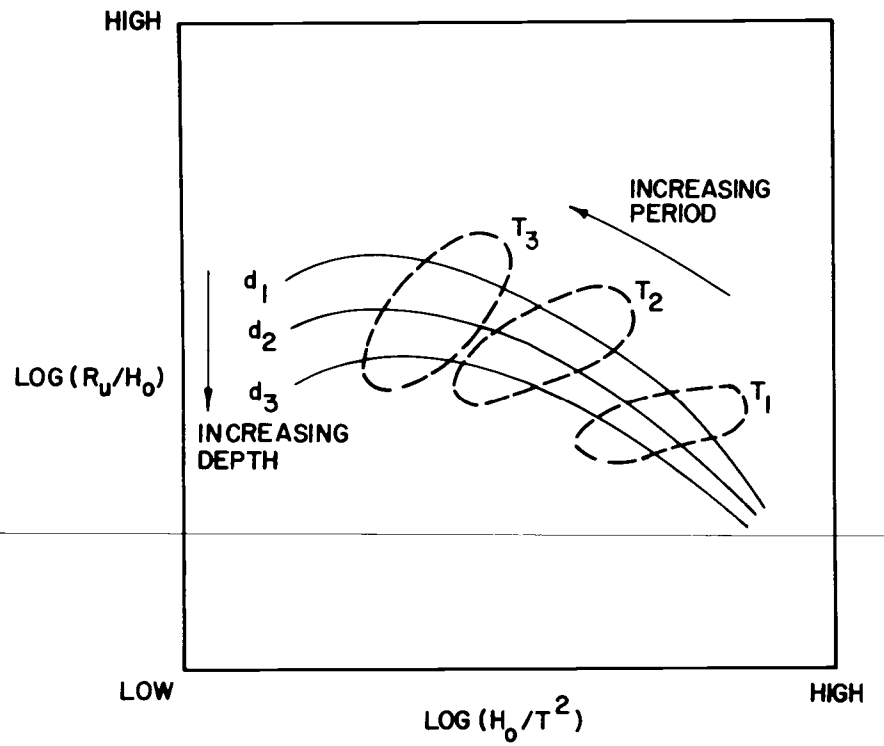

Fig. 4-2. Hypothesized Behavior of Relative Runup

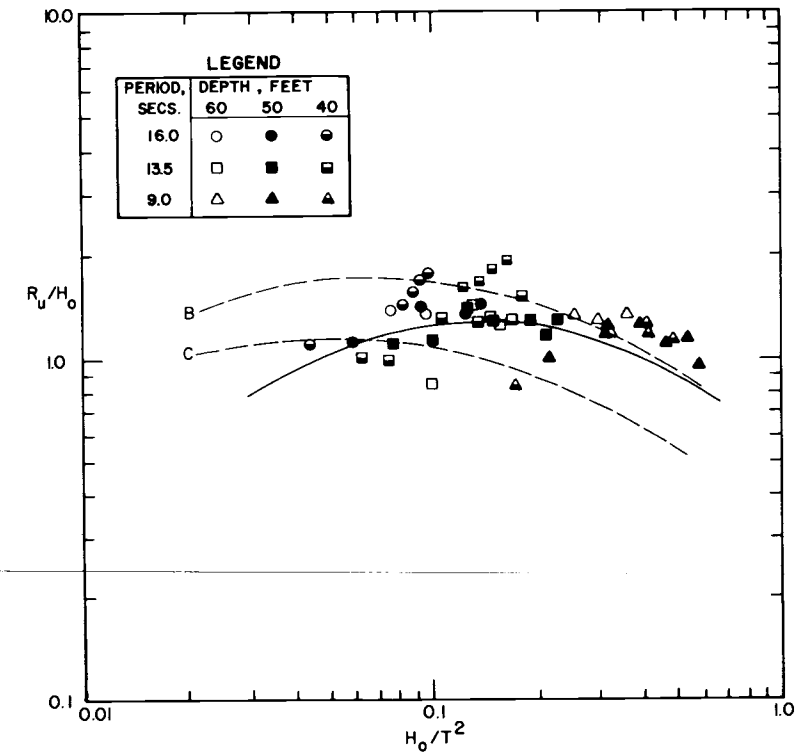

Figure 4-3. Relative Runup Versus Deep Water Wave Steepness, 1:10 Scale Model

Fig. 4-3 shows a composite of relative runup versus deep-water steepness in the 1:10 model for all waves recording runup (non-overtopping). This graph exhibits good correlation with previous data; runup increases to a maximum and then drops off as breaking increases. Although the data are skewed towards shorter periods at high steepness it is apparent that where overlap does occur the shorter waves yield less runup at the same steepness. Therefore wave period, T, as well as H_o/T^2 is important.

Fig. 4-4 illustrates data taken in the 1:20 tests. This composite of all data is somewhat higher than the 1:10 test data but shows good correlation along the upper boundary. Stability analysis of overtopping waves was the primary effort at the 1:20 scale, hence there are insufficient runup data points to warrant analysis of the individual frequencies. However, the same basic wave period trends displayed at 1:10 scale are apparent at 1:20 scale.

Fig. 4-5 shows the data taken in the 1:100 tests with the sloped bottom. The plot shows runup to be less than at the larger scales but in reasonable agreement with the lower bound. The individual frequencies show a marked separation in the peak of relative runup. This displacement of the peak for shorter waves indicates that period is an important consideration in runup.

Fig. 4-6 illustrates the data for the 1:100 test with the flat bottom configuration. Considerable low scatter exists with a

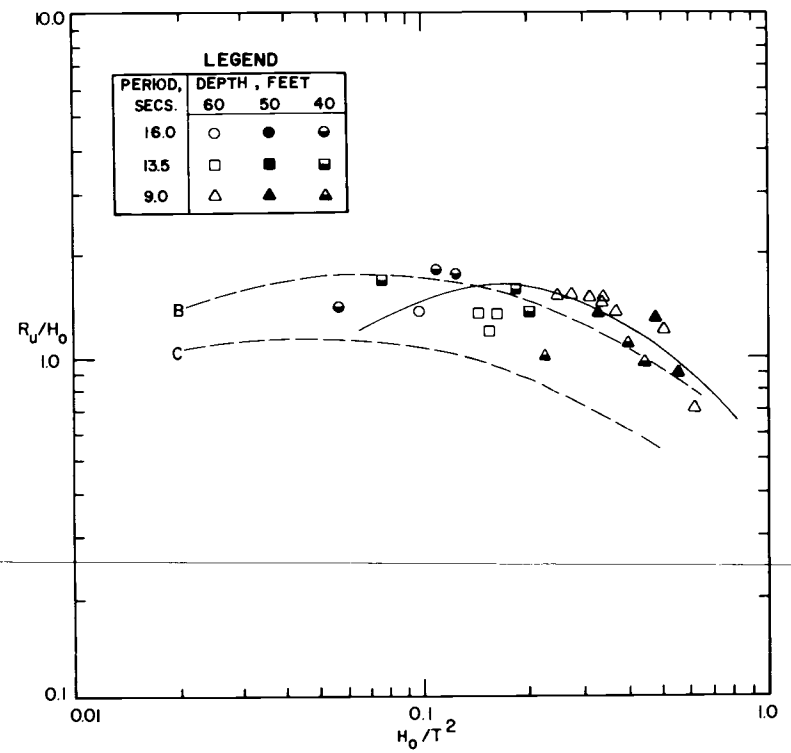

Fig. 4-4. Relative Runup Versus Deep Water Wave Steepness, 1:20 Scale Model

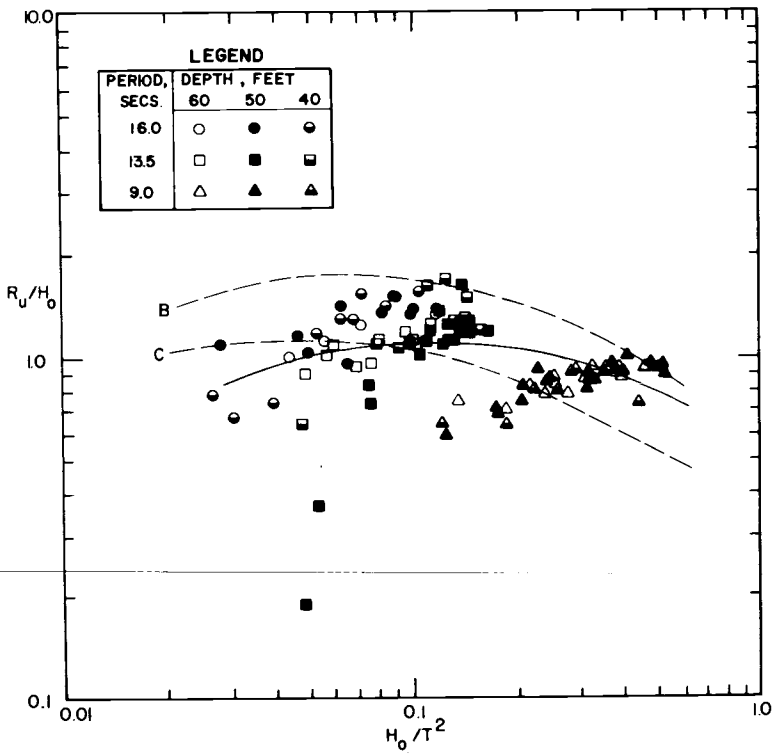

Fig. 4-5. Relative Runup Versus Deep Water Wave Steepness, 1:100 Scale Model, Sloped Bottom Configuration

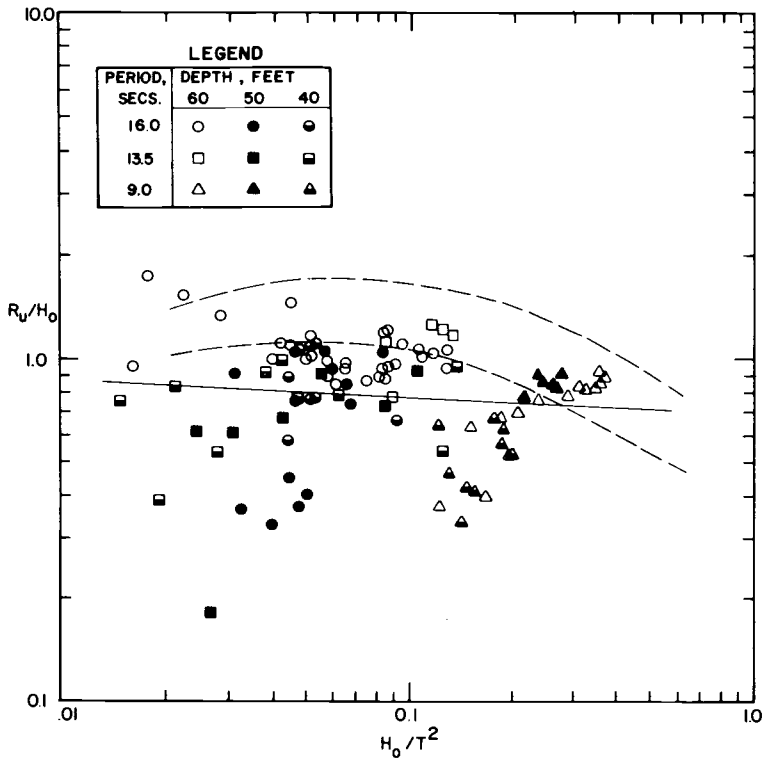

Fig. 4-6. Relative Runup Versus Deep Water Wave Steepness, 1:100 Scale Model, Flat Bottom Configuration

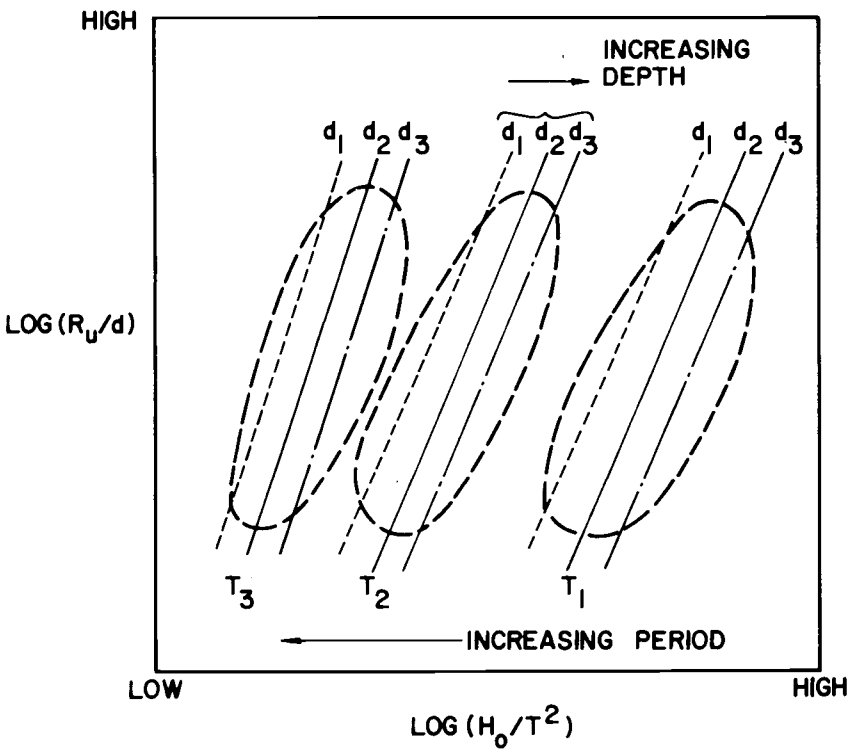

Fig. 4-7. Hypothesized Behavior of Runup Divided by Depth Versus Deep Water Wave Steepness

majority of the points falling below the range of the previous data. The best fit line is well below that of the sloped bottom noted for the waves with nine second periods. The distribution of the nine second data clearly indicates a period dependence beyond that of steepness, e.g., shorter periods produce less relative runup at a given steepness. To further investigate this effect, the data were replotted using other dimensionless combinations. The most descriptive of these was R_u/d versus H_o/T^2.

R_u/d tends to expand the scale of the runup data compared to R_u/H_o because as H_o increases, R_u increases, retaining a near constant value of R_u/H_o whereas decreasing depth results in increasing runup thereby amplifying the value of R_u/d. This amplification of data increases the separation of wave period. Fig. 4-7 depicts the expected behavior for the plot of R_u/d versus H_o/T^2. Increased values of T^2/d cause increased shoaling, increasing wave crest height, thereby increasing runup. Similarly, increasing values of H/d are related to increasing values of crest height, thus causing increased runup.

In plotting values, it is not necessary to plot isolines of T^2/d and H/d because one set of isolines uniquely defines each point. Since the close correlation between wave height and runup has been long established, the data in Figs. 4-8 through 4-11 have been plotted to identify values of T and D.

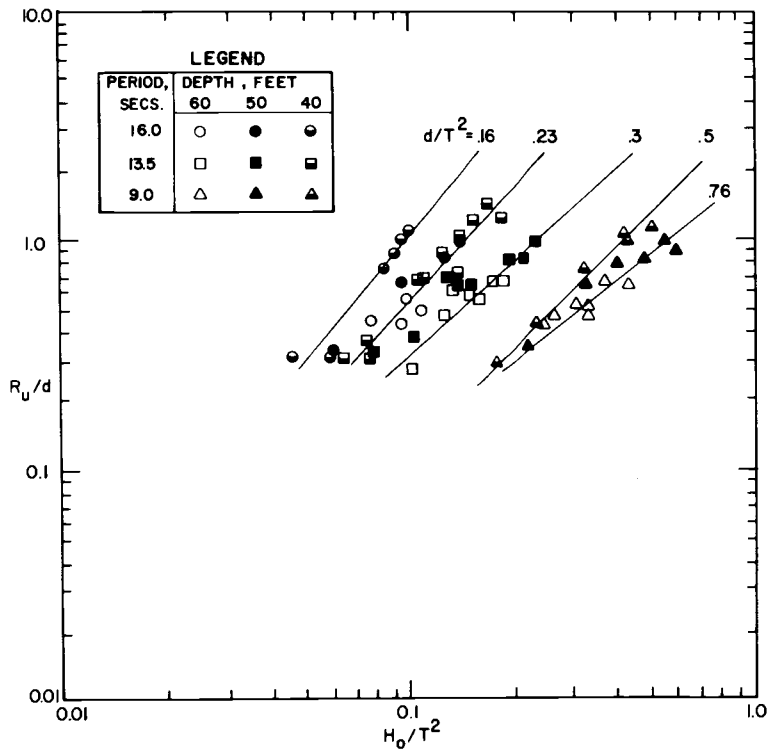

Fig. 4-8. Runup Divided by Depth Versus Deep Water Wave Steepness, 1:10 Scale Model

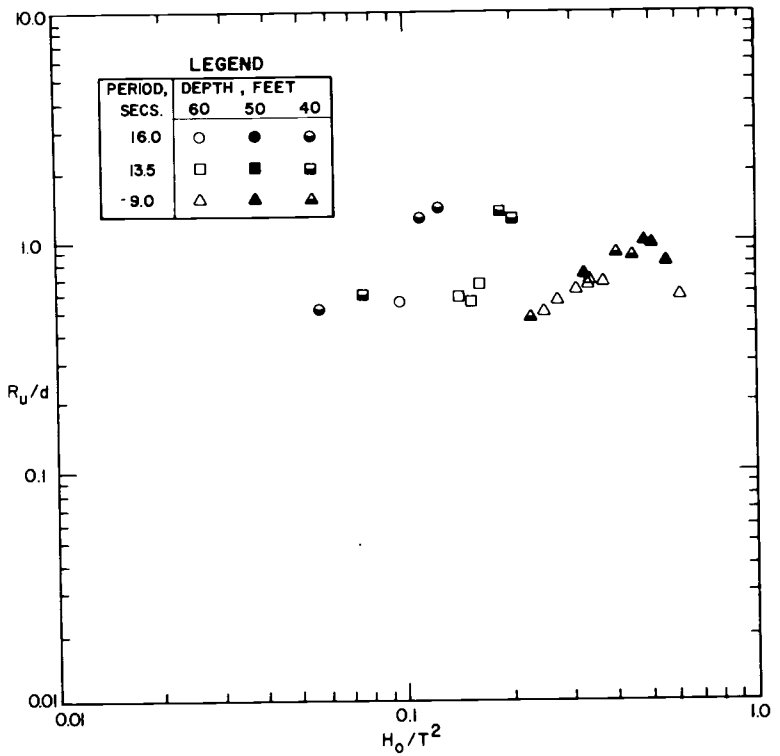

Fig. 4-9. Runup Divided by Depth Versus Deep Water Wave Steepness, 1:20 Scale Model

Fig. 4-8 shows a composite plot of all data taken in the 1:10 scale model. The separation of the nine second waves is readily apparent. Separation of the 13.5 and 16 second wave is not as well defined since T^2/d is .22 for a 13.5 second wave in 40 feet of water and .23 for a 16 second wave in 60 feet of water. Variations in runup due to depth can also be seen although the effect is less than that of period.

Fig. 4-9 shows data for the 1:20 test. As described previously, the 1:20 test was undertaken as a stability test and provides only limited runup data. Separation of the data by period is observable and shows good agreement with the 1:10 data.

Fig. 4-10 illustrates the runup data taken in the 1:100 scale model with the flat bottom installed. The nine second waves once again clearly separate from the longer waves and show some sorting with depth. The longer wave lengths are distinguishable, probably due to the effect of the bottom on the length of the wave. Although the waves tested do not coincide exactly with those in the 1:10 test, reasonable agreement is apparent.

The 1:100 sloped bottom test data shown in Fig. 4-11 display the best separation both in period and depth. Excellent agreement with anticipated results and other scales can be seen.

The use of this type plot provides advantages over the traditional single line plot of R_u/H_o versus H_o/T^2. It maps the total runup

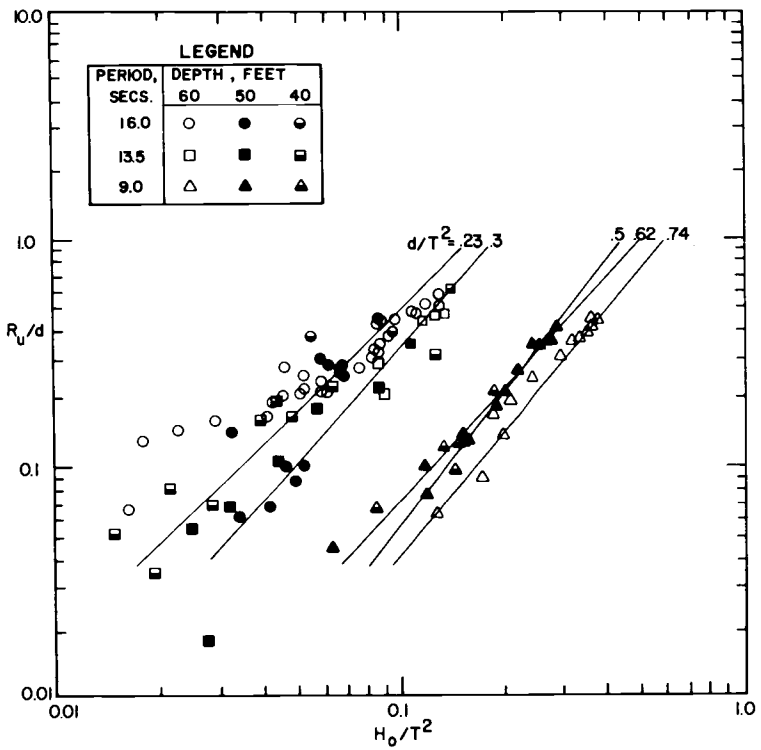

Fig. 4-10. Runup Divided by Depth Versus Deep Water Wave Steepness, 1:100 Scale Model, Flat Bottom Configuration

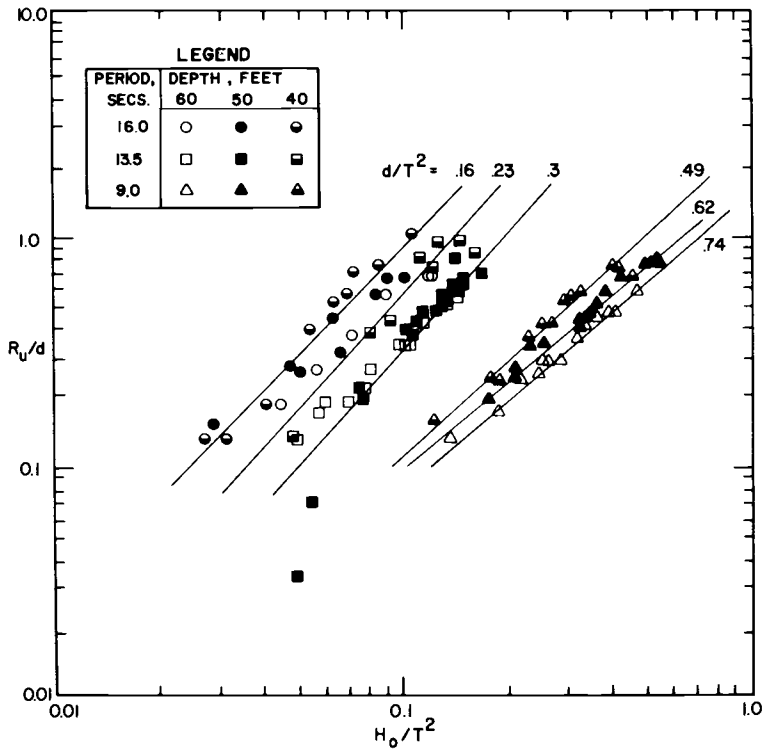

Fig. 4-11. Runup Divided by Depth Versus Deep Water Wave Steepness, 1:100 Scale Model, Sloped Bottom Configuration

behavior. With a complete set of T^2/d isolines, a design may be tested for sensitivity to depth, period, and wave height. The separation of period effects should also improve the interpretation of runup spectra from wave height spectra.

A plot with isolines also provides an improved tool for evaluating the effects of bottom slope and scale. The observed variations in runup with period and depth will cause any R_u/H_o versus H_o/T^2 best fit line to be dependent on the distribution of the samples taken. Thus variations due to depth and period might be mistakenly interpreted as scale or bottom effects.

The effect of bottom slope is most apparent from a comparison of the 1:100 model data for sloped and flat bottoms, Figs. 4-5 and 4-6. The best fit line for the flat bottom configurations averages 16.8% less than the sloped bottom configuration. This value is in agreement with the reductions in runup observed by Saville (40) and Nagai (33). If, however, the effect of bottom slope is interpreted using plots of R_u/d versus H_o/T^2 (Figs. 4-10 and 4-11) and comparing equal values of T^2/d, the variations are considerably different. At T^2/d equal to 0.27 (13.5 second wave in 50 feet of water) the variation averages 9.4% less in the flat bottom case and for all values of T^2/d, the flat bottom case averages 6.8% less than the sloped bottom case. This value is much less than that previously derived and is only slightly greater than the accuracy of the measurements taken.

This indicates that by simplifying runup to a single line plot, previous works may have overestimated the effect of bottom slope.

In order to evaluate scale effects, the data were analyzed in the same manner as for the effect of bottom slope. Since only a limited number of runup values was taken in the 1:20 test and since the 1:10 test was conducted primarily with a sloped bottom, the best comparison available for scale effects on runup is between the 1:10 scale and the 1:100 scale sloped bottom. A visual comparison of Figs. 4-3 and 4-4, however, does indicate that very little difference exists between the 1:10 and 1:20 data. Comparison of the 1:100 and 1:10 data shows a reduction of 17.7% in R_u/H_o and reduction of 10.8% in R_u/d in the 1:100 model. Both numbers are in reasonable agreement with the 13% reduction predicted by the Shore Protection Manual (46) but the difference indicates that neglecting the effects of depth and period can cause an overestimation of scale effects.

4.3 Rundown

While the reporting of runup when testing rubble-mound stability is common practice, the reporting of rundown, though not unprecedented, is rare. Hudson and Jackson (21) provide the most complete treatment of the subject. The placed stone construction technique of the breakwater studied in this research dictates the need to consider rundown. The lower reaches of the armor layer are of

smaller randomly placed stones. This creates a potentially weak region when exposed to waves with excessive rundown and may allow rundown failures as described by Svee (42). A progressive failure of this type in the A minus rock could eventually cause the structure to fail.

The measurement of rundown is complicated in much the same way as runup. During the entire duration of rundown, water flows out of the breakwater, tending to obscure a well defined maximum rundown point. In addition, the leading edge of the oncoming wave changes shape with wave steepness, e.g. the leading edge of a plunging wave appears markedly different from a non-breaking wave. Fig. 4-12 shows two different cases of rundown illustrating this difficulty. The value of rundown used in this study represents the greatest vertical distance below the mean water level attained by the leading edge of the oncoming wave. This point is somewhat subjective and is considered to be accurate to within 10%.

Anticipated rundown behavior is quite different from that of runup. The most notable difference is that variation in depth causes an opposite reaction in rundown compared to runup. This is the result of finite amplitude effects on the wave profile. The decreased trough amplitude reduces the maximum amount to which the water might descend, thereby reducing rundown. Similarly a higher wave traveling in relatively shallow water will tend to distort

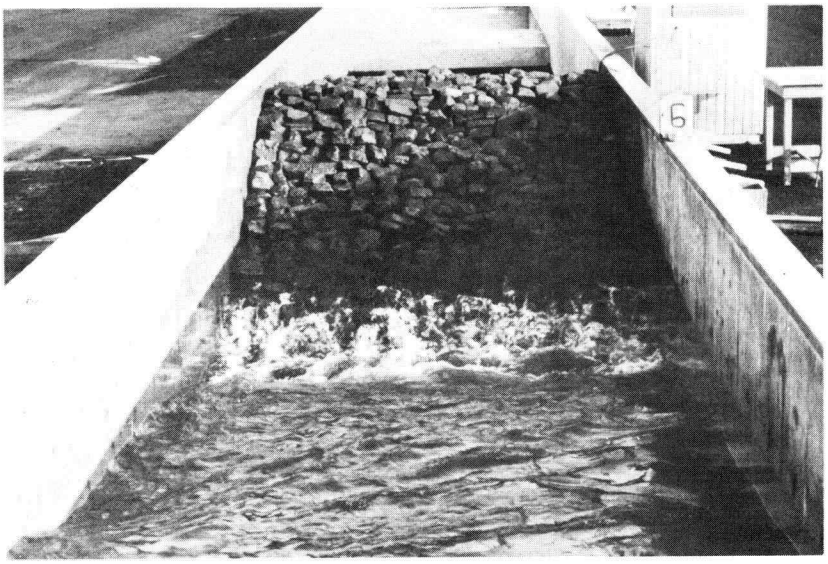

a) Non-breaking

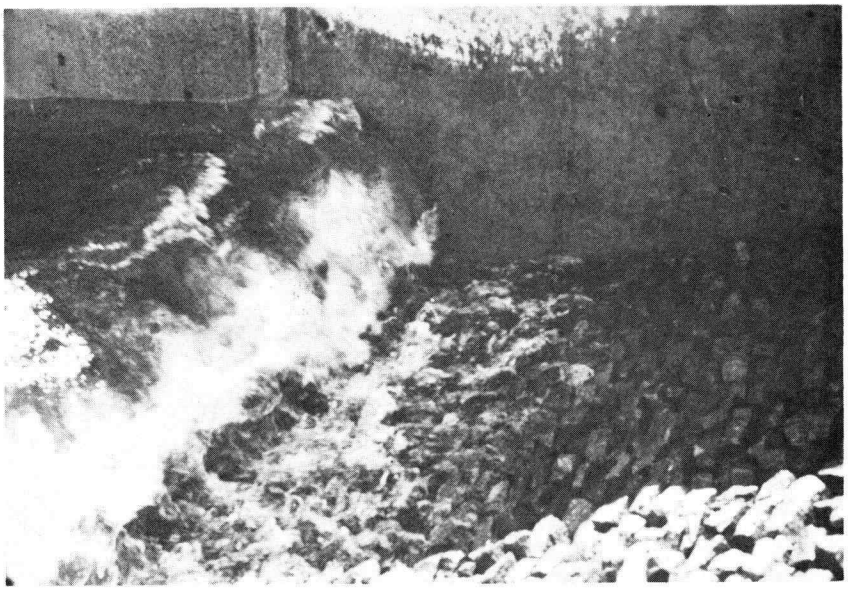

b) Breaking

Fig. 4-12. Rundown Profiles

the wave trough further, hence relative rundown decreases despite an increase in absolute rundown. The effect of period is more confusing. Increasing period does increase trough amplitude for a given height of wave and the lengthened period allows rundown to fully develop.

For a given wave height, the trough amplitude will increase with: 1) increasing depth; (2) increasing period; and (3) decreasing wave steepness due to finite amplitude effects. It is anticipated that rundown responds similarly, as indicated in Fig. 4-13.

Fig. 4-14 shows data from the 1:10 scale model with Hudson and Jackson's results for a 1:2 graded riprap slope plotted as a dashed line. The shape of a second degree polynomial fit, shown by the solid line, is similar to Hudson and Jackson's result, but averages only 50% of the previous findings. This is, to some extent, predictable since Hudson and Jackson's data were for $d/H < 3$. A distinct increase in rundown with depth is apparent through the data. The variation of rundown with period is somewhat obscured by the data scatter and by the lack of comparative steepnesses.

Fig. 4-15 shows the result of the 1:20 scale model to be considerably greater than the 1:10 model data and in better agreement with previous data. Variations with depth and period are obscured as only waves of high steepness were measured.

Figs. 4-16 and 4-17 illustrate the data taken in the 1:100 scale models in the flat and sloped bottom configurations. Both the sloped

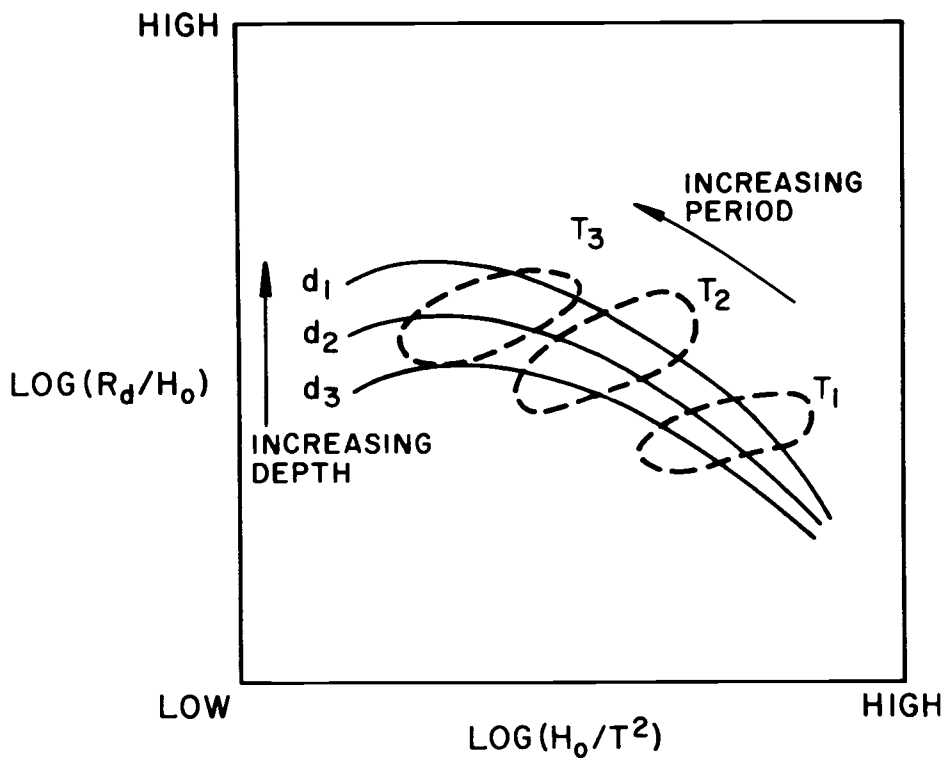

Fig. 4-13. Hypothesized Behavior of Relative Rundown

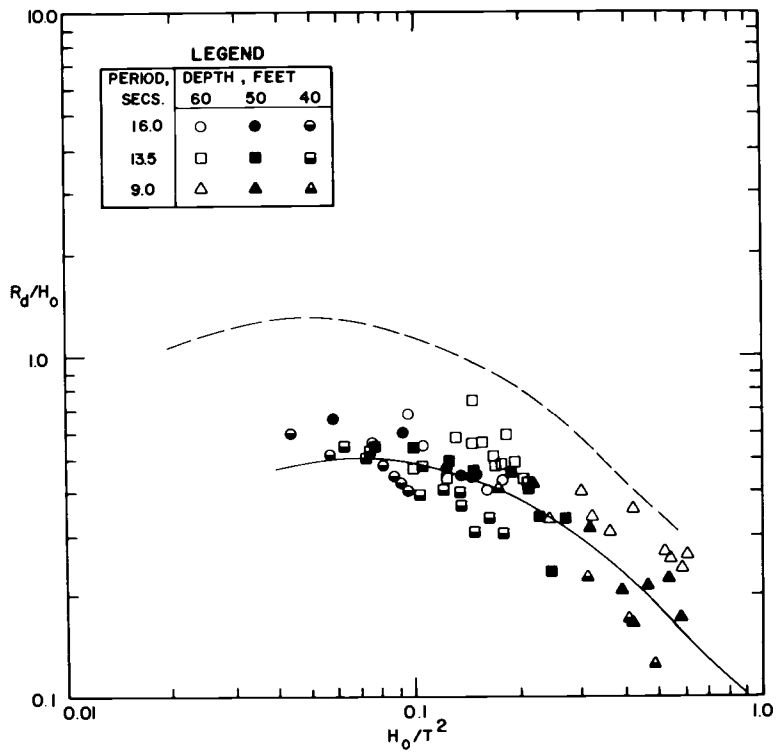

Fig. 4-14. Relative Rundown Versus Deep Water Wave Steepness, 1:10 Scale Model

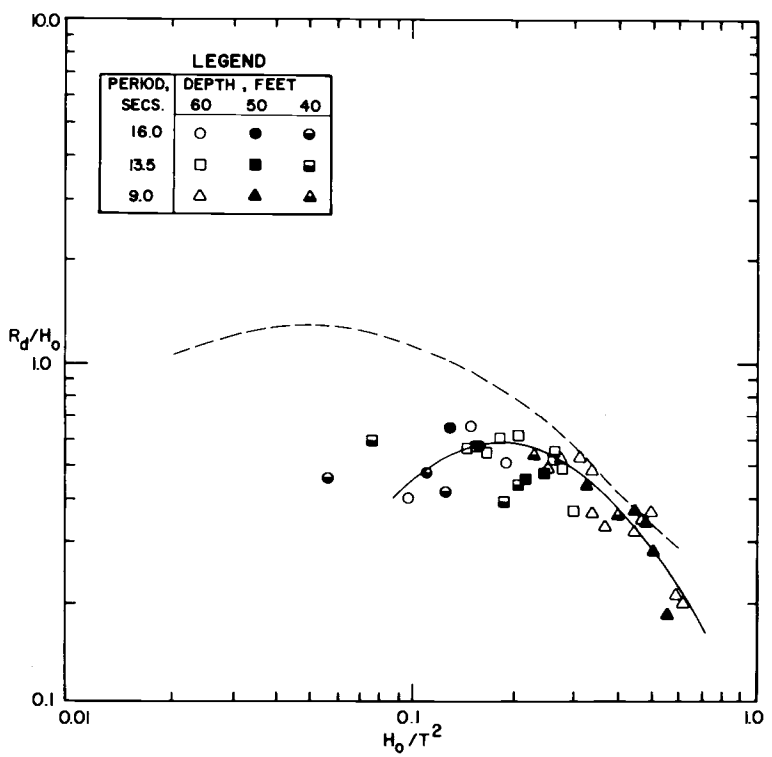

Fig. 4-15. Relative Rundown Versus Deep Water Wave Steepness, 1:20 Scale Model

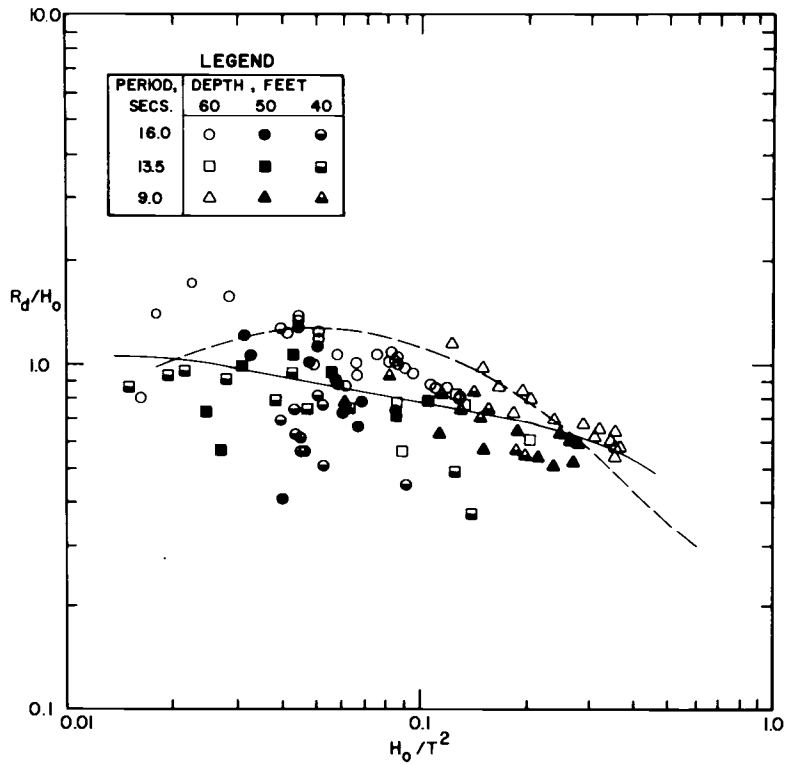

Fig. 4-16. Relative Rundown Versus Deep Water Wave Steepness, 1:100 Scale Model, Flat Bottom Configuration

and flat bottom data agree fairly closely with the 1:20 data. These results cover a greater range of steepness than the other scale models and show the best agreement with previous data although considerably lower. A grouping of data by depth, as hypothesized in Fig. 4-13, is obvious at the two extremes of steepness but is indistinct when $0.1 < H_o/T^2 < 0.2$.

As with the runup data, several other combinations of dimensionless variables were plotted for rundown. No combination provided any improvement on these interpretations.

The comparison of data to determine scale effects and bottom slopes was conducted in a manner identical to that for runup. Comparison of Figs. 4-16 and 4-17 clearly indicates that the effect of bottom slope is extremely small. Except in the steeper waves, the 1:100 scale sloped and flat bottom lines are coincidental and the effect in the 1:10 model is only slightly greater. By selecting ten values for H_o/T^2 and averaging the percentage difference, the 1:100 flat bottom data proved to be 6.9% larger, well below the accuracy of the measurement. The variation between the 1:10 sloped and flat bottom data was greater, 7.9%.

The rundown observed in the 1:10 model was substantially less than either the 1:20 or 1:100 models. Calculating in the same manner as for bottom effects, rundown in the 1:100 test was found to be

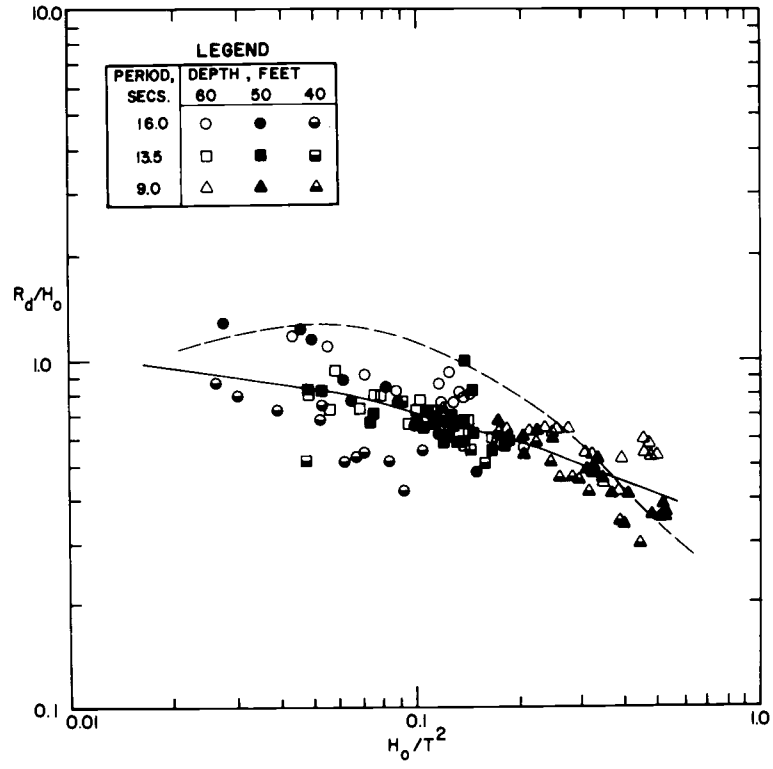

Fig. 4-17. Relative Rundown Versus Deep Water Wave Steepness, 1:100 Scale Model, Sloped Bottom

69.7% larger than the 1:10 test and rundown in the 1:20 test was 64% larger.

It is clear that the measured rundown behavior with regard to scale is opposite to that of runup. In addition, rundown scale effects are much greater than runup effects even when restated in terms of the smaller scale model. (Rundown in the 1:10 model was 41% less than the 1:100 model and 39% less than the 1:20 model.) This response can be explained in terms of the cyclic behavior of runup and rundown. Each event repeats once each wave period so that if a greater portion of a period is required for runup, then less time will be available for rundown before the next runup cycle begins. In large models, relative runup is increased and a greater fraction of the wave period is required for maximum runup to be attained. A reduced fraction of the wave period remains for rundown, hence, maximum rundown is reduced in large models. Conversely, small models take less time for reduced runup so more time is available to yield increased rundown. The scale effect is accentuated in rundown, since rundown is a smaller value.

4.4 Reflection Coefficient

In the past, wave reflection characteristics have had little impact on breakwater design. Design waves for breakwater stability have generally been selected independent of reflection since this

provides a conservative estimate for breaking wave heights. However, wave reflection often causes incident waves to break prematurely, thereby providing some degree of protection to the reflecting structure. Also, reflected wave activity on the seaward side of a breakwater establishes sediment shoaling patterns and makes ship navigation more difficult at the entrance to jetty protected inlets.

Previous investigations of wave reflection have been concerned primarily with the validation of analytical models. Investigations into the effects of slope, permeability, wave height and period have been limited. Comparisons with previous studies were not undertaken since no common standard has been established. Deep water wave steepness was once again selected as the independent variable.

The reflection coefficient presented is the ratio of the reflected wave height to the incident wave height. This ratio was calculated using the equation:

$$C_r = \frac{H_{reflected}}{H_{incident}} = \frac{H_{max} - H_{min}}{H_{max} + H_{min}}$$

as previously discussed and defined in Fig. 2-2.

In the perfect standing wave case the distance between runup and rundown is the antinodal distance, H_{max}. As a result, one might expect the general shape of reflection curves to follow the plots of runup and rundown. Steeper waves should produce less reflection

due to increased energy dissipation (breaking) at the breakwater. While long, low steepness waves will reflect without breaking, some energy loss will always result from frictional resistance along the slope and within the interstices of the structure. Consequently, even low steepness waves should reflect less than 100% of the incident wave. Period and depth effects tend to be less pronounced due to the opposing influence on runup and rundown.

The occurrence of overtopping has been eliminated in the presentation of reflection data. Reflection is reduced by overtopping. Since more overtopping existed in the deeper water cases, the data would distort depth effects if the overtopping cases were included.

Fig. 4-18 shows 1:10 scale model reflection coefficient results. The shape is similar to that of runup and rundown but is more steeply sloped at higher wave steepnesses. This is attributed to the increased breaking and friction losses at large steepnesses. It was observed during testing, that although runup was relatively high, the volume of water carried by these waves was reduced by the inclusion of trapped air. The reflected energy is derived from the potential energy created during runup. The energy available in the reflected wave is reduced if the volume of runup is reduced. Hence, wave reflection

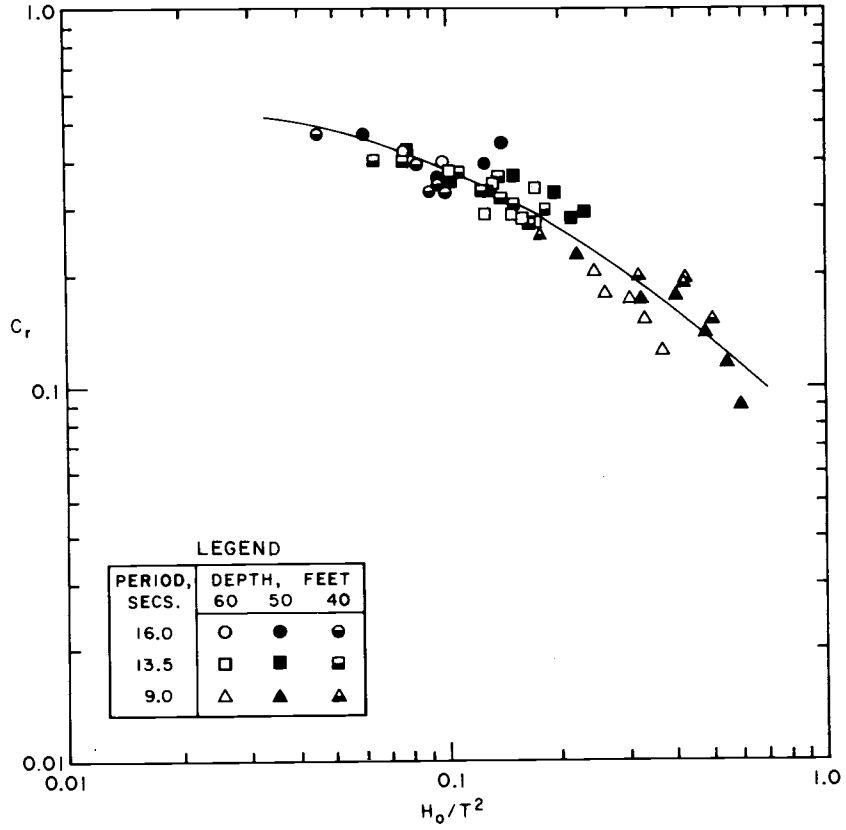

Fig. 4-18. Reflection Coefficient Versus Deep Water Wave Steepness, 1:10 Scale Model

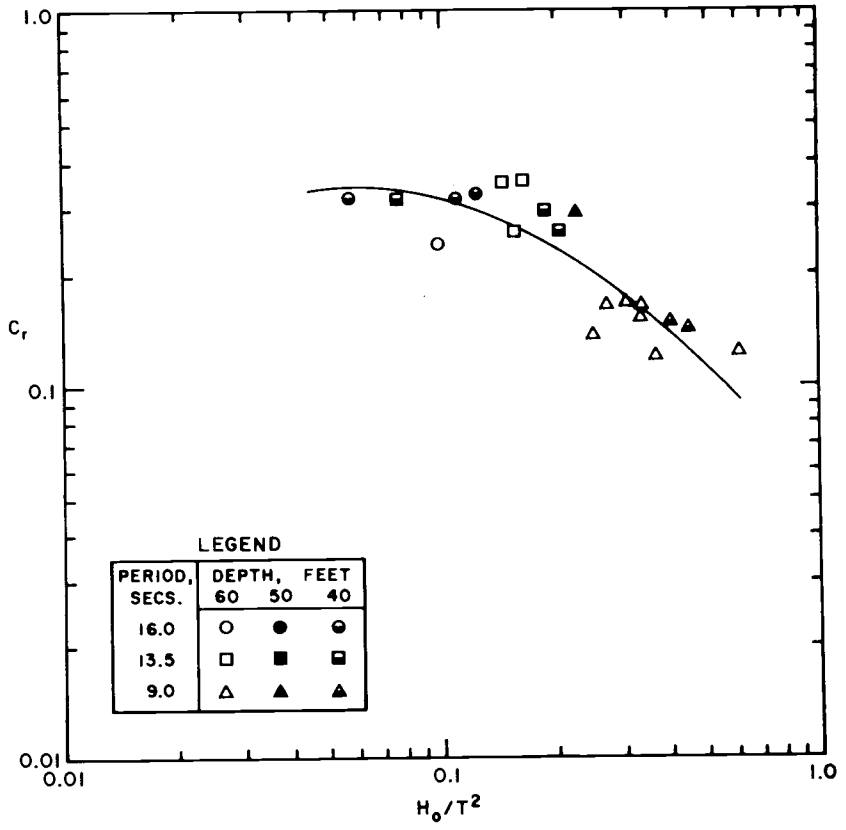

Fig. 4-19. Reflection Coefficient Versus Deep Water Wave Steepness, 1:20 Scale Model

is reduced at high runup due to air entrainment and turbulent dissipation along the breakwater slope.

Some increase in reflection with decreasing depth can be seen in the nine second waves but it is not visible in the other periods. Very little sorting of data with respect to period can be seen other than that naturally occurring from the use of H_o/T^2 as the independent variable. An indication of increased reflection is seen between the 13.5 second and 16.0 second waves at 40 feet and 50 feet but the majority of the 16 second data was not plotted due to overtopping.

Fig. 4-19 shows the results of the 1:20 scale model and confirms the shape observed in Fig. 4-18. The lack of data points due to overtopping prevents any analysis for depth and period effects.

Fig. 4-20 illustrates the data taken during the sloped bottom portion of the 1:100 test. The form of the 1:10 data is clearly matched by the 1:100 testing. The reflection at the 60 foot depth is generally less than that observed in the shallower cases. The 40 feet and 50 feet depths are separable in the less steep waves but are mixed in the steeper waves. Some indication of increased reflection with period can be seen.

Fig. 4-21 presents the data during the 1:100 scale tests with the flat bottom installed. These data closely follow those of the other cases tested. No dependence on depth or period is visible except that nine second waves generally experience less reflection.

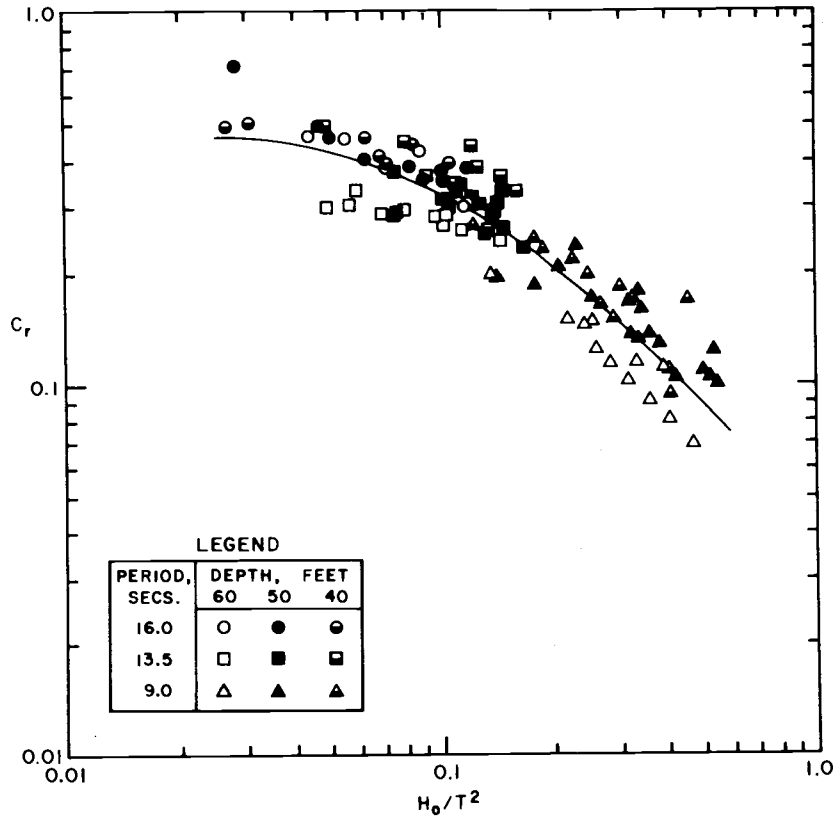

Fig. 4-20. Reflection Coefficient Versus Deep Water Wave Steepness, 1:100 Scale Model, Sloped Bottom Configuration

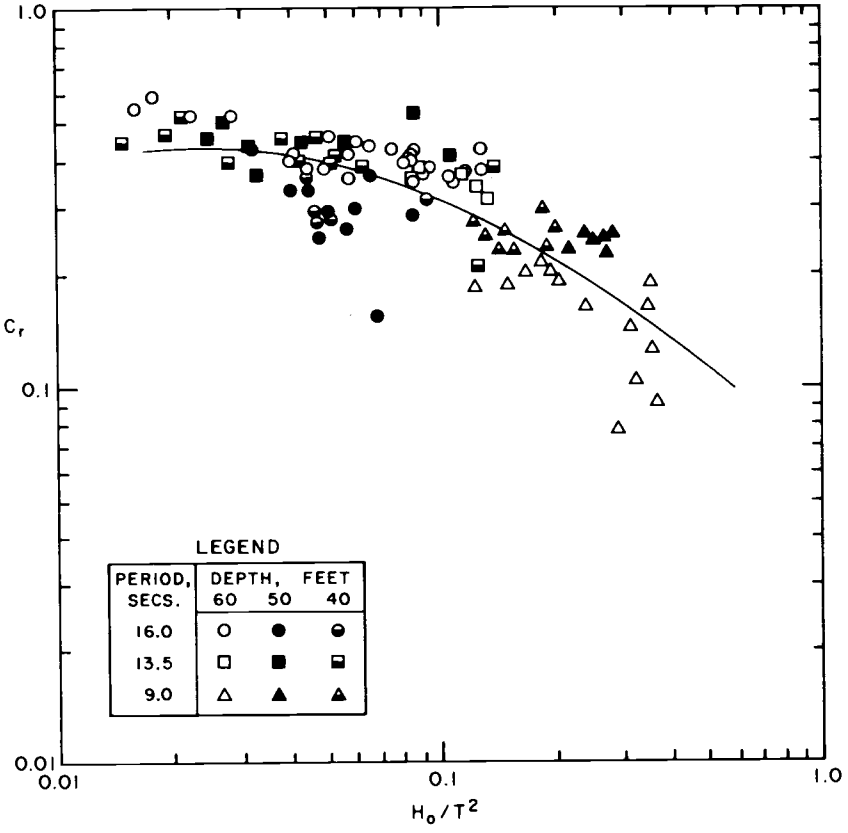

Fig. 4-21. Reflection Coefficient Versus Deep Water Wave Steepness, 1:100 Scale Model, Flat Bottom Configuration

Summarizing, it appears that reflection increases with: 1) increasing period; 2) decreasing steepness; and 3) decreasing depth. The results with respect to depth and period are not conclusive and indicate that additional investigations over several periods and several depths are required to resolve this behavior.

Table 4-1 shows a comparison of reflection coefficients for the six combinations of model size and bottom configuration. The comparison shown is similar to the calculations for scale and bottom effects in runup and rundown discussions. The value presented is an average of the deviations calculated at several identical values of H_o/T^2. The effect of bottom slope is only slightly greater than the 5% experimental error level. The effect of scale is significant, nearly 20% between the largest and smallest model. This is not appreciably larger than the scale effect noted for runup and it can be concluded that the same mechanism causes this scale effect, i.e., greater dissipation due to low Reynolds number damping reduces runup and reflection at small model scales.

4.5 Breakwater Stability

The determination of a stability or damage coefficient is dependent upon the establishment of some level of damage for use as a standard for comparing different breakwater types. The wave height

Table 4-1. Comparison of Reflection Coefficient for Effect of Bottom Slope and Scale.

Cr_1	Cr_2	$\frac{Cr_1 - Cr_2}{Cr_2}$
1:10 flat	1:10 sloped	+ 5.4%
1:100 flat	1:100 sloped	+ 5.4%
1:100 flat	1:10 flat	-19.1%
1:20 sloped	1:10 sloped	-13.0%
1:100 sloped	1:10 sloped	-18.0%
1:100 sloped	1:20 sloped	-10.3%

creating zero damage is the most common standard. As previously discussed, the use of this criteria has been disputed by some authors, however, the majority of cases suitable for comparison in this study utilize some form of zero damage measurement. Since the most common stability coefficient, Hudson's K_D, requires cubing the zero damage wave height to determine the required armor unit weight, it is especially important that the same criteria be applied.

The measurement of damage is usually made by comparing the number, area or volume of stones disturbed to the number, area or volume of stones in the armor layer. The placed stone configuration greatly facilitates the measurement of the area and/or number of stones disturbed during a test sequence. Unfortunately, the different types of armor stones used on the front face of this design complicate the calculation of relative damage. Specifically, one must decide to what number, volume, or area should the damage be compared. In

order to overcome this complication, the zero damage wave height was determined in two ways.

1. The smallest wave that dislodged A minus, A or A select stones. This point corresponds with the bottom of the 3A zone in Baird and Paul's (36) modes of failure diagram.
2. A graphical solution following that used by Thomsen et al. (44).

Figs. 4-22, 4-23 and 4-24 depict the modes of failure diagrams for the 1:10, 1:20 and 1:100 scale models respectively. According to Baird and Paul's (36) definition:

Zone 1	No movement of stone
Zone 2	In place oscillation of some stones (not recorded in this study)
Zone 3a	Displacement of up to ten stone per 100 lineal feet of prototype breakwater
Zone 3	Displacement of more than ten stone per 100 feet, establishing an equilibrium state in which continued attack will not result in failure of the breakwater
Zone 4	Damage such that continued wave attack over a long period of time would eventually cause complete failure of the breakwater
Zone 5	Immediate and widespread damage to the breakwater with complete failure imminent

The diagrams include one refinement; T^2/d is plotted along the abscissa to give an indication of the effect of period and depth. In general, longer waves in shallower water caused greater damage. This result agrees with the conclusion reached by Thomsen, et al (44).

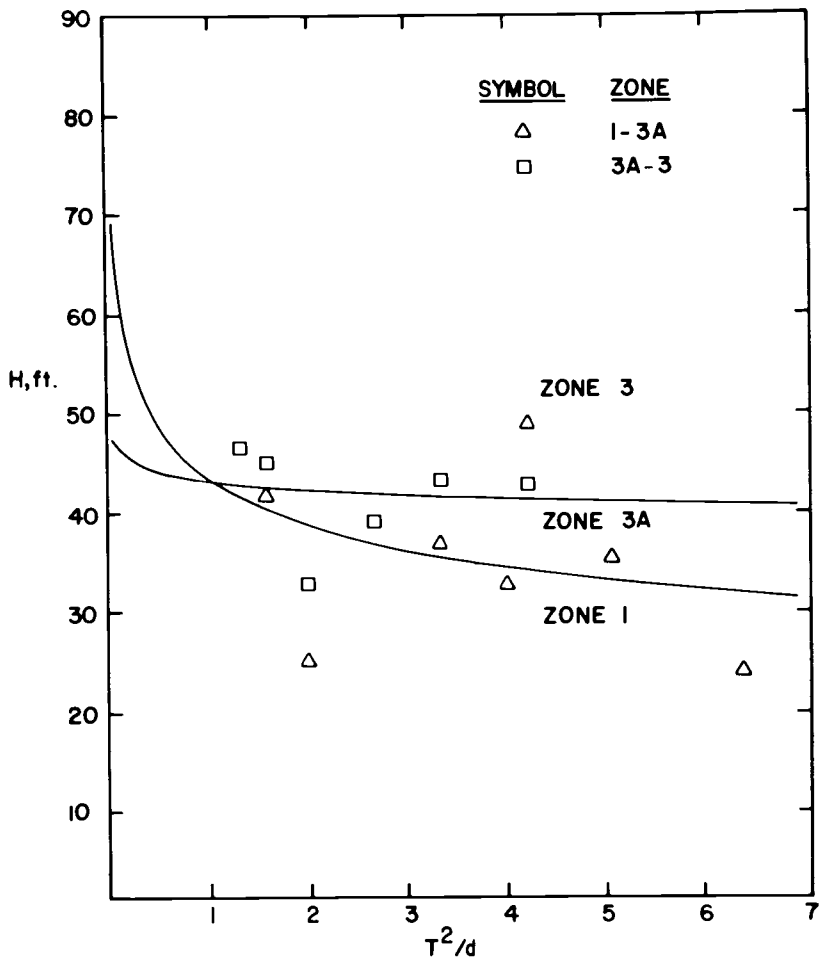

Fig. 4-22. Modes of Failure Diagram, 1:10 Scale Model

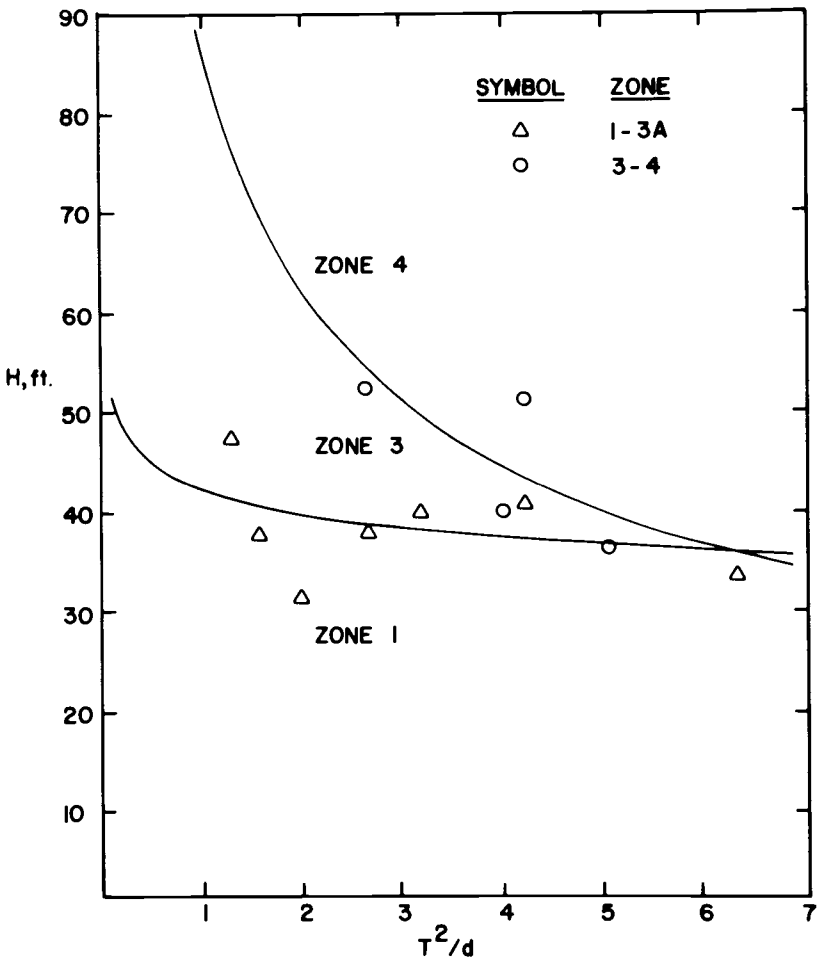

Fig. 4-23. Modes of Failure Diagram, 1:20 Scale Model

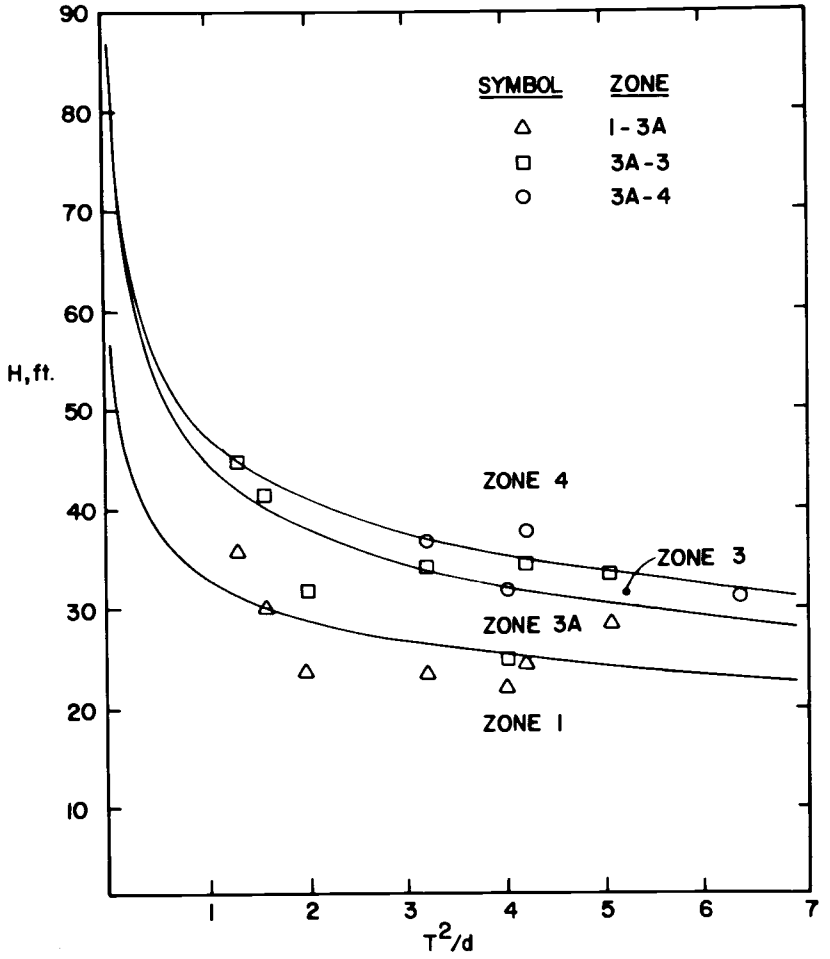

Fig. 4-24. Modes of Failure Diagram, 1:100 Scale Model

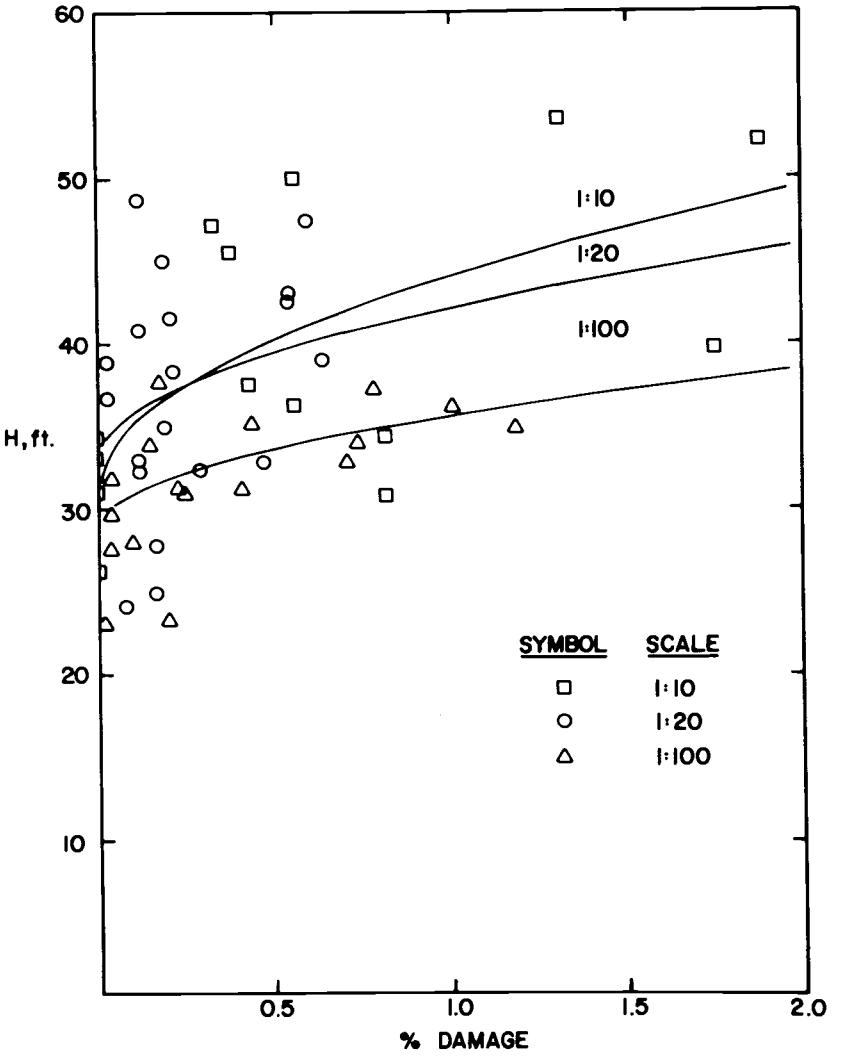

Fig. 4-25. Wave Height Corresponding to Percent Areal Damage

For comparison of no damage wave heights, the wave height corresponding to the lower limit of the 3A Zone for a 13.5 second wave in 50 feet of water was selected. This gives no damage wave heights of 34, 35 and 25 feet for the 1:10, 1:20 and 1:100 tests.

Thomsen, et al. (44) determine the no damage wave height by plotting wave height versus a dimensionless areal damage coefficient,

$$B = \frac{JL}{b}$$

where L is a linear dimension representing the armor unit width and J is the number of stones displaced from a section of width, b. As shown in Fig. 4-25, the damage remains small until the wave height increases to a critical point after which the damage increases rapidly. The no damage wave height is selected by projecting the flat portion of the curve back to zero. This technique eliminates the question of which percent damaged area should be used to select an appropriate no damage or limited damage wave height. The shape of the damage curve remains the same regardless of the width used. Using this technique, no damage wave heights of 36, 35, and 30 feet were determined for the 1:10, 1:20, and 1:100 scale models, respectively.

These wave heights demonstrate excellent agreement with the modes of failure results for the 1:10 and 1:20 models but significant spread at the 1:100 scale is apparent. In order to reduce this discrepancy, the 1:100 failure modes are replotted in Fig. 4-26 using

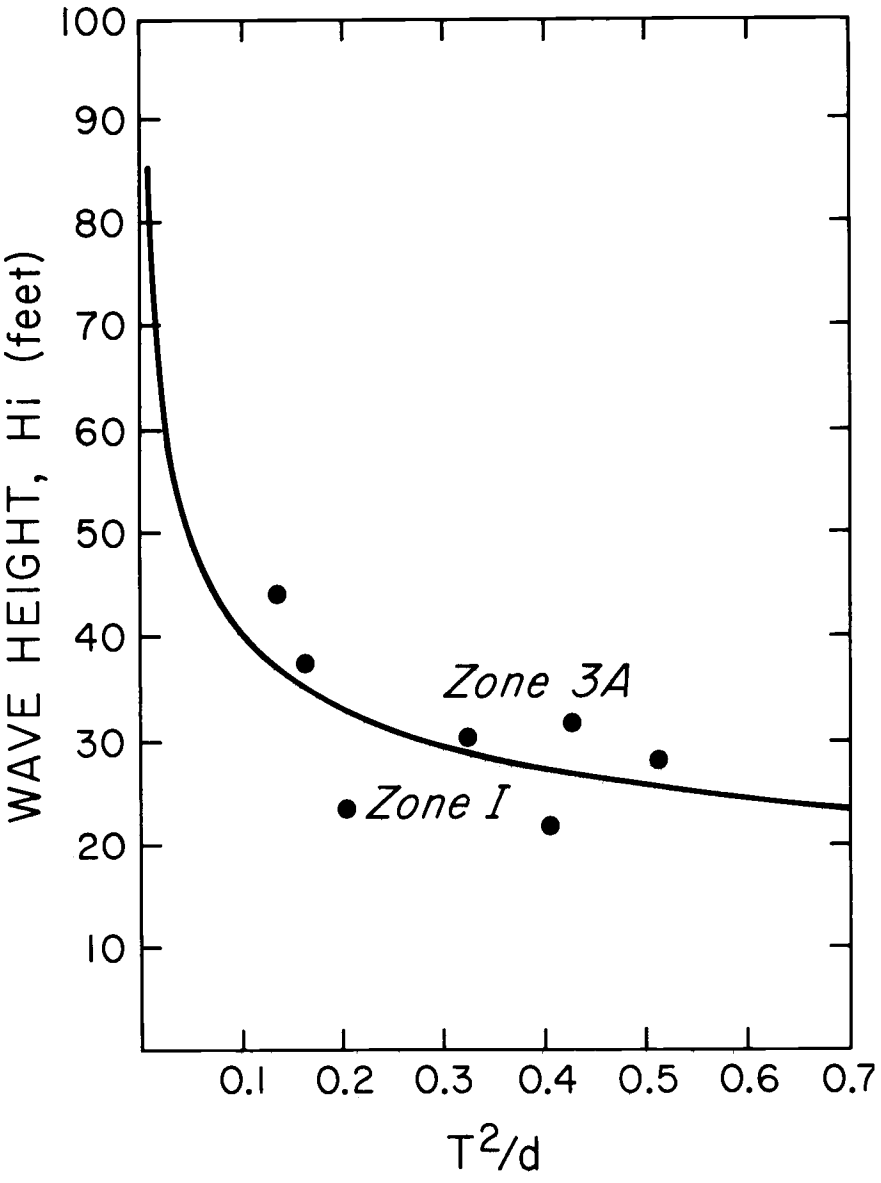

Fig. 4-26. Modes of Failure Diagram, 1:100 Scale Model, Revised

displacement of more than two stones as a no damage criterion. This increases the no damage wave height to 28 feet at the 1:100 scale.

Combining the modes of failure and areal damage results provides the following estimates for no damage wave heights at the three model scale ratios:

Model Scale	No Damage Wave Height
1:10	35 feet
1:20	35 feet
1:100	28 feet

Using these no damage wave heights as inputs to the calculation of Hudson's stability coefficient, K_D, Table 4-2 lists K_D for this and several related tests. The tabulated summary demonstrates that placed stone armor compares favorably with dolos armor. It is also significantly better than the placed stone results from the Siuslaw jetty testing, but is similar to the placed stones tested by Thomsen, et al. and to placed cubes.

It should be noted that values of no damage wave height selected are quite conservative in that displacement of A minus stone was considered damage. The onset of damage in the A select and A zones did not occur until much higher waves were encountered. Failure in the placed stone portion of the front face can be generally equated with the boundary between Zone 3 and Zone 4 in Fig. 4-22. In the 1:20 and 1:100 model this wave height is about one-third greater than the selected no damage wave. In the 1:10 model no more than two A

Table 4-2. Table of Hudson Stability Coefficient

Armor Type	Damage Criteria	K_D	Recommended by Shore Protection Manual
Umpqua placed stone	average no damage conditions		
1:10		29.8	
1:20		29.8	
1:100		15.4	
Placed Quartzite	Zero damage by Thomsen, et al.		4.8
large		34.1	
medium		10.3	
small		6.3	
Dumped Quartzite	Zero damage by Thomsen, et al.		
large		30.5	3.5
medium		8.9	
Dumped Boulders	Zero damage by Thomsen, et al.		2.1
large		6.1	
small		1.2	
Dolos 1:16 scale	Lower limit of Zone 3A for modes of		22.0
0.19 tons	failure diagram	17.3	
0.65 tons		25.7	
0.70 tons		25.5	
0.75 tons		32.3	
Tetrapod 1:16 scale	Lower limit of Zone 3A for modes of		7.2
1.53 tons	failure diagram	6.8	
3.5 tons		11.5	
Stones 1:16 scale	Lower limit of Zone 3A for modes of		2.1
6-7 tons	failure diagram	3.8	
Siuslaw Jetty Placed Stones	Not given	4.8	4.8
Cubes	Not given		
Random		7.8	6.8
Placed		13.7	

A or A select stones were dislodged in any tests. These tests included several long duration tests in which the highest attainable waves were applied to the structure. In view of the level of stability exhibited in the 1:10 tests, it is reasonable to predict that, as designed, the breakwater is capable of withstanding the design wave of 43 feet at 13.5 seconds.

In a composite breakwater with several types and sizes of facing material, it is also necessary to evaluate the nature and distribution of the various failures that occur. This evaluation indicates which areas may be under or over designed. The overall high stability exhibited by the design studied makes this evaluation quite subjective, however the failures observed were found to be of three types:

1. Failure near the waterline.
2. Failure at the A minus/A select interface
3. Failure of the back face at the interface of the B stones and the caisson.

The first type of failure is similar to that commonly seen in other rubble mound structures wherein the action of the wave caused displacement and removal of A or A select stones on the seaward face of the breakwater. This type of failure was infrequent but generally occurred in the presence of very high waves and in relatively deep water. On numerous occasions, this type of failure ceased after the

removal of one or two stones in an area. In general, this failure mechanism initially occurred near or below the waterline in the A select stone and spread into the A stone. The overall high stability exhibited by the design indicates that this type of failure is not a design weakness.

Failure at the interface of the A minus and A select stones was generally experienced in the low water conditions for waves with large rundown. This resulted from long term loss of A minus stone and subsequent deterioration of the A select foundation stones. This type of failure was not as prevalent as initially expected, although in several of the small model tests it was obvious that extensive exposure beyond 500 waves would have resulted in this type of failure. Success at the larger scales indicates that the sizing of the stone was acceptable. It was found, however, that the maintenance of the 1:1.5 slope in the A minus stone was very difficult. Under moderately high waves, the slope rapidly deteriorated to approximately 1:2. This slope was very stable, losing additional stones only to much higher waves.

Failure of the back face, as previously discussed, prompted an early modification of the design. Originally the B minus under layer was terminated at the back edge of the breakwater crest and C stone was placed directly under the back face. Early major failures in the

1:20 scale model indicated that the layer of B minus stone should be extended to the back face.

Failures in the back face were limited in the 1:10 scale model but did occur several times in the 1:100 scale model. Nearly all of the failure in the back face occurred at the interface with the caisson in conditions of high water and significant overtopping. The primary cause of the failure was the large volume of water running out of the back face of the breakwater during high waves. Most of the water traveled along the top of the caisson and on numerous occasions was as deep as the smallest dimension of the B stone, approximately three feet at full scale. The velocity was not measured but was approximated at several feet per second, full scale. During failures this flow removed stones along the interface, removing support for the other stones. The subsequent loosening of this layer allowed the wash of the waves to destroy major portions of the back face. This type of failure appears to be the result of poor interfacial contact at the surface of the caisson. As designed, the flat top of the caisson makes the placement of the first two layers of stones very difficult. The contact area between the stone is reduced since the major plane of the stones cannot be placed parallel to each other. Redesign of the caisson as shown in Fig. 4-27 should greatly reduce this type of failure and facilitate stone placement on the back face.

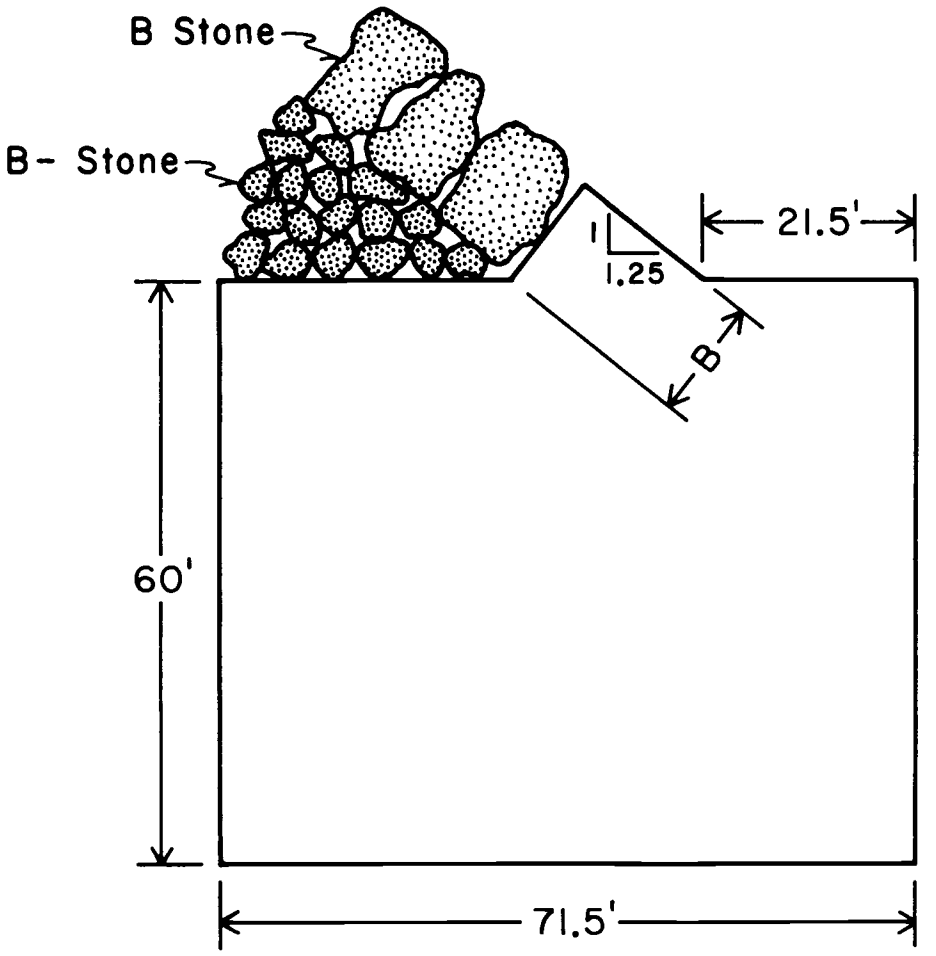

Fig. 4-27. Proposed Modified Caisson Design

4.6 Stability Scale Effects

Very few studies have investigated the effect of model size on breakwater stability. The Shore Protection Manual (45) states that Reynolds Number larger than 6×10^4 should produce full scale results. Thomsen, et al. (44) showed that a Reynolds number defined as

$$R_e = \frac{\gamma_f}{\mu} \frac{(W)^{1/3}}{(\gamma)^{1/3}} \frac{(H)^{1/2}}{(g)^{1/2}} > 3 \times 10^5$$

produced results equivalent to full scale. This may also be written as

$$R_e = \frac{\rho}{\mu} \left(\frac{W}{\gamma}\right)^{1/3} (gH)^{1/2}$$

where $(W/\gamma)^{1/3}$, the cube root of the armor volume, is the characteristic length and $(gH)^{1/2}$ is characteristic velocity. A more appropriate velocity scale might be formed from H/T to include the effect of wave period, however, period data are not presented in the Thomsen study (44). Nevertheless, the Thomsen study is the most thorough investigation of scale effects and serves as a comparison for this study. Three ranges of Reynolds Number were investigated by Thomsen, et al. (44), $2 - 3 \times 10^4$, $4 - 6 \times 10^4$ and greater than 5×10^5. A normalized zero damage stability coefficient N'_{ZD}/N_{ZD} was defined where

$$N_{ZD} = \frac{H_{ZD}}{(W/\ )^{1/3}\ (s-1)}$$

and N'_{ZD} represents the largest scale tested. This parameter is proportional to the cube root of Hudson's stability coefficient but does not separate the effect of slope. This parameter was plotted as a function of Reynolds Number and an exponential decay relationship was found. Fig. 4-28 shows Thomsen's curve (44) and the zero damage points developed in the present study. Since this normalized coefficient allows comparison of any similarly established zero damage wave heights, N'_{ZD}/N_{ZD} for the points corresponding to the lower boundary of Zone 4 of the modes of failure diagram are plotted. The data show fair agreement with the curve although they are generally lower. This is considered to be the result of being unable to substantially damage the cover layer in the 1:10 testing. Although the rise in damage of the A minus stones indicates that instability of the armor layer was approached, the actual value of N'_{ZD} is likely larger than that used. This increase would generally elevate the plotted points improving the correlation with the previous investigation. In general, this study agrees with the conclusion of Thomsen, et al. that $Re > 3 \times 10^5$ produces model results roughly equivalent to full scale. This indicates that both the 1:20 and 1:10 scale models are satisfactory for interpretation of prototype behavior for the design wave conditions required in this study. However, smaller prototypes

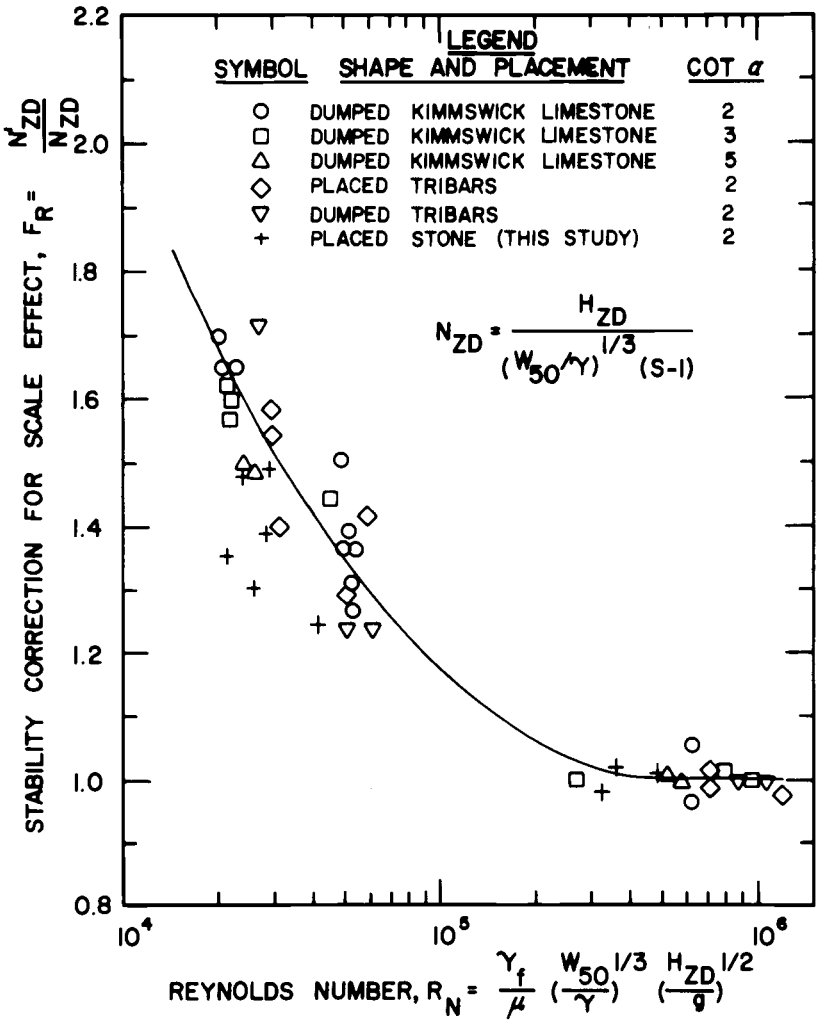

Fig. 4-28. Scale Effect for Zero Damage Stability

may require relatively larger model scale ratios in order to maintain the minimum Reynolds Number requirements.

CHAPTER V

SUMMARY AND CONCLUSIONS

5.1 Synthesis

This study has examined a breakwater designed to protect a floating nuclear power plant experiencing breaking wave heights in water depths of 40 to 60 feet. The models were tested using a placed stone construction technique employed by the Umpqua Division of the Bohemia Corporation. The purpose of this study was to quantify the unusually high stability exhibited by several existing breakwaters, and to investigate the interaction of waves and the breakwater in the form of runup, rundown and reflection.

Three different scales were tested (1:10, 1:20 and 1:100) at three different depths (40 feet, 50 feet and 60 feet), three different wave periods (9.0 seconds, 13.5 seconds and 16.0 seconds) and two bottom slopes (flat and 1:12). A total of 370 test cases were completed providing a large body of data for comparison for the effect of depth, period, bottom slope and scale.

With regard to these factors, all three models generally confirmed that:

1. Increased depth results in
   a) decreased runup
   b) increased rundown

c) decreased reflection
d) increased stability

2. Increased period results in

a) increased runup
b) increased rundown
c) increased reflection
d) decreased stability

3. Increased wave height results in

a) decreased relative runup
b) decreased relative rundown
c) decreased reflection
d) decreased stability

4. Increased bottom slope

a) increased runup
b) no change in rundown
c) no change in reflection

5. Increased model size

a) increased runup
b) decreased rundown
c) increased reflection
d) increased stability

These results agreed with the hypothesized behavior.

Values of runup correlated well with previous data lying between that for random stones on an impermeable slope and that for random stones on a permeable slope. It was found by plotting runup divided by depth (instead of runup divided by wave height) versus wave steepness that the effect of depth and period were separable from steepness. Based on plots of R_u/d versus H_o/T^2 the measured effects of bottom slope and model scale were smaller than in previous

investigations and it was concluded that the classical use of R_u/H_o as a dependent variable may result in overestimation of these effects. Values of runup determined in this method showed an increase of only 7% in the sloped bottom case and 10% in the larger scale model as compared to 17% and 18% when R_u/H_o was used.

Values of rundown were considerably less than those found in previous investigations. This is attributable to the fact that previous investigations were conducted in deep water. It was also found that rundown decreases with scale size and that this decrease is related to the increase in runup with model scale.

Reflection was found to be relatively low when compared to that of smooth surfaces. Reflection was greatly reduced in waves of high steepness.

The breakwater was exceptionally stable exhibiting a Hudson's stability coefficient of 30. This compares favorably with that assigned to dolos. Scale testing indicated that the 1:100 scale test underestimated Hudson's K_D by a factor of two whereas the 1:20 model provided results similar to the 1:10 model.

5.2 Recommendations for Future Studies

In general the designed breakwater was found suitable for the proposed application. The question of the volume of overtopping has not been addressed in this study. Although such information is not

required in jetty applications, it would be useful to estimate drainage requirements for enclosed systems. The design tested did exhibit higher runups than those of an ordinary rubble mound indicating that design crest height calculations should account for this condition. The studies of runup, rundown and reflection indicate that changes in depth and period have considerable effect. This study provides significant information regarding these effects on runup and to a certain extent rundown. The lack of repeatability of the runup and rundown measurements is of some concern. Visual measurement against a grid is somewhat subjective and some form of electronic sensing device could improve measurement procedures. The use of several sensors, placed across the face of the breakwater, in tests utilizing many wave periods and depths may provide additional information on the behavior of breakwater failures, distributions of runup and volume of overtopping.

The design breakwater when tested at 1:10 scale exhibited no major structural failures in any of the design conditions and the no damage wave height was deduced from damage to the toe material (A minus). This condition places a lower limit on K_D and restricts the interpretation of results for deeper water and higher waves. To make the results more general for the placed stone section, it is suggested that a uniform model slope, made up entirely of similar placed stones at the 1:20 or 1:10 scale, be tested at various depths,

wave heights and periods. Additional testing of the A minus stone and the A select/A minus interface should not be required since the results of this study adequately quantify this type of damage.

REFERENCES

1. Ahrens, John P., Influence of Breaker Type on Riprap Stability, Proceedings of the Twelfth Conference on Coastal Engineering, Vol. III, September 1970, pp. 1557-1566.

2. Castro, Eduardo, Diques de escolleru, Revista de Obras Publicas, April 1933.

3. Carstens, T., Torum, Alf and Traetteberg, Anton, The Stability of Rubble Mound Breakwaters against Irregular Wave, Proceedings of the Tenth Conference on Coastal Engineering, Vol. II, September 1966, pp. 958-971.

4. Cross, R.H. and Sollitt, C.K., Wave Transmission by Overtopping, Technical Note No. 15, Ralph M. Parsons Laboratory, Massachusetts Institute of Technology, July 1971.

5. d'Angremond, K., Span, H. J. Th., van der Weide, J. and Woestenek, A. J., Use of Asphalt in Breakwater Construction, Proceedings of the Twelfth Conference on Coastal Engineering, Vol. III, September 1971, pp. 601-628.

6. Dai, Y. B. and Kamel, A. M., Scale Effect Test for Rubble Mound Breakwaters, Research Report H-69-2 U.S. Army Engineer Waterways Experiment Station, Corps of Engineers, Vicksburg, Mississippi, December 1969.

7. de Carvalho, J. J. R. and Vera-Cruz, D., On the Stability of Rubble-Mound Breakwaters, Proceedings of the Seventh Conference on Coastal Engineering, August 1960, pp. 633-658.

8. Epstein, H. and Tyrrel, F., Design of Rubble-Mound Breakwaters, Proceedings of the Seventeenth International Navigation Congress, Section II Communication 4, July 1949.

9. Font, J. B., Effect of Storm Duration on Rubble-Mound Breakwater Stability, Proceedings of the Eleventh Conference on Coastal Engineering, Vol. II, September 1968, pp. 779-796.

10. Font, J. B., Damage Function for a Rubble-Mound Breakwater under the Effect of Swell, Proceedings of the Twelfth Conference on Coastal Engineering, Vol. III, September 1971, pp. 1567-1586.

11. Galvin, C. J., Breaker Type Classification on Three Laboratory Beaches, Journal of Geophysical Research, Vol. 73, No. 12, June 1968, pp. 3650-3661.

12. Galvin, C. J., Breaker Travel and Choice of Design Wave Heights, Journal of the Waterways and Harbors Division, Proceedings of the American Society of Civil Engineers, Vol. 95, No. WW2, May 1969, pp. 175-200.

13. Goda, Y. and Abe, Y., Apparent Coefficient of Partial Reflection of Finite Amplitude Waves, Report of the Port and Harbour Research Institute, Vol. 7, No. 3, September 1968, pp. 3-58.

14. Goda, Y., Re-analysis of Laboratory Data on Wave Transmission over Breakwaters, Report of the Port and Harbour Research Institute, Vol. 8, No. 3, September 1969, pp. 3-18.

15. Grantham, K. N., Wave Run-up on Shore Structures, Transactions of the American Geophysical Union, Vol. 34, No. 5, pp. 590-609.

16. Hickson, R. and Rudolf, F., Design and Construction of Jetties, Proceedings of the First Conference on Coastal Engineering, October 1950, pp. 227-245.

17. Hudson, R. Y., Wave Forces on Breakwaters, Transactions of the American Society of Civil Engineers, Vol. 118, 1953, pp. 653-674.

18. Hudson, R. Y., Laboratory Investigations of Rubble-Mound Breakwaters, Journal of the Waterways and Harbors Division, Proceedings of the American Society of Cifil Engineers, Vol. 85, No. WW3, September 1959, pp. 93-121.

19. Hudson, R. Y. and Houseley, J. G., Designs for Rubble-Mound Breakwater, Nawiliwili Harbor, Nawiliwili, Hawaii, Hydraulic Model Investigation, Miscellaneous Paper No. 2-377, U.S. Army Engineer Waterways Experiment Station, Corps of Engineers, Vicksburg, Mississippi, February 1960.

20. Hudson, R. Y., Wave Forces on Rubble-Mound Breakwaters and Jetties, Miscellaneous Paper No. 2-453, U.S. Army Engineer Waterways Experiment Station, Corps of Engineers, Vicksburg, Mississippi, December 1969.

21. Hudson, R. Y. and Jackson, R. A., Stability of Rubble Mound Breakwaters, Technical Memorandum No. 2-365, U.S. Army Engineer, Waterway Experiment Station, Corps of Engineers, Vicksburg, Mississippi, 1953.

22. Hunt, I. A., Design of Seawalls and Breakwaters, Journal of the Waterways and Harbors Division, Proceedings of the American Society of Civil Engineers, Vol. 85, No. WW3, September 1959, pp. 123-152.

23. Ippen, A. T., Estuary and Coastline Hydrodynamics, McGraw-Hill Book Co., Inc., New York, 1966.

24. Iribarren, R., Una Formula Para el Calcula de los Disques de Escollera, Revista de Obrus Publicus, 1938.

25. Iverson, H. W., Waves and Breakers in Shoaling Water, Proceedings of the Third Conference on Coastal Engineering, October 1952, pp. 1-12.

26. Jackson, R. A., Stability of South Jetty Siuslaw River, Oregon, Technical Report No. 2-631, U.S. Army Engineer Waterways Experiment Station, Corps of Engineers, Vicksburg, Mississippi, July 1963.

27. Johnson, J. W., Kondo, H., and Wallihan, R., Scale Effects in Wave Action through Porous Structures, Proceedings of the Tenth Conference on Coastal Engineering, Vol. II, September 1966, pp. 895-912.

28. Kidby, H. A., Powell, S. B., Roberts, A. L., "Placed-Stone" Jetty, Stone Weight Coefficients, Journal of the Waterways and Harbors Division, Proceedings of the American Society of Civil Engineers, Vol. 90, No. WW4, November 1964, pp. 77-86.

29. Kidby, H. A. and Price, C. D., Umpqua Jetty Surveillance Program, Proceedings of the American Society of Civil Engineers Specialty Conference, Coastal Engineering, October 1965, pp. 845-861.

30. Le Mehaute, B., Koh, R. C., and Hwang, Li-San, Synthesis on Wave Run-up, Journal of the Waterway and Harbors Division, Proceedings of the American Society of Cifil Engineers, Vol. 94, No. WW1, February 1968, pp. 77-92.

31. Merrifield, E. M. and Zwamborn, J. A., The Economic Value of a New Breakwater Armour Unit "Dolos," Proceedings of the Tenth Conference on Coastal Engineering, Vol. II, September 1966, pp. 885-912.

32. Merryfield, E. M., Dolos Concrete Armor Protection, Civil Engineering--ASCE, December 1968, pp. 38-41.

33. Nagai, S., Research on Sea Walls, Proceedings of the Twelfth Conference on Coastal Engineering, Vol. III, September 1971, pp. 1431-1450.

34. Oulett, Y., Effects of Irregular Wave Trains on Rubble Mound Breakwaters, Journal of the Waterways, Harbors and Coastal Engineering Division, Proceedings of the American Society of Civil Engineers, Vol. 98, No. WW1, February 1972, pp. 1-14.

35. Paape, A. and Wather, A. W., Akmon Armour Units for Cover Layers of Rubble-Mount Breakwaters, Proceedings of the Eighth Conference on Coastal Engineering, November 1913, pp. 430-443.

36. Paul, M. W. and Baird, W. F., Discussion of Breakwater Armor Units, The First International Conference on Port and Ocean Engineering under Arctic Conditions, Vol. II, August 1971, pp. 1-27.

37. Rogan, A. J., Destruction Criteria for Rubble Mound Breakwaters, Proceedings of the Eleventh Conference on Coastal Engineering, Vol. II, September 1968, pp. 761-778.

38. Savage, R. P., Wave Run-up on Roughened and Permeable Slopes, Transactions of the American Society of Civil Engineers, Vol. 124, 1959, Paper No. 3003, pp. 852-870.

39. Saville, T., Jr., Wave Runup on Composite Slopes, Proceedings of the Sixth Conference on Coastal Engineering, December 1957, pp. 691-699.

40. Saville, T., Jr., Wave Runup on Shore Structures, Transactions of the American Society of Civil Engineers, Vol. 123, 1958, pp. 139-150.

41. Sollitt, C. K. and Cross, R. H., Wave Reflection and Transmission at Permeable Breakwaters, Report No. 147,

Ralph M. Parsons Laboratory, Massachusetts Institute of Technology, March 1972.

42. Svee, R., Traetteberg, A., and Torum, A., The Stability Properties of the Svee-Block, Proceedings of the Twenty-First International Navigation Congress, Section 2, Subject 1, 1965, pp. 133-162.

43. Svee, R., Formulas for Design of Rubble Mound Breakwaters, Journal of the Waterways and Harbors Division, Proceedings of the American Society of Divil Engineers, Vol. 88, No. WW2, May 1962, pp. 11-21.

44. Thomsen, A. L., Wohlt, P. E. and Harrison, A. S., Riprap Stability on Earth Embankments Tested in Large and Small Scale Wave Tanks, Technical Memorandum No. 37, U.S. Army Corps of Engineers, Coastal Engineering Research Center and Missouri River Division, June 1972.

45. U.S. Army Engineers Coastal Engineering Research Center, Shore Protection Manual, Department of the Army Corps of Engineersl 1973.

46. U.S. Army Engineer District, Portland, Oregon, Surveillance of Umpqua River, South Jetty, June 1971.

47. Van Oorchot, F. and d'Angremound, K., The Effect of Wave Energy on Wave Run-up, Proceedings of the Eleventh Conference on Coastal Engineering, Vol. II, September 1968, pp. 888-901.

48. Vera-Cruz, D., Overtopping of Sloped Breakwaters, Bulletin of the Permanent International Association of Navigation Congresses, No. 12, 1972, pp. 97-105.

49. Wassing, F., Model Investigations on Wave Run-up Carried Out in the Netherlands during the Last Twenty Years, Proceedings of the Sixth Conference on Coastal Engineering, December 1957, pp. 700-714.

50. Weggel, J. R., Maximum Breaker Height, Journal of the Waterways, Harbors and Coastal Engineering Division, Proceedings of the American Society of Civil Engineers, Vol. 98, No. WW4, November 1972, pp. 529-548.

51. Wilson, K. W. and Cross, R. H., Scale Effects in Rubble Mound Breakwaters, Proceedings of the Thirteenth Conference on Coastal Engineering, Vol. III, July 1972, pp. 1873-1884.

APPENDICES

APPENDIX A

PHOTO ESSAY OF MODEL CONSTRUCTION AND WAVE INDUCED DAMAGE

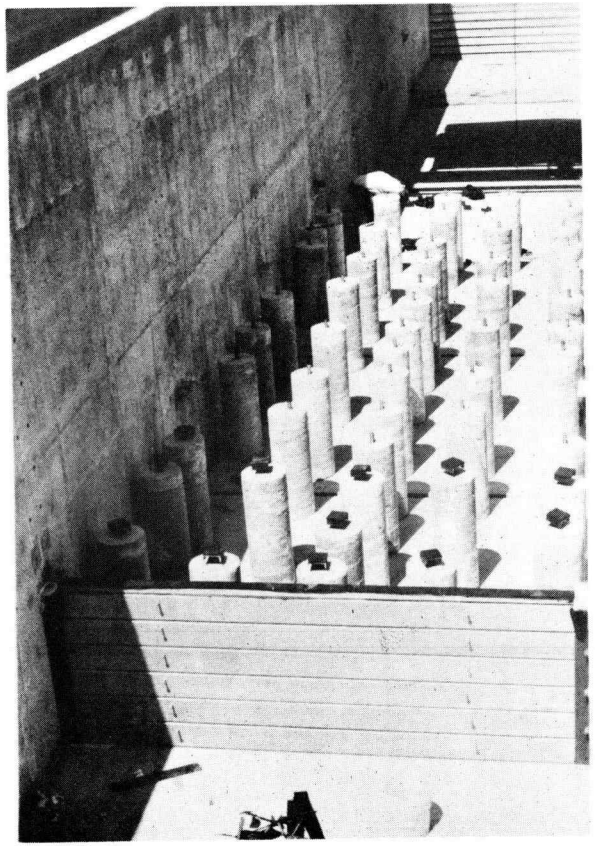

Fig. A-1. Concrete Support Columns for Model Foundation Slab

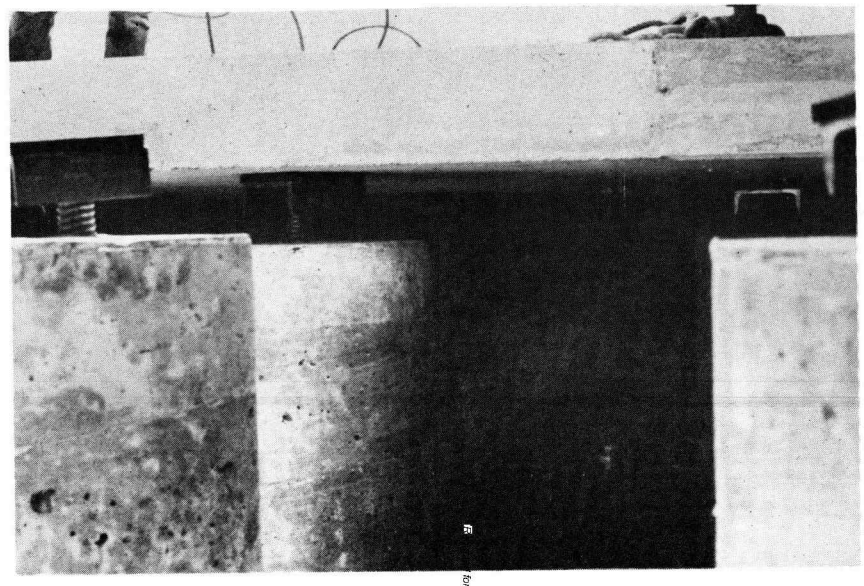

Fig. A-2. Threaded Shims and Rubber Pads Under 12' x 12' Foundation Slabs

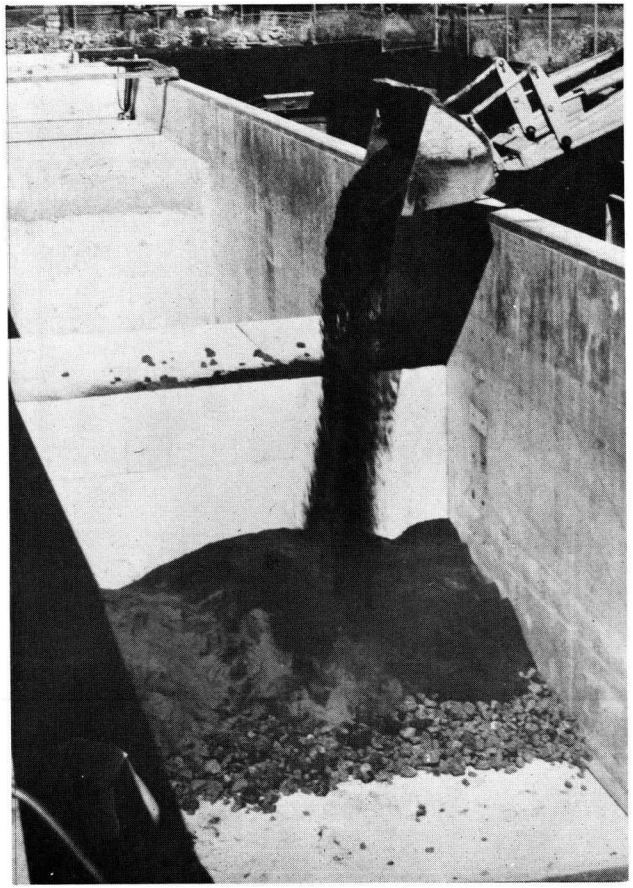

Fig. A-3. Caisson, Foundation Blanket and Placement of Sand Core, 1:10 Scale Model

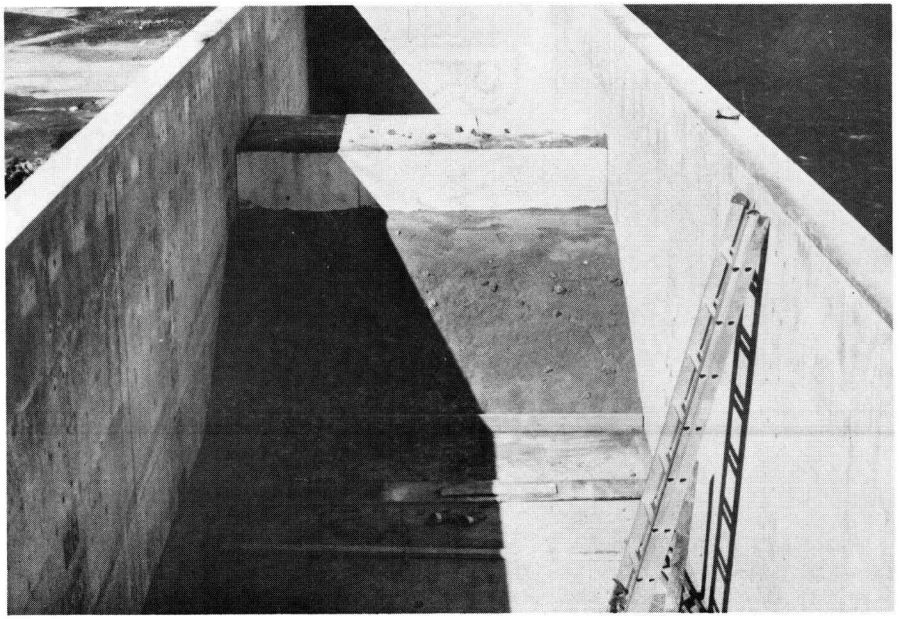

Figure A-4. Caisson and Completed Sand Core, 1:10 Scale Model

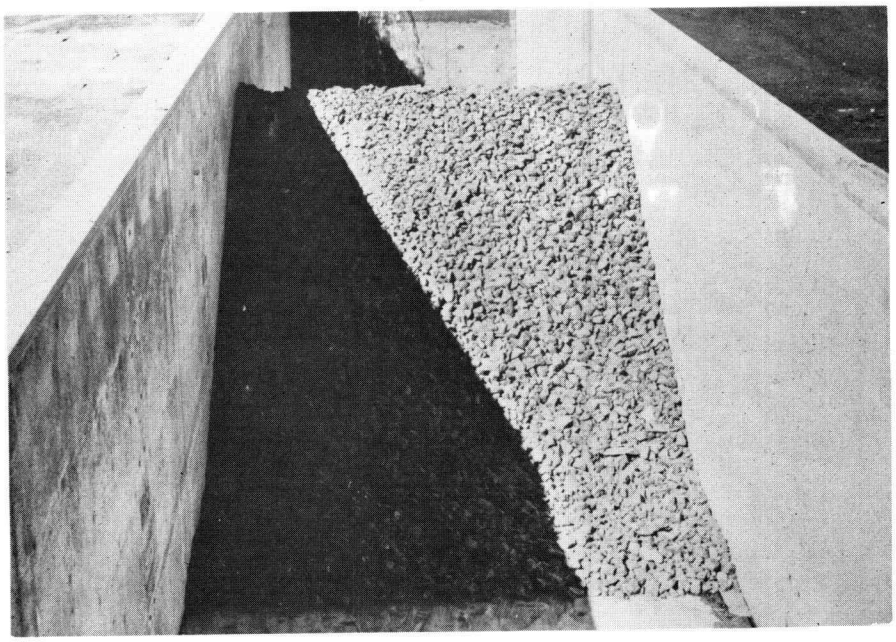

Fig. A-5. C Stone, 1:10 Scale Model

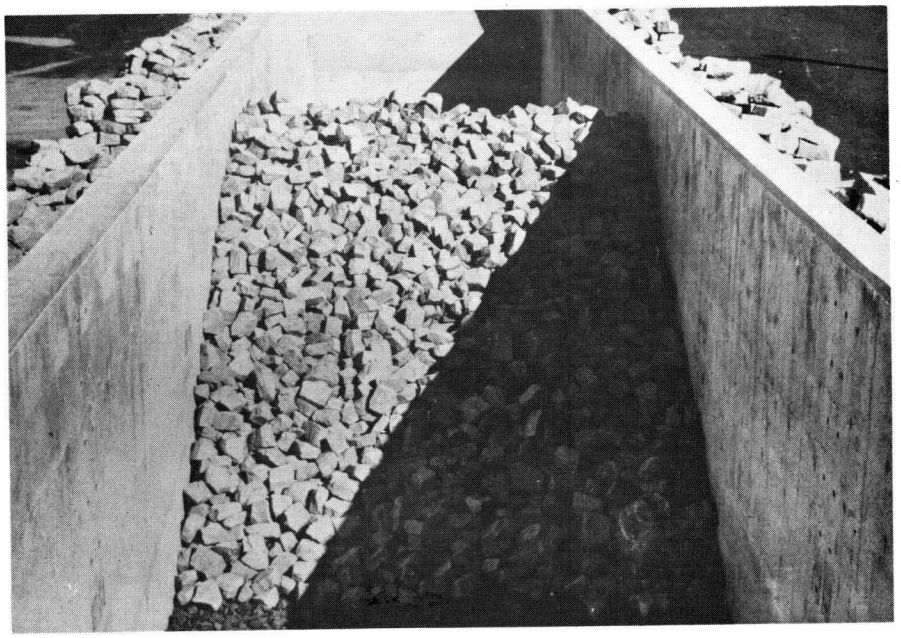

Fig. A-6. B- Stone, 1:10 Scale Model

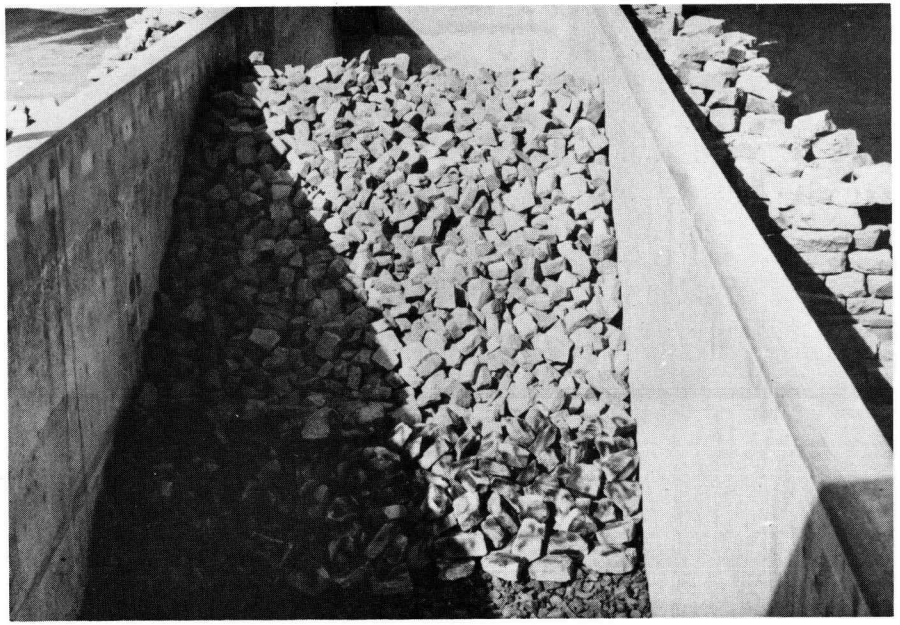

Fig. A-7. A- Stone Placed at Toe of Slope, 1:10 Scale Model

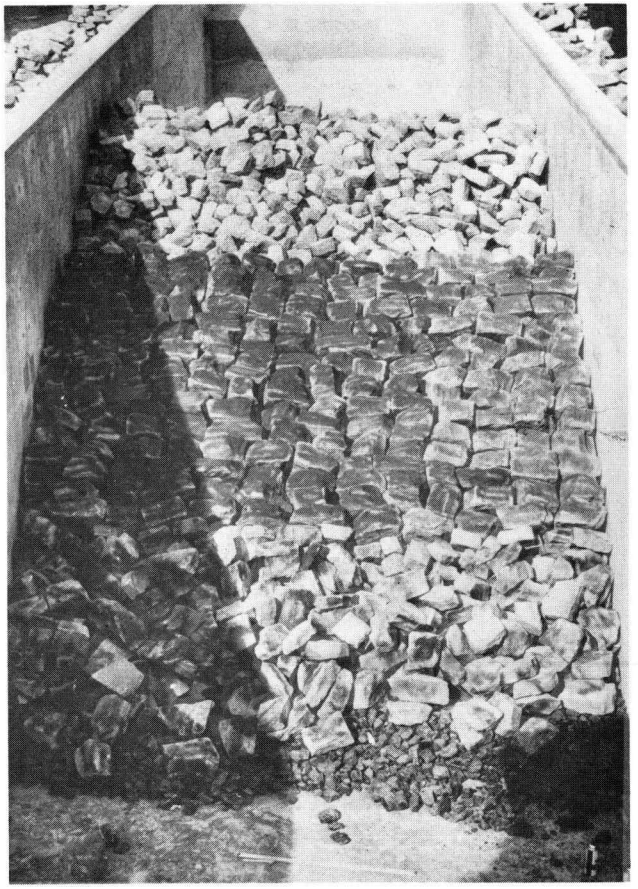

Fig. A-8. A+ Stone, 1:10 Scale Model

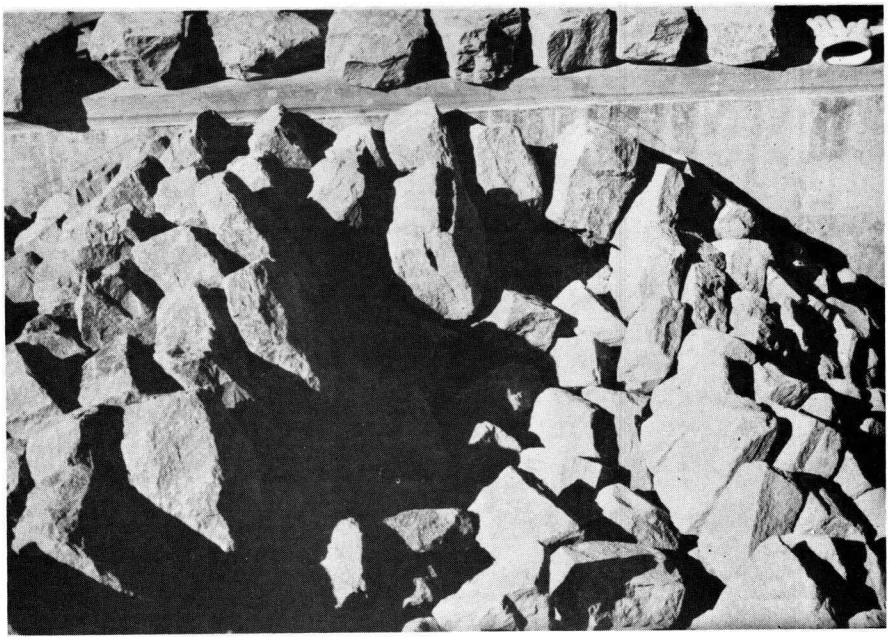

Fig. A-9. A Stone Placement at Breakwater Crest, 1:10 Scale Model

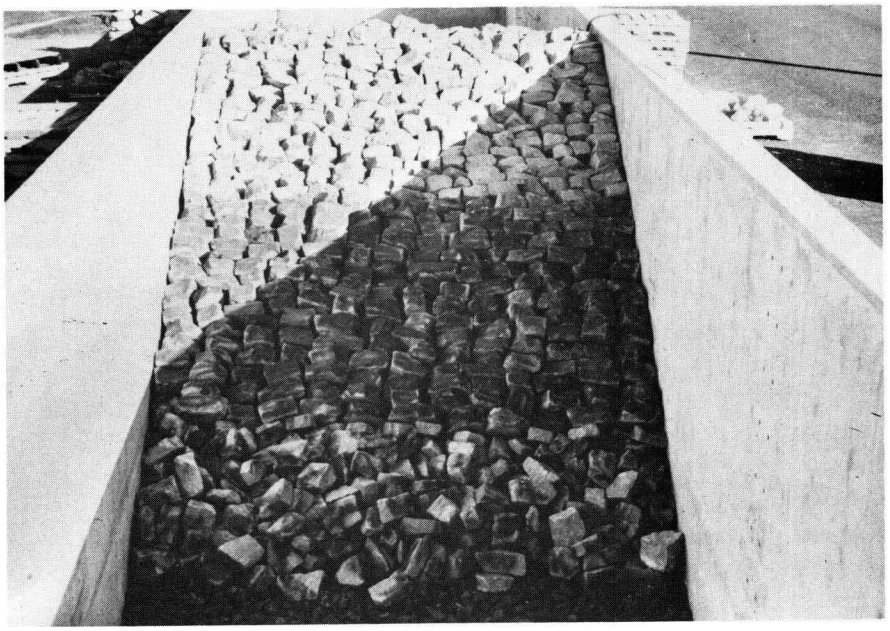

Fig. A-10. Seaward Slope of Completed 1:10 Scale Model

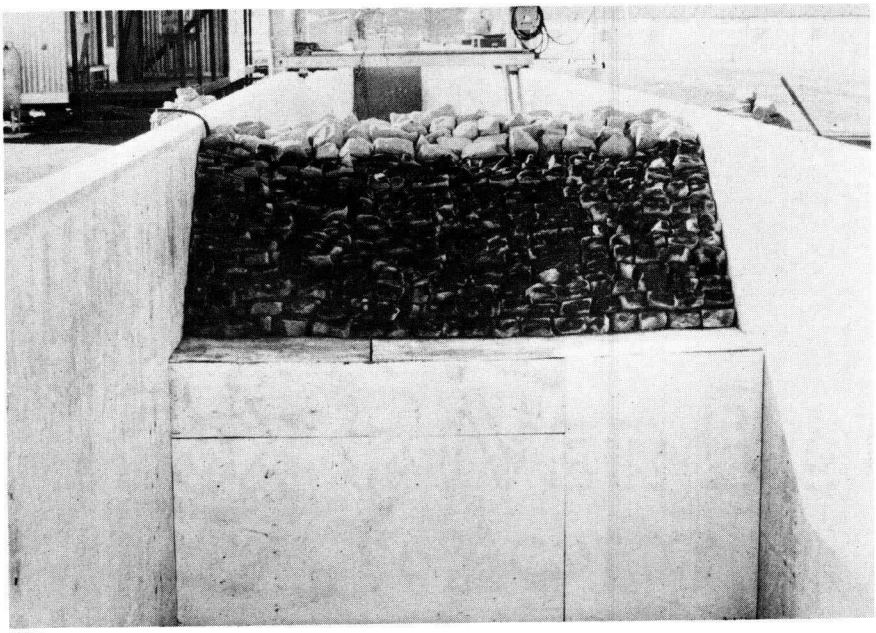

Fig. A-11. B Stones on Back Face of Completed 1:10 Scale Model

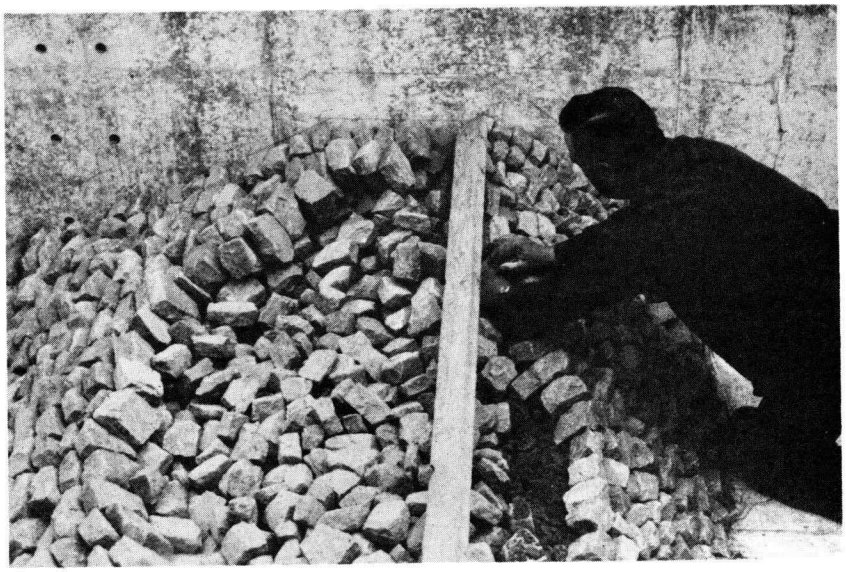

Fig. A-12. Placement of A and B Stones, 1:20 Scale Model

Fig. A-13. Grid Used to Measure Runup and Rundown

Fig. A-14. Runup, 1:10 Scale Model

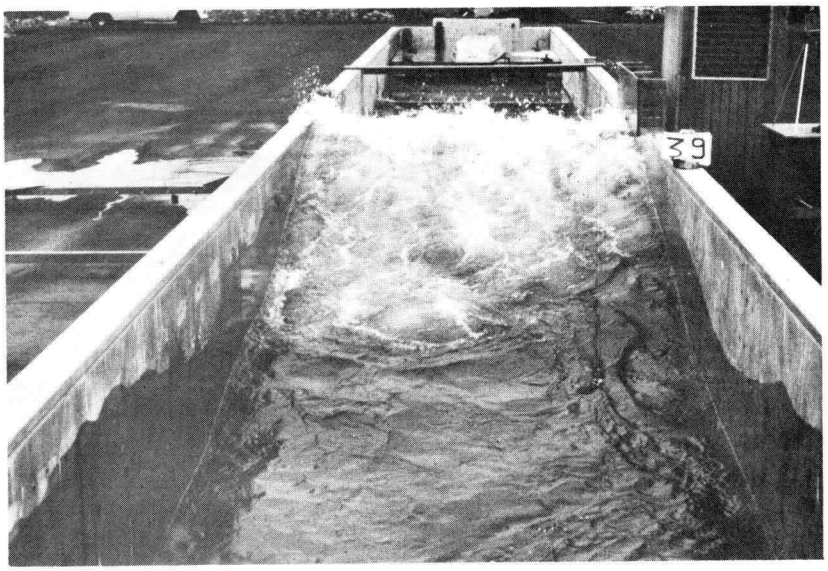

Fig. A-15. Non-Breaking Overtopping, 1:10 Scale Model

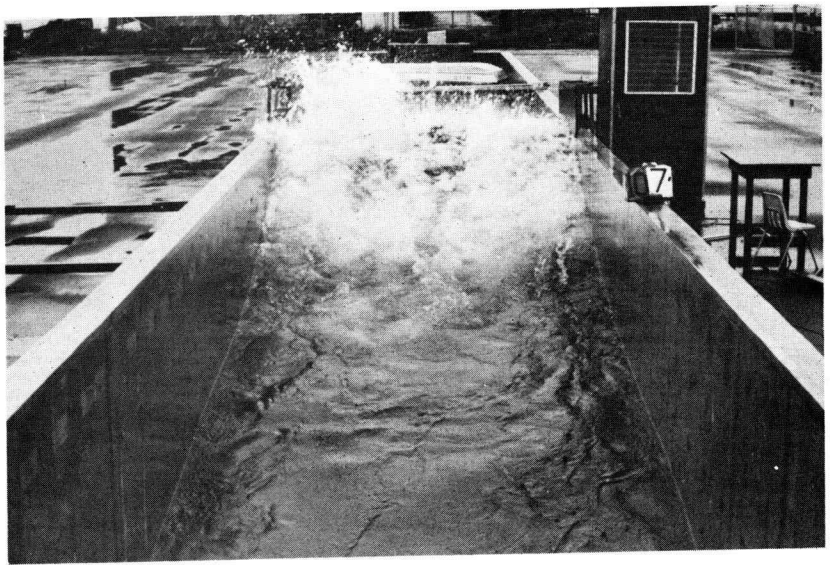

Fig. A-16. Breaking Overtopping, 1:10 Scale Model

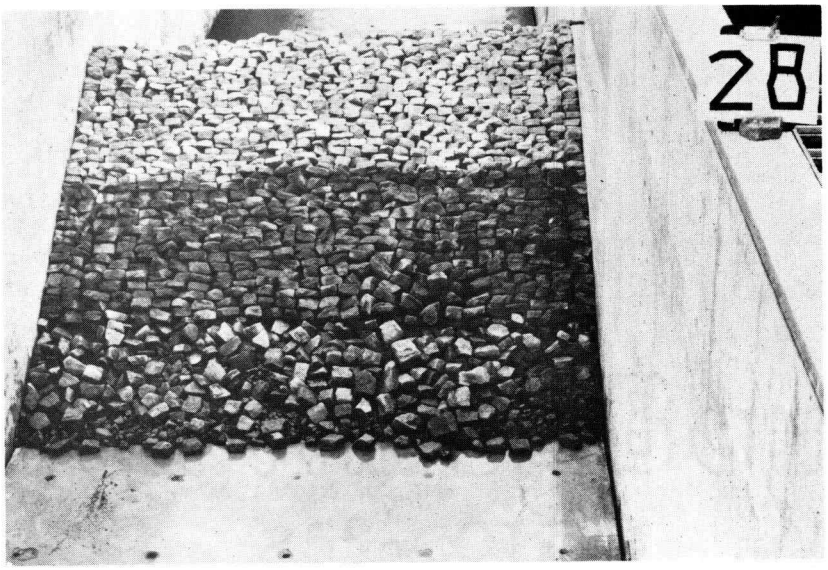

Fig. A-17. Example Damage to A- and A+ Stones, 1:20 Scale Model

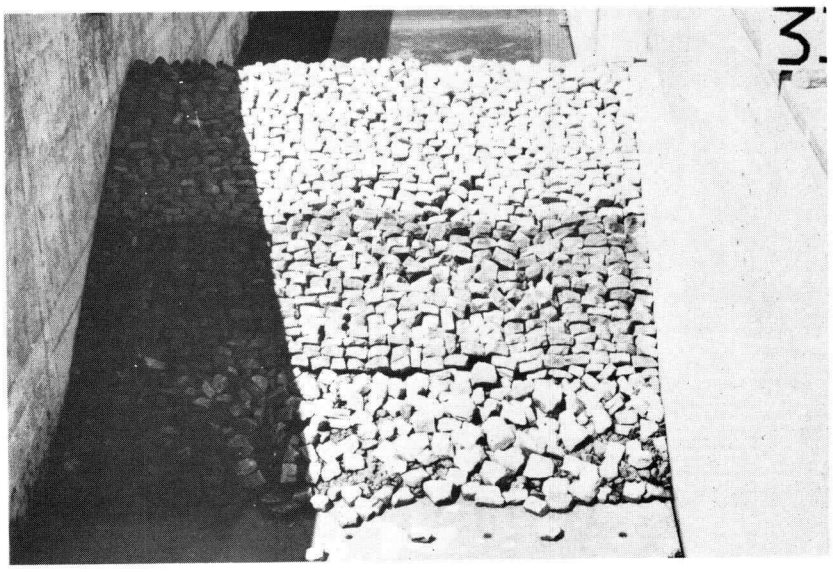

Fig. A-18. Example Moderate Damage to A+ Stones, 1:20 Scale Model

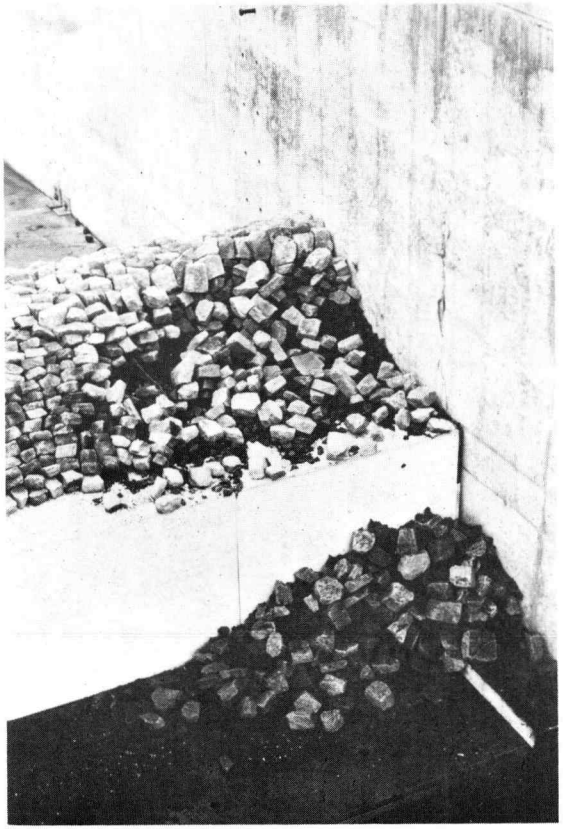

Fig. A-19. Example Damage to B Stone, 1:20 Scale Model

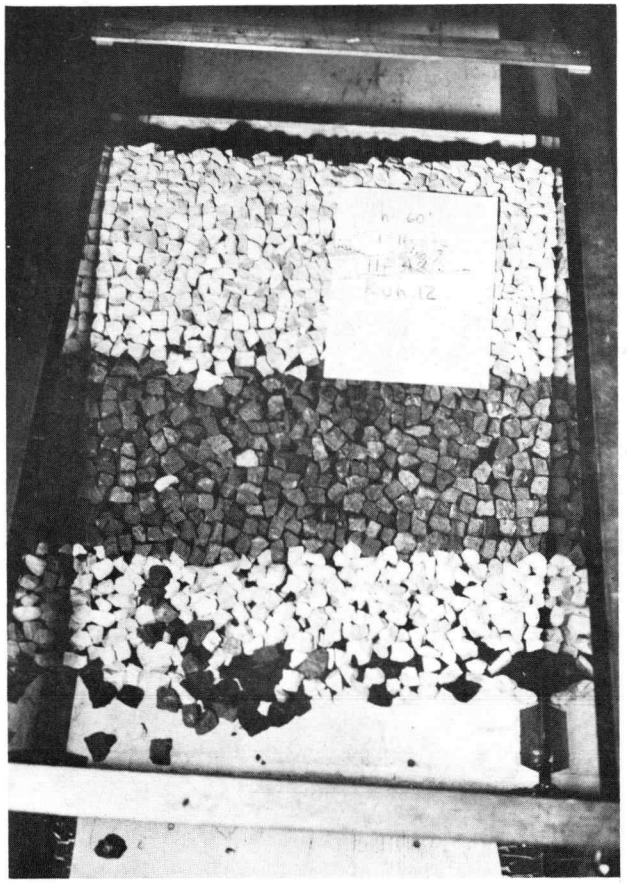

Fig. A-20. Example Damage to A-, A, and A+ Stone, 1:100 Scale Model

APPENDIX B

ARMOR STONE WEIGHT DISTRIBUTIONS

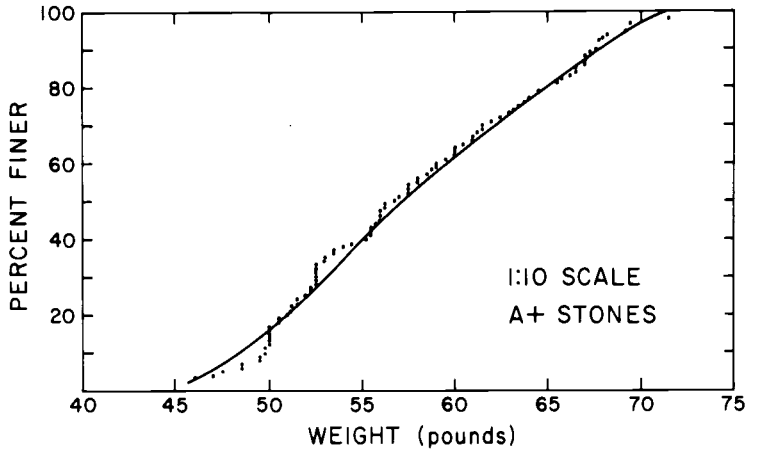

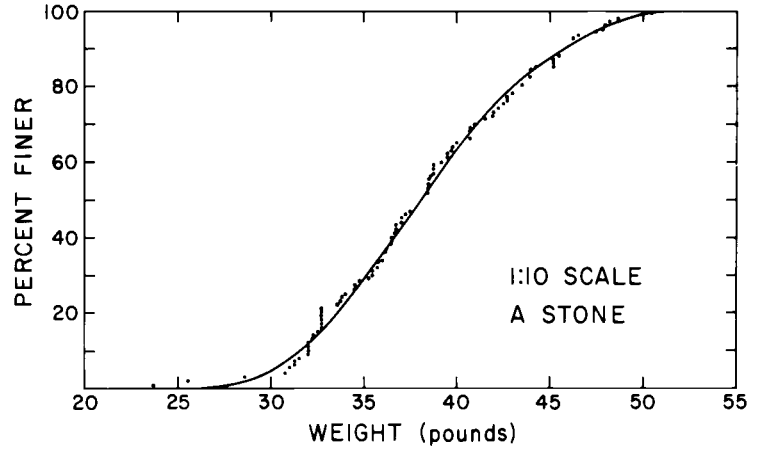

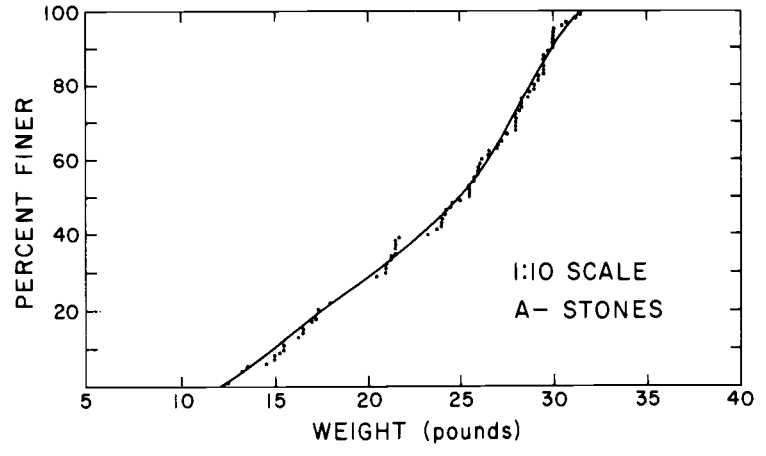

Fig. B-1. 1:10 Scale Model Stone Weight Distribution

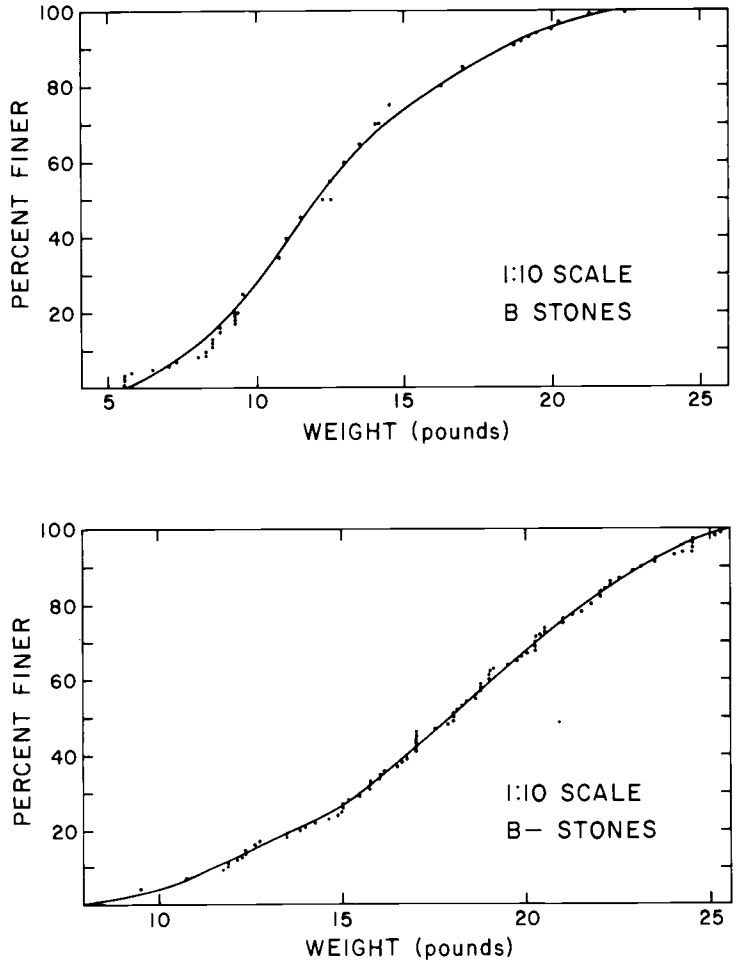

Fig. B-2. 1:10 Scale Model Stone Weight Distribution

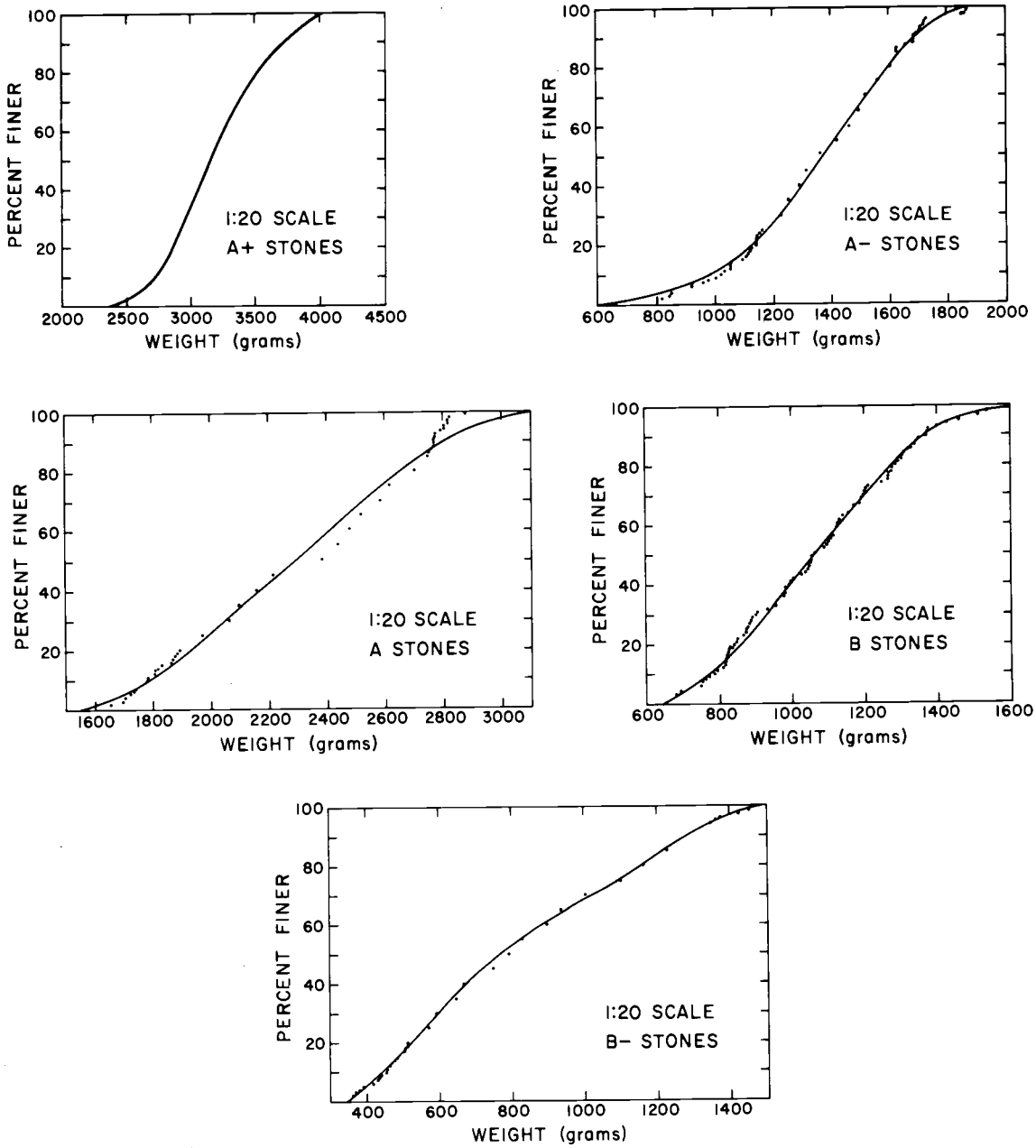

Fig. B-3. 1:20 Scale Model Stone Weight Distribution

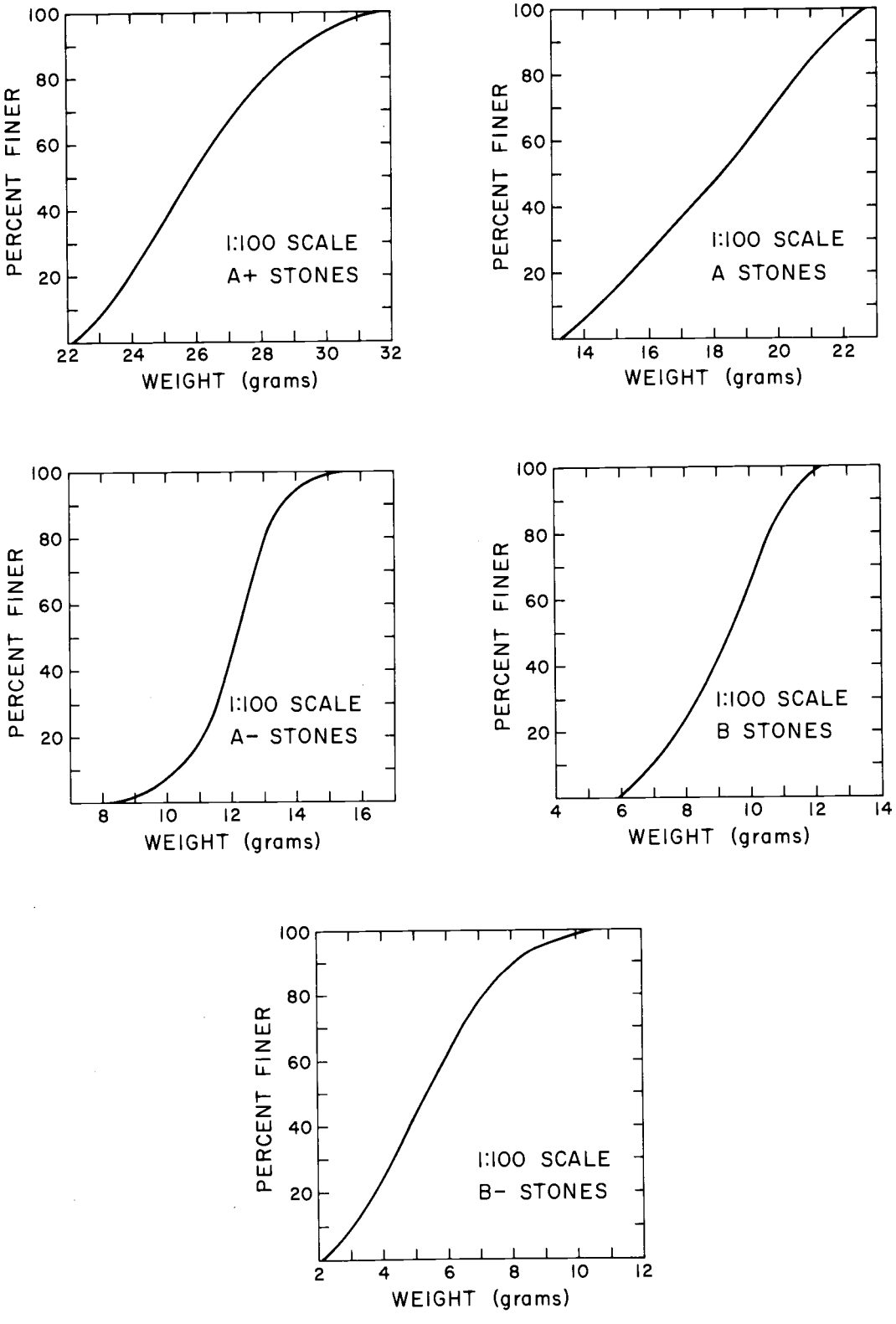

Fig. B-4. 1:100 Scale Model Stone Weight Distribution

APPENDIX C

DATA TABULATIONS

All data are converted to prototype scale. Lengths are in feet, time in seconds. "Height" refers to the local incident wave height on flat section in front of breakwater.

C-1

1:10 Scale Data

RUN NO	BOTTOM	HEIGHT	PERIOD	DEPTH	RUNUP	RUNDOWN	REFLECT.
1	FLAT	32.1	9.0	60.0	38.3	12.5	.201
2	FLAT	33.4	13.5	60.0	40.0	20.0	.361
3	FLAT	28.6	16.0	60.0	30.0	15.0	.324
4	FLAT	27.7	10.0	60.0	30.0	17.0	.190
5	FLAT	26.7	13.5	60.0	35.0	20.0	.358
6	FLAT	24.9	16.0	60.0	25.8	8.9	.268
7	FLAT	24.6	9.0	60.0	28.3	7.6	.153
8	FLAT	27.5	14.0	50.0	32.5	6.7	.360
9	FLAT	17.7	9.0	40.0	17.5	4.0	.246
10	FLAT	20.2	13.5	40.0	27.5	7.5	.370
11	FLAT	16.6	16.0	40.0	12.5	7.5	.287
12	FLAT	14.1	13.5	40.0	15.0	6.7	.395
13	FLAT	27.6	15.0	60.0	38.4	17.7	.379
14	SLOPED	39.4	9.0	60.0	O.T.	11.6	.099
15	SLOPED	41.0	9.0	60.0	O.T.	11.6	.094
16	SLOPED	44.0	9.0	60.0	O.T.	11.6	.088
17	SLOPED	45.8	9.0	60.0	O.T.	13.3	.068
18			NO DATA	.			
19	SLOPED	30.9	13.5	60.0	40.0	15.0	.271
20	SLOPED	32.2	13.5	60.0	O.T.	15.8	.273
21	SLOPED	35.2	13.5	60.0	O.T.	17.5	.322
22	SLOPED	37.5	13.5	60.0	O.T.	16.7	.301
23	SLOPED	38.4	13.5	60.0	O.T.	16.7	.289
24	SLOPED	48.2	16.0	60.0	O.T.	20.0	.357
25	SLOPED	18.2	9.0	60.0	25.8	6.7	.201
26	SLOPED	19.5	9.0	60.0	28.3	7.3	.178
27	SLOPED	22.6	9.0	60.0	31.7	10.0	.171
28	SLOPED	24.5	9.0	60.0	30.8	9.1	.150
29	SLOPED	27.3	9.0	60.0	40.0	9.1	.123
30	SLOPED	26.6	13.5	60.0	35.0	15.0	.283

RUN NO	BOTTOM	HEIGHT	PERIOD	DEPTH	RUNUP	RUNDOWN	REFLECT.
31	SLOPED	30.6	13.5	60.0	40.0	15.8	.332
32	SLOPED	24.0	10.0	60.0	28.3	9.1	.158
33	SLOPED	26.1	11.0	60.0	32.5	11.7	.184
34	SLOPED	26.1	12.0	60.0	30.8	13.3	.192
35	SLOPED	26.1	13.0	60.0	33.3	15.0	.276
36	SLOPED	25.9	14.0	60.0	36.8	15.0	.342
37	SLOPED	24.6	15.0	60.0	33.3	15.0	.397
38	SLOPED	25.8	16.0	60.0	33.3	16.7	.392
39	SLOPED	43.3	16.0	60.0	O.T.	16.7	.389
40	SLOPED	24.3	9.0	50.0	32.5	8.3	.173
41	SLOPED	25.6	10.0	50.0	32.5	8.3	.234
42	SLOPED	24.8	11.0	50.0	32.5	8.3	.229
43	SLOPED	25.0	12.0	50.0	32.5	9.2	.288
44	SLOPED	25.1	13.0	50.0	32.5	11.7	.361
45	SLOPED	25.7	14.0	50.0	35.0	12.5	.331
46	SLOPED	25.2	15.0	50.0	32.5	12.5	.393
47	SLOPED	25.8	16.0	50.0	33.3	14.2	.364
48	SLOPED	29.8	9.0	50.0	40.0	6.7	.175
49	SLOPED	35.4	9.0	50.0	41.7	8.3	.139
50	SLOPED	40.7	9.0	50.0	50.0	10.0	.116
51	SLOPED	44.1	9.0	50.0	45.0	8.3	.090
52	SLOPED	31.3	13.5	50.0	O.T.	N.D.	.333
53	SLOPED	32.4	13.0	50.0	41.7	15.0	.329
54	SLOPED	36.0	13.0	50.0	41.7	15.0	.281
55	SLOPED	39.0	13.0	50.0	50.0	13.3	.292
56	SLOPED	42.2	13.0	50.0	O.T.	10.0	.333
57	SLOPED	46.5	13.0	50.0	O.T.	15.8	.258
58	SLOPED	34.4	16.0	50.0	42.5	15.0	.391
59	SLOPED	38.1	16.0	50.0	50.0	15.8	.439
60	SLOPED	40.8	16.0	50.0	O.T.	16.7	.313

RUN NO	BOTTOM	HEIGHT	PERIOD	DEPTH	RUNUP	RUNDOWN	REFLECT.
61	SLOPED	41.9	16.0	50.0	O.T.	17.5	.388
62	SLOPED	16.4	9.0	50.0	17.5	7.5	.224
63	SLOPED	16.9	10.0	50.0	18.3	8.3	.263
64	SLOPED	17.5	11.0	50.0	18.3	7.5	.242
65	SLOPED	16.5	12.0	50.0	18.3	8.3	.312
66	SLOPED	17.0	13.0	50.0	19.2	9.2	.348
67	SLOPED	15.5	14.0	50.0	16.6	8.3	.423
68	SLOPED	17.5	15.0	50.0	17.5	9.2	.422
69	SLOPED	16.3	16.0	50.0	16.7	10.0	.468
70	SLOPED	13.3	9.0	40.0	11.7	5.8	.252
71	SLOPED	13.1	10.0	40.0	12.5	5.8	.312
72	SLOPED	13.4	11.0	40.0	12.5	6.7	.304
73	SLOPED	14.0	12.0	40.0	13.3	6.7	.310
74	SLOPED	13.3	13.0	40.0	12.5	6.7	.395
75	SLOPED	13.2	14.0	40.0	12.5	6.7	.396
76	SLOPED	13.2	15.0	40.0	12.5	5.8	.449
77	SLOPED	12.8	16.0	40.0	12.5	6.7	.471
78	SLOPED	24.2	9.0	40.0	30.0	5.8	.195
79	SLOPED	32.2	9.0	40.0	40.0	5.8	.192
80	SLOPED	31.8	9.0	40.0	42.5	5.8	.188
81	SLOPED	37.7	9.0	40.0	45.0	5.0	.151
82	SLOPED	24.9	10.0	40.0	32.5	7.5	.267
83	SLOPED	24.6	11.0	40.0	30.0	8.3	.279
84	SLOPED	25.1	12.0	40.0	27.5	10.0	.282
85	SLOPED	23.9	13.0	40.0	29.1	9.1	.361
86	SLOPED	23.6	13.5	40.0	35.8	9.1	.330
87	SLOPED	26.4	13.5	40.0	41.7	9.1	.316
88	SLOPED	28.8	13.5	40.0	49.2	8.3	.304
89	SLOPED	31.7	13.5	40.0	57.5	10.0	.270
90	SLOPED	35.0	13.5	40.0	50.0	10.0	.294

RUN NO	BOTTOM	HEIGHT	PERIOD	DEPTH	RUNUP	RUNDOWN	REFLECT.
91	SLOPED	22.4	14.0	40.0	27.5	10.0	.370
92	SLOPED	24.2	15.0	40.0	32.5	10.0	.418
93	SLOPED	23.7	16.0	40.0	30.0	10.0	.388
94	SLOPED	25.5	16.0	40.0	35.0	10.0	.327
95	SLOPED	26.7	16.0	40.0	40.0	10.0	.345
96	SLOPED	28.2	16.0	40.0	44.2	10.0	.327
97	SLOPED	20.0	10.0	60.0	25.0	5.8	.188
98	SLOPED	19.9	11.0	60.0	25.8	6.7	.195
99	SLOPED	20.2	12.0	60.0	25.8	7.5	.220
100	SLOPED	20.6	13.0	60.0	28.3	9.2	.285
101	SLOPED	19.6	14.0	60.0	16.7	9.2	.372
102	SLOPED	20.2	15.0	60.0	28.3	10.0	.341
103	SLOPED	20.3	16.0	60.0	26.7	10.8	.416

C-2

1:20 Scale Data

RUN NO	BOTTOM	HEIGHT	PERIOD	DEPTH	RUNUP	RUNDOWN	REFLECT.
201	FLAT	27.2	10.0	60.0	35.0	15.0	.176
202	FLAT	28.1	13.5	60.0	33.4	16.4	.253
203	FLAT	25.9	16.0	60.0	33.4	10.0	.236
204	FLAT	25.1	9.0	60.0	38.4	13.3	.150
207	FLAT	17.4	9.0	40.0	18.4	10.0	.287
208	FLAT	14.7	13.5	40.0	23.2	8.3	.311
209	FLAT	16.3	16.0	40.0	20.0	6.7	.313
210	SLOPED	18.6	9.0	60.0	30.0	10.0	.134
211	SLOPED	20.3	9.0	60.0	33.2	11.7	.162
212	SLOPED	23.0	9.0	60.0	36.8	13.3	.164
213	SLOPED	25.2	9.0	60.0	40.0	10.0	.161
214	SLOPED	27.5	9.0	60.0	40.0	10.0	.118
215	SLOPED	33.2	9.0	60.0	O.T.	11.7	.092
216	SLOPED	35.2	9.0	60.0	O.T.	13.3	.084
217	SLOPED	37.2	9.0	60.0	O.T.	15.0	.081
218	SLOPED	43.5	9.0	60.0	O.T.	10.0	.113
219	SLOPED	45.8	9.0	60.0	35.0	10.0	.122
220	SLOPED	26.0	13.5	60.0	35.0	15.0	.342
221	SLOPED	29.7	13.5	60.0	40.0	16.6	.346
222	SLOPED	32.6	13.5	60.0	O.T.	20.0	.331
223	SLOPED	37.1	13.5	60.0	O.T.	23.4	.323
224	SLOPED	49.7	13.5	60.0	O.T.	25.0	.284
225	SLOPED	53.2	13.5	60.0	O.T.	20.0	.262
226	SLOPED	30.5	9.0	40.0	35.0	11.7	.146
228	SLOPED	34.0	9.0	40.0	34.4	13.5	.141
228	SLOPED	39.3	13.5	40.0	50.0	16.6	.257
229	SLOPED	31.7	16.0	40.0	50.0	13.5	.314
230	SLOPED	35.9	16.0	40.0	55.0	13.5	.322
231	SLOPED	35.9	13.5	40.0	53.5	13.5	.289
232	SLOPED	46.8	13.5	60.0	O.T.	25.0	.265

RUN NO	BOTTOM	HEIGHT	PERIOD	DEPTH	RUNUP	RUNDOWN	REFLECT.
233	SLOPED	47.1	13.5	60.0	O.T.	26.6	.201
234	SLOPED	39.4	16.0	60.0	O.T.	25.0	.648
235	SLOPED	50.6	16.0	60.0	O.T.	25.0	.499
236	SLOPED	24.4	9.0	50.0	35.0	11.7	.125
237	SLOPED	36.0	9.0	50.0	50.0	13.5	.092
238	SLOPED	38.1	9.0	50.0	48.5	11.7	.102
239	SLOPED	41.8	9.0	50.0	40.0	8.4	.123
240	SLOPED	40.2	13.5	50.0	O.T.	18.4	.263
241	SLOPED	45.6	13.5	50.0	O.T.	21.6	.247
242	SLOPED	35.7	16.0	50.0	O.T.	21.6	.356
243	SLOPED	43.4	16.0	50.0	O.T.	23.4	.372
244	SLOPED	43.3	11.2	50.0	O.T.	20.0	.099

C-3

1:100 Scale Data

RUN NO	BOTTOM	HEIGHT	PERIOD	DEPTH	RUNUP	RUNDOWN	REFLECT.
1031	FLAT	13.8	16.0	60.0	15.3	15.3	.455
1032	FLAT	16.2	16.0	60.0	13.0	13.2	.438
1033	FLAT	12.1	16.0	60.0	16.8	15.1	.378
1034	FLAT	15.4	16.0	60.0	13.0	12.7	.351
1035	FLAT	17.5	16.0	60.0	15.6	15.4	.429
1036	FLAT	13.3	16.0	60.0	12.6	12.6	.375
1037	FLAT	13.7	16.0	60.0	13.3	16.1	.455
1038	FLAT	15.4	16.0	60.0	14.4	15.6	.405
1039	FLAT	17.5	16.0	60.0	16.1	16.8	.429
1040	FLAT	20.0	16.0	60.0	16.4	20.1	.417
1041	FLAT	21.7	16.0	60.0	18.1	20.7	.385
1042	FLAT	22.7	16.0	60.0	18.9	21.6	.394
1043	FLAT	22.1	16.0	60.0	19.6	22.5	.396
1044	FLAT	22.9	16.0	60.0	20.7	22.7	.345
1045	FLAT	24.2	16.0	60.0	22.4	22.4	.362
1046	FLAT	22.5	16.0	60.0	25.6	21.7	.407
1047	FLAT	22.9	16.0	60.0	26.4	21.7	.418
1048	FLAT	25.4	16.0	60.0	26.7	22.7	.377
1049	FLAT	28.3	16.0	60.0	28.9	23.6	.353
1050	FLAT	29.2	16.0	60.0	28.2	23.7	.343
1051	FLAT	31.2	16.0	60.0	31.0	25.3	.360
1052	FLAT	34.2	16.0	60.0	30.6	25.5	.415
1053	FLAT	34.2	16.0	60.0	34.6	25.8	.366
1054	FLAT	6.2	9.0	40.0	2.6	6.1	.333
1055	FLAT	8.8	9.0	40.0	3.0	7.7	.333
1056	FLAT	10.0	9.0	40.0	5.0	7.9	.250
1057	FLAT	11.2	9.0	40.0	5.1	8.3	.259
1058	FLAT	10.8	9.0	40.0	3.9	9.5	.231
1059	FLAT	11.9	9.0	40.0	5.3	9.4	.228
1060	FLAT	14.2	9.0	40.0	8.6	8.4	.294

RUN NO	BOTTOM	HEIGHT	PERIOD	DEPTH	RUNUP	RUNDOWN	REFLECT.
1061	FLAT	15.2	9.0	40.0	8.6	8.8	.260
1062	FLAT	9.2	9.0	60.0	3.7	11.6	.182
1063	FLAT	11.2	9.0	60.0	7.8	12.1	.185
1064	FLAT	14.6	9.0	60.0	8.3	13.3	.200
1065	FLAT	12.5	9.0	60.0	5.4	11.9	.200
1066	FLAT	13.7	9.0	60.0	10.1	10.8	.212
1067	FLAT	15.4	9.0	60.0	11.7	13.4	.189
1068	FLAT	17.9	9.0	60.0	14.8	13.7	.163
1069	FLAT	21.7	9.0	60.0	18.4	15.9	.077
1070	FLAT	24.2	9.0	60.0	21.4	17.1	.103
1071	FLAT	25.8	9.0	60.0	23.0	17.0	.161
1072	FLAT	26.7	9.0	60.0	24.4	15.7	.188
1073	FLAT	23.3	9.0	60.0	21.1	15.7	.143
1074	FLAT	26.7	9.0	60.0	24.4	18.4	.125
1075	FLAT	26.7	9.0	60.0	26.8	16.8	.125
1076	FLAT	27.5	9.0	60.0	26.3	17.3	.091
1077	FLAT	4.6	9.0	50.0	2.2	3.8	.273
1078	FLAT	8.5	9.0	50.0	5.1	5.8	.268
1079	FLAT	11.2	9.0	50.0	7.1	6.8	.259
1080	FLAT	14.2	9.0	50.0	9.4	9.8	.235
1081	FLAT	16.2	9.0	50.0	13.6	9.5	.231
1082	FLAT	17.9	9.0	50.0	17.4	9.8	.256
1083	FLAT	18.7	9.0	50.0	17.2	12.7	.244
1084	FLAT	20.4	9.0	50.0	18.1	11.4	.224
1085	FLAT	21.2	9.0	50.0	20.8	13.6	.255
1086	FLAT	20.0	9.0	50.0	18.1	12.9	.250
1087	FLAT	8.7	16.0	50.0	7.3	9.7	.429
1088	FLAT	9.2	16.0	50.0	3.1	8.9	.364
1089	FLAT	11.2	16.0	50.0	3.4	4.2	.333
1090	FLAT	13.3	16.0	50.0	4.5	12.3	.250

RUN NO	BOTTOM	HEIGHT	PERIOD	DEPTH	RUNUP	RUNDOWN	REFLECT.
1091	FLAT	18.7	16.0	50.0	12.7	13.4	.156
1092	FLAT	12.5	16.0	50.0	5.2	14.6	.333
1093	FLAT	14.2	16.0	50.0	5.3	14.6	.294
1094	FLAT	15.8	16.0	50.0	15.3	12.9	.263
1095	FLAT	16.7	16.0	50.0	14.3	11.1	.300
1096	FLAT	18.3	16.0	50.0	14.2	11.1	.364
1097	FLAT	23.3	16.0	50.0	22.4	15.6	.286
1098	FLAT	12.9	16.0	40.0	6.7	7.3	.355
1099	FLAT	13.5	16.0	40.0	9.1	6.7	.323
1100	FLAT	15.4	16.0	40.0	10.5	6.8	.351
1101	FLAT	13.5	16.0	40.0	12.7	7.3	.292
1102	FLAT	13.7	16.0	40.0	13.0	7.0	.273
1103	FLAT	12.9	16.0	40.0	10.2	8.5	.355
1104	FLAT	15.0	16.0	40.0	10.2	9.3	.389
1105	FLAT	15.0	16.0	40.0	14.7	9.5	.278
1106	FLAT	15.4	16.0	40.0	15.4	10.4	.405
1107	FLAT	26.7	16.0	40.0	15.8	10.2	.313
1108	SLOPED	9.3	9.0	40.0	6.4	7.3	.273
1109	SLOPED	14.4	9.0	40.0	9.6	9.3	.235
1110	SLOPED	13.5	9.0	40.0	9.8	9.0	.250
1111	SLOPED	17.4	9.0	40.0	14.8	10.9	.220
1112	SLOPED	19.0	9.0	40.0	16.9	10.5	.200
1113	SLOPED	22.0	9.0	40.0	20.9	11.0	.154
1114	SLOPED	20.3	9.0	40.0	17.1	10.1	.167
1115	SLOPED	24.6	9.0	40.0	23.1	11.2	.172
1116	SLOPED	22.9	9.0	40.0	22.1	11.3	.185
1117	SLOPED	30.9	9.0	40.0	29.2	11.5	.096
1118	SLOPED	30.5	9.0	40.0	30.1	11.5	.111
1119	SLOPED	34.7	9.0	40.0	27.0	11.2	.171
1120	SLOPED	9.5	9.0	50.0	6.0	6.2	.217

RUN NO	BOTTOM	HEIGHT	PERIOD	DEPTH	RUNUP	RUNDOWN	REFLECT.
1121	SLOPED	13.2	9.0	50.0	10.1	9.8	.188
1122	SLOPED	15.7	9.0	50.0	12.6	10.5	.211
1123	SLOPED	15.7	9.0	50.0	13.8	9.3	.211
1124	SLOPED	19.0	9.0	50.0	17.7	12.4	.174
1125	SLOPED	17.4	9.0	50.0	17.1	12.1	.238
1126	SLOPED	24.0	9.0	50.0	20.6	12.9	.138
1127	SLOPED	24.0	9.0	50.0	22.1	12.7	.172
1128	SLOPED	25.2	9.0	50.0	22.8	13.8	.180
1129	SLOPED	25.6	9.0	50.0	23.4	14.8	.161
1130	SLOPED	24.8	9.0	50.0	22.5	13.0	.133
1131	SLOPED	26.9	9.0	50.0	25.9	13.7	.138
1132	SLOPED	28.5	9.0	50.0	29.3	13.2	.130
1133	SLOPED	31.4	9.0	50.0	33.9	14.4	.105
1134	SLOPED	37.2	9.0	50.0	38.5	14.8	.111
1135	SLOPED	38.9	9.0	50.0	39.0	15.2	.106
1136	SLOPED	39.7	9.0	50.0	41.0	17.1	.125
1137	SLOPED	40.5	9.0	50.0	38.8	15.8	.102
1138	SLOPED	40.5	9.0	50.0	38.5	16.1	.102
1139	SLOPED	10.2	9.0	60.0	8.2	7.5	.200
1140	SLOPED	14.0	9.0	60.0	10.7	9.7	.159
1141	SLOPED	16.3	9.0	60.0	14.6	11.2	.150
1142	SLOPED	18.1	9.0	60.0	15.4	12.7	.146
1143	SLOPED	19.5	9.0	60.0	17.7	13.7	.125
1144	SLOPED	21.2	9.0	60.0	17.9	14.8	.115
1145	SLOPED	19.1	9.0	60.0	18.0	13.0	.149
1146	SLOPED	23.6	9.0	60.0	21.9	14.1	.103
1147	SLOPED	24.8	9.0	60.0	25.0	14.6	.115
1148	SLOPED	26.9	9.0	60.0	26.7	13.3	.091
1149	SLOPED	29.3	9.0	60.0	28.2	13.5	.111
1150	SLOPED	30.1	9.0	60.0	28.2	17.4	.081

RUN NO	BOTTOM	HEIGHT	PERIOD	DEPTH	RUNUP	RUNDOWN	REFLECT.
1001	FLAT	16.0	13.5	60.0	12.6	9.1	.375
1002	FLAT	15.4	13.5	60.0	17.4	12.1	.351
1003	FLAT	20.8	13.5	60.0	26.5	18.2	.361
1004	FLAT	22.5	13.5	60.0	28.0	18.9	.333
1005	FLAT	24.1	13.5	60.0	28.6	18.6	.311
1006	FLAT	36.6	13.5	60.0	O.T.	22.4	.273
1007	FLAT	2.9	13.5	40.0	2.1	2.3	.439
1008	FLAT	3.7	13.5	40.0	1.4	3.3	.459
1009	FLAT	4.1	13.5	40.0	3.3	3.7	.512
1010	FLAT	5.4	13.5	40.0	2.8	4.7	.389
1011	FLAT	7.5	13.5	40.0	6.5	5.6	.450
1012	FLAT	9.2	13.5	40.0	6.8	6.5	.454
1013	FLAT	8.3	13.5	40.0	7.9	7.4	.398
1014	FLAT	12.1	13.5	40.0	9.1	8.6	.378
1015	FLAT	24.1	13.5	40.0	12.6	11.2	.207
1016	FLAT	26.6	13.5	40.0	24.2	9.3	.376
1017	FLAT	5.0	13.5	50.0	.9	2.8	.500
1018	FLAT	4.6	13.5	50.0	2.8	3.3	.451
1019	FLAT	5.8	13.5	50.0	3.5	5.6	.431
1020	FLAT	8.1	13.5	50.0	5.3	8.4	.441
1021	FLAT	10.4	13.5	50.0	9.3	9.3	.442
1022	FLAT	15.8	13.5	50.0	11.4	10.9	.525
1023	FLAT	19.6	13.5	50.0	17.7	15.1	.407
1024	FLAT	4.3	16.0	60.0	3.9	3.3	.535
1025	FLAT	4.8	16.0	60.0	7.9	6.3	.579
1026	FLAT	6.0	16.0	60.0	8.8	9.7	.517
1027	FLAT	7.7	16.0	60.0	9.7	11.4	.516
1028	FLAT	10.8	16.0	60.0	10.2	13.0	.389
1029	FLAT	11.2	16.0	60.0	11.9	13.0	.411
1030	FLAT	12.1	16.0	60.0	12.6	15.8	.378

RUN NO	BOTTOM	HEIGHT	PERIOD	DEPTH	RUNUP	RUNDOWN	REFLECT.
1151	SLOPED	35.0	9.0	60.0	34.8	20.9	.070
1152	SLOPED	35.0	9.0	60.0	35.2	23.0	.070
1153	SLOPED	36.6	9.0	60.0	O.T.	21.4	.067
1154	SLOPED	35.8	9.0	60.0	O.T.	22.7	.091
1155	SLOPED	38.3	9.0	60.0	O.T.	22.5	.106
1156	SLOPED	43.2	9.0	60.0	O.T.	N.D.	.057
1157	SLOPED	44.0	9.0	60.0	O.T.	N.D.	.074
1158	SLOPED	8.9	13.5	60.0	8.0	7.3	.300
1159	SLOPED	10.2	13.5	60.0	10.4	7.6	.304
1160	SLOPED	10.7	13.5	60.0	11.6	10.2	.333
1161	SLOPED	12.4	13.5	60.0	11.8	9.3	.286
1162	SLOPED	13.8	13.5	60.0	13.3	11.3	.290
1163	SLOPED	14.4	13.5	60.0	16.3	12.0	.292
1164	SLOPED	17.3	13.5	60.0	20.5	11.8	.282
1165	SLOPED	18.2	13.5	60.0	20.5	13.5	.268
1166	SLOPED	18.7	13.5	60.0	20.5	14.8	.286
1167	SLOPED	20.4	13.5	60.0	25.8	14.9	.261
1168	SLOPED	24.0	13.5	60.0	30.7	16.3	.259
1169	SLOPED	25.8	13.5	60.0	33.1	17.7	.241
1170	SLOPED	25.8	13.5	60.0	33.5	16.4	.241
1171	SLOPED	30.2	13.5	60.0	O.T.	18.6	.235
1172	SLOPED	31.1	13.5	60.0	O.T.	18.6	.086
1173	SLOPED	31.5	13.5	60.0	O.T.	18.6	.268
1174	SLOPED	9.1	13.5	50.0	1.7	7.6	.300
1175	SLOPED	10.0	13.5	50.0	3.5	8.3	.273
1176	SLOPED	14.0	13.5	50.0	10.1	10.1	.290
1177	SLOPED	19.5	13.5	50.0	19.4	12.7	.302
1178	SLOPED	18.6	13.5	50.0	20.2	12.4	.317
1179	SLOPED	20.4	13.5	50.0	22.0	14.9	.333
1180	SLOPED	22.6	13.5	50.0	24.2	15.4	.320

RUN NO	BOTTOM	HEIGHT	PERIOD	DEPTH	RUNUP	RUNDOWN	REFLECT.
1181	SLOPED	23.6	13.5	50.0	25.6	16.6	.308
1182	SLOPED	25.8	13.5	50.0	29.8	14.9	.298
1183	SLOPED	25.4	13.5	50.0	30.0	15.1	.286
1184	SLOPED	23.6	13.5	50.0	28.5	15.5	.308
1185	SLOPED	25.4	13.5	50.0	31.0	17.2	.286
1186	SLOPED	24.5	13.5	50.0	26.6	14.4	.259
1187	SLOPED	27.2	13.5	50.0	31.2	17.1	.267
1188	SLOPED	30.8	13.5	50.0	35.6	17.2	.235
1189	SLOPED	33.5	13.5	50.0	O.T.	19.4	.243
1190	SLOPED	35.8	13.5	50.0	O.T.	0.0	.266
1191	SLOPED	34.4	13.5	50.0	O.T.	20.5	.421
1192	SLOPED	13.8	13.5	50.0	11.2	9.3	.377
1193	SLOPED	20.8	13.5	50.0	24.2	14.0	.348
1194	SLOPED	25.8	13.5	50.0	41.0	26.1	.298
1195	SLOPED	26.3	13.5	50.0	29.8	16.8	.310
1196	SLOPED	34.4	13.5	50.0	O.T.	20.5	.421
1197	SLOPED	27.2	13.5	50.0	33.5	22.4	.333
1198	SLOPED	9.3	13.5	40.0	5.6	4.7	.500
1199	SLOPED	15.3	13.5	40.0	15.8	12.1	.455
1200	SLOPED	17.6	13.5	40.0	17.7	13.0	.368
1201	SLOPED	21.3	13.5	40.0	32.6	14.9	.348
1202	SLOPED	24.1	13.5	40.0	38.2	14.9	.385
1203	SLOPED	30.6	13.5	40.0	34.5	14.9	.333
1204	SLOPED	23.2	13.5	40.0	29.8	13.0	.440
1205	SLOPED	27.8	13.5	40.0	39.1	14.9	.367
1206	SLOPED	11.8	16.0	60.0	11.2	13.4	.462
1207	SLOPED	19.1	16.0	60.0	22.4	16.8	.381
1208	SLOPED	23.6	16.0	60.0	33.5	18.6	.423
1209	SLOPED	31.8	16.0	60.0	40.2	23.3	.314
1210	SLOPED	15.0	16.0	60.0	15.8	15.8	.455

RUN NO	BOTTOM	HEIGHT	PERIOD	DEPTH	RUNUP	RUNDOWN	REFLECT.
1211	SLOPED	31.3	16.0	60.0	40.2	26.1	.304
1212	SLOPED	33.6	16.0	60.0	O.T.	29.8	.378
1213	SLOPED	35.9	16.0	60.0	O.T.	27.9	.367
1214	SLOPED	34.5	16.0	60.0	O.T.	25.2	.316
1215	SLOPED	38.6	16.0	60.0	O.T.	29.8	.365
1216	SLOPED	36.8	16.0	60.0	O.T.	27.9	.358
1217	SLOPED	55.2	16.0	60.0	O.T.	29.8	.103
1218	SLOPED	7.8	16.0	50.0	7.8	9.3	.726
1219	SLOPED	13.0	16.0	50.0	13.8	14.9	.500
1220	SLOPED	13.9	16.0	50.0	13.0	14.9	.467
1221	SLOPED	18.1	16.0	50.0	15.8	13.0	.179
1222	SLOPED	22.8	16.0	50.0	27.9	17.9	.388
1223	SLOPED	24.6	16.0	50.0	33.5	17.5	.358
1224	SLOPED	17.2	16.0	50.0	22.4	14.2	.405
1225	SLOPED	27.6	16.0	50.0	33.5	16.8	.378
1226	SLOPED	28.1	16.0	50.0	35.4	17.5	.355
1227	SLOPED	32.5	16.0	50.0	41.0	18.6	.386
1228	SLOPED	41.8	16.0	50.0	O.T.	18.6	.267
1229	SLOPED	11.5	16.0	40.0	7.5	7.5	.500
1230	SLOPED	15.3	16.0	40.0	15.8	9.3	.500
1231	SLOPED	19.6	16.0	40.0	22.4	9.3	.415
1232	SLOPED	7.7	16.0	40.0	5.2	6.0	.500
1233	SLOPED	8.9	16.0	40.0	5.2	6.3	.514
1234	SLOPED	20.6	16.0	40.0	27.9	10.1	.395
1235	SLOPED	18.0	16.0	40.0	20.5	8.2	.467
1236	SLOPED	24.2	16.0	40.0	29.8	11.2	.446
1237	SLOPED	30.2	16.0	40.0	41.0	14.9	.397